NATURAL GROUNDWATER RECHARGE IN THE ALAŞEHİR SUB-BASIN (GEDİZ BASIN, TURKEY)

A Thesis Submitted to
the Graduate School of Engineering and Sciences of
İzmir Institute of Technology
in Partial Fulfillment of the Requirements for the Degree of

MASTER OF SCIENCE

in Energy Systems Engineering

by
Serhat TONKUL

November 2018
İZMİR

We approve the thesis of **Serhat TONKUL**

Examining Committee Members:

Prof. Dr. Alper BABA
Department of Civil Engineering, İzmir Institute of Technology

Prof. Dr. Celalettin ŞİMŞEK
Department of Drilling Technology, Dokuz Eylül University

Prof. Dr. Gülden Gökçen AKKURT
Department of Energy Engineering, İzmir Institute of Technology

Prof. Dr. Gökmen TAYFUR
Department of Civil Engineering, İzmir Institute of Technology

Assoc. Prof. Dr. Orhan GÜNDÜZ
Department of Environmental Engineering, Dokuz Eylül University

23 November 2018

Prof. Dr. Alper BABA
Supervisor, Department of Civil Engineering
İzmir Institute of Technology

Prof. Dr. Celalettin ŞİMŞEK
Co-Supervisor, Department of Drilling Technology
Dokuz Eylül University

Prof. Dr. Gülden Gökçen AKKURT
Head of the Department of Energy Systems Engineering

Prof. Dr. Aysun SOFUOĞLU
Dean of the Graduate School of Engineering and Sciences

ACKNOWLEDGMENTS

I am very grateful to the supervisor of my thesis, Prof. Dr. Alper BABA, for his invaluable theoretical support, guidance and trust during the preparation.

I would like to express my especial gratitude to my co-supervisor Prof. Dr. Celalettin ŞİMŞEK for his great support, academic guidance, helpful advice and feedbacks.

I would like to thank Assist. Prof. Dr. Seda DURUKAN and Assoc. Prof. Dr. Ali Can DEMİRKESEN for their valuable support and contributions.

I would also like to extend my thankfulness to Murat Ozan ÖZDAYI for his support during field studies.

Financial support of Scientific and Technological Research Council of Turkey (TÜBİTAK), which gave me the honor of being a scholar of such an institution devoted to science, is gratefully appreciated.

Finally, I want to express my deepest gratitude to a very special person in my life, my mother Mine VURAL, for her support, love and patience in every aspect of my life.

ABSTRACT

NATURAL GROUNDWATER RECHARGE IN THE ALAŞEHİR SUB-BASIN (GEDİZ BASIN, TURKEY)

The increase in water utilization due to climate change in recent years, as well as excessively growing population causes to an increase in usage of groundwater and threatens water resources. Dams and artificial lakes are being constructed to ensure the sustainability of water resources, but there is much evaporation on large surface of these structures. Due to reason that the evaporation losses are not experienced, the groundwater recharge by direct rainfall becomes important. Groundwater recharge protects the water without too much evaporation in the basins and increases the potential of water resources and ensures sustainability. The aim of this study is to determine alluvial aquifer recharge in Alaşehir (Manisa) sub-basin using numerical and chemical methods. In addition to this aim, the mechanism of mixing of groundwater and geothermal fluid has also been examined.

The Gediz Basin, located in the west of Turkey constitutes 2% of the country, has an important groundwater potential in the area where it is used. The Alasehir sub-basin, located in the southeast of the Gediz Basin and having extensive withdrawal for irrigation, constitutes the study area. Alluvial aquifer is the main groundwater bearing lithological unit in the plain. Twenty-five research wells, which is ranging from 20 m to 50 m in depth, were opened for the calculation of the recharge of the aquifer. Soil characterization was done on the core samples and the aquifer characterization was performed and the alluvial aquifer recharge was calculated. As a result, the recharge value of annual precipitation is range from 21.78 mm to 68.52 mm and average recharge from precipitation is 43.09 mm in the wells which are opened into the alluvium aquifer. According to the numerical model, this amount of recharge corresponds to 10% of the amount of annual rainfall. This estimated recharge ratio directly represents recharge from precipitation into the aquifer. According to the results of the chemical method, it is understood that the average recharge value from precipitation is 16.38%. In addition, the mixing ratio of the groundwater and geothermal fluid is 17% in the sub-basin.

Keywords Aquifer Characterization, Alaşehir, Precipitation Recharge, Numerical Modelling

ÖZET

ALAŞEHİR ALT HAVZASINDA DOĞAL YERALTISUYU BESLENİMİ

Son yıllarda iklim değişikliğine bağlı su kullanımının artması ve buna ek olarak aşırı nüfus artışı, yeraltısuyu kullanımını arttırmakta ve su kaynaklarını tehdit etmektedir. Su kaynaklarının sürdürülebilirliğinin sağlanması için barajlar ve yapay göller inşa edilmekte, ancak bu yapıların geniş yüzey alanlarında çok fazla buharlaşma görülmektedir. Dolayısı ile yeraltı suyunun, buharlaşma kayıplarının yaşanmadığı direkt yağış ile beslenen yeraltısuyu beslenmesi önem kazanmaktadır. Yeraltısuyu beslenmesi, havzalardaki suyu fazla buharlaşmadan korur ve su kaynaklarının potansiyelini artırıp, sürdürülebilirliğini sağlar. Bu çalışma kapsamında nümerik ve kimyasal metotlar kullanılarak, Alaşehir (Manisa) havzasında alüvyon akiferin beslenmesinin belirlenmesi amaçlanmıştır. Ayrıca yeraltısuyu ve jeotermal sistemin karışım mekanizması incelenmiştir. Türkiye'nin batısında yer alan ve ülkenin %2'sini oluşturan Gediz Havzası, önemli bir yeraltı suyu potansiyelinin olduğu ve kullanıldığı alan konumundadır.

Gediz havzasının güneydoğusunda bulunan ve önemli sulama suyu çekiminin yapıldığı Alaşehir alt havzası çalışma alanını oluşturur. Çalışma alanında yer alan alüvyon akifer ise en önemli yeraltısuyu akiferidir. İçme ve sulama suyunun tamamına yakını bu akiferden karşılanır. Çalışma kapsamında akifer beslenmesinin hesaplanması için 25 noktada derinliği 20 m ile 50 m arasında değişen araştırma kuyuları açılmıştır. Karot örnekleri üzerinden zemin tanımlamaları yapılarak akifer karakterizasyonu yapılmış ve alüvyon akiferin beslenmesi hesaplanmıştır. Sonuç olarak, çalışma alanında alüvyon akifere açılan kuyulara uygulanan yıllık yağıştan beslenme değeri 21,78 mm ile 68,52 mm arasında değişmekte olup, ortalama yağıştan beslenme değeri 43,09 mm olarak elde edilmiştir. Nümerik modele göre elde edilen bu beslenme miktarı yağış miktarının %10'una karşılık gelmektedir. Bu beslenme doğrudan yağıştan süzülme değeri olarak ele alınmalıdır. Kimyasal yöntem sonuçlarına göre ortalama beslenme değerinin %16.38 olduğu anlaşılmıştır. Ayrıca havzada yeraltısuyu ve jeotermal sistemin %17 oranında karışım miktarı elde edilmiştir.

Anahtar kelimeler Akifer Karakterizasyonu, Alaşehir, Yağıştan Süzülme, Nümerik Modelleme

TABLE OF CONTENTS

LIST OF FIGURES

LIST OF TABLES

LIST OF ABBREVIATIONS

μS/cm	Microsiemens Per Centimeter
BS 5930	British Standard Soil Classification System
DSİ	General Directorate of State Hydraulic Works
EC	Electrical Conductivity
h	Hour
ha	Hectare
HCI	Hydrochloric acid
HDPE	High Density Polyethylene
Km^2	Square Kilometers
m/d	Meter Per Day
m/s	Meter Per Second
m	Meter
m^3/s	Cubic Meter Per Second
min	Minute
ml	Milliliter
mm	Millimeter
mm/y	Millimeter Per year
MT	Weather Station
PET	Potential Evapotranspiration
pH	Power of Hydrogen
TS 1500	Turkish Standard Soil Classification System
USCS	Unified Soil Classification System
USDA	Triangular Classification System
WTF	Water Table Fluctuation
YM	Rainwater Sample

LIST OF SYMBOLS

q	Flow Rate [$L^3 T^{-1}$]
K	Hydraulic Conductivity [$L T^{-1}$]
K_x, K_y, K_z	Hydraulic Conductivities along x, y and z axes [$L T^{-1}$]
K_v	Vertical Hydraulic Conductivity [$L T^{-1}$]
A	Cross Sectional Area [L^2]
r	Radius [L]
°C	Centigrade
h	Pressure Head [L]
S_s	Specific Storage for Confined Aquifer [L^{-1}]
S_y	Specific Yield of Unconfined Aquifer [-]
t	Time [T]
T	Transmissibility [$L^2 T^{-1}$]
b	Thickness of unconfined aquifer [L]
θ	Water Content [-]
G_s	Specific Gravity [-]
γ	Density [$M L^{-3}$]
e	Void Ratio [-]
n	Porosity [-]
V	Volume [L^3]
I_x, I_y, I_z	Mass Entering Control Volume
O_x, O_y, O_z	Mass Leaving Control Volume
S	Sink Term [$L^3 L^{-3} T^{-1}$]
z	Vertical Distance [L]
R	Recharge [$L T^{-1}$]
P	Precipitation [$L T^{-1}$]
I	Heat Index [-]
Δh	Difference in Water Levels [L]
Ca^{2+}	Calcium
Mg^{2+}	Magnesium

Na^+	Sodium
K^+	Potassium
SO_4^{2-}	Sulphate
HCO_3^-	Bicarbonate
CO_3^-	Carbonate
Cl^-	Chloride
B	Boron
Br^-	Bromide
$\delta^{18}O$	Oxygen Isotope
$\delta^{2}H$	Hydrogen Isotope
$\delta^{3}He$	Helium Isotope
^{14}C	Carbon Isotope

CHAPTER 1

INTRODUCTION

1.1. Problem Description

The freshwater reserves, including the water bodies in icecaps on Earth, are 2.5%. About 35% of this water forms the fresh groundwater resources (Margat and Van der Gun, 2013). There are 25 water basins in Turkey. When the geographical and topographic features of Turkey considered, these water basins are concentrated in the Aegean and Marmara regions where the population and industry concentrated. In the Aegean region, especially the Gediz Basin with its significant groundwater potential is the basin where irrigation made. Irrigation, industry and drinking water consumption depend on the groundwater in this region. Excessive water withdrawals cause groundwater decline at dry period and threaten groundwater resources (Gündüz and Şimşek, 2011).

The old-aged irrigation technology also increases the water consumption considerably. Groundwater resources cannot be stored enough in the aquifer due to excessive withdrawal pressure and the storage reserves are constantly decreasing due to climate change. Considering the global climate change that creates pressure on the world and on growing population, studies are needed for more effectively usage of groundwater to meet the water needs in the future. The investigation of the groundwater and the establishment of the management plans are only possible by realizing the hydrological characteristics of the region and by determining the character of the groundwater system. The most difficult parameter to be determined from all these studies is the recharge. Calculation of the amount of groundwater recharge is one of the most difficult parameters because of the lack of concrete methods for determining the amount of groundwater recharge (Healy, 2010). There are some studies in the literature to determine the amount of recharge using different methods which are used to determine the amount of recharge in the unsaturated and saturated zone (Scanlon et al., 2002; Weight, 2008; Healy, 2010; Leaney et al., 2011). Generally, physical measurement methods, tracer and chemical monitoring methods (stable isotopes and environmental monitoring), groundwater level change methods have been used for determining recharge. In addition, numerical models

have been used to predict the recharge of groundwater. In this study, chemical and numerical methods were used to determine recharge in alluvium aquifer. Furthermore, the relation between cold groundwater resources and geothermal fluids was evaluated. The mixing mechanism of the groundwater and the geothermal fluid is revealed.

1.2. Population and Industry

The study area is a quite wide geographical area. High number of villages and large-scale districts are located therein. Population distribution is mostly concentrated in the Salihli and Alaşehir which is industrial centre (Figure 1.1). In rural areas, population is low and livelihoods are agriculture and animal husbandry. The region is in a trend of population growth in recent years. The biggest reason for this is the increase in industrial companies in the provinces. For example, the Salihli Industrial region covers an area of 115 ha.

Another important economic development has been the increase of geothermal activities in the whole of the plain and the increase of operating facilities for electricity production. In this view, many geothermal wells are opened in the Alaşehir sub-basin and electricity production is being done. Alaşehir sub-basin is one of the most important basins in terms of both groundwater and geothermal. Especially considering the geothermal potential, deep geothermal drilling which reaches 3000 meters was carried out in Alaşehir sub-basin. Agriculture and energy in the basin continue together.

Grape, tobacco, barley, wheat, maize, cotton are the main agricultural products in the basin. Sesame, olive, cherry and pear are also grown at the local scale. There are 60 grape exporting firms and, 40 grape enterprises, Tariş integrated grape processing facilities, Suma factory and Sarıkız mineral water factory are located in Alaşehir. The most important item of all these products is the grape cultivation.

1.3. Irrigation Area

About 32044 ha area is irrigated by surface water irrigation facilities which were constructed by General Directorate of State Hydraulic Works (DSİ) in the study site. The surface water irrigation facilities, constructed by Manisa Special Provincial

Administration are used to irrigate 1628 ha area. A total surface area of 33672 ha is irrigated by irrigation facilities in the study area accordingly. In addition to these, an area of 2370 ha is irrigated by 14 irrigation cooperatives owned by General Directorate of State Hydraulic Works (DSİ). An area of 4049 ha is irrigated by Manisa Special Provincial Administration. A total area of 6419 ha is irrigated with groundwater in the study area accordingly. A total area of 40091 ha is irrigated with surface and groundwater in the study area. The most part of irrigation areas are located within the study area (Figure 1.1). The irrigated farming is performed on the most important aquifer system.

A number of wells have been drilled by General Directorate of State Hydraulic Works (DSİ) for irrigation purpose, drinking and industrial water supply. According to DSİ data, it is revealed that 86.5% of groundwater is used for agricultural irrigation, 11.6% for water usage, and 1.5% for drinking water purpose. The result shows that a considerable part of water consumption is used in irrigation in the basin. It has been shown that the area used for irrigation is approximately 74595 acres in the study area (DSİ, 2014).

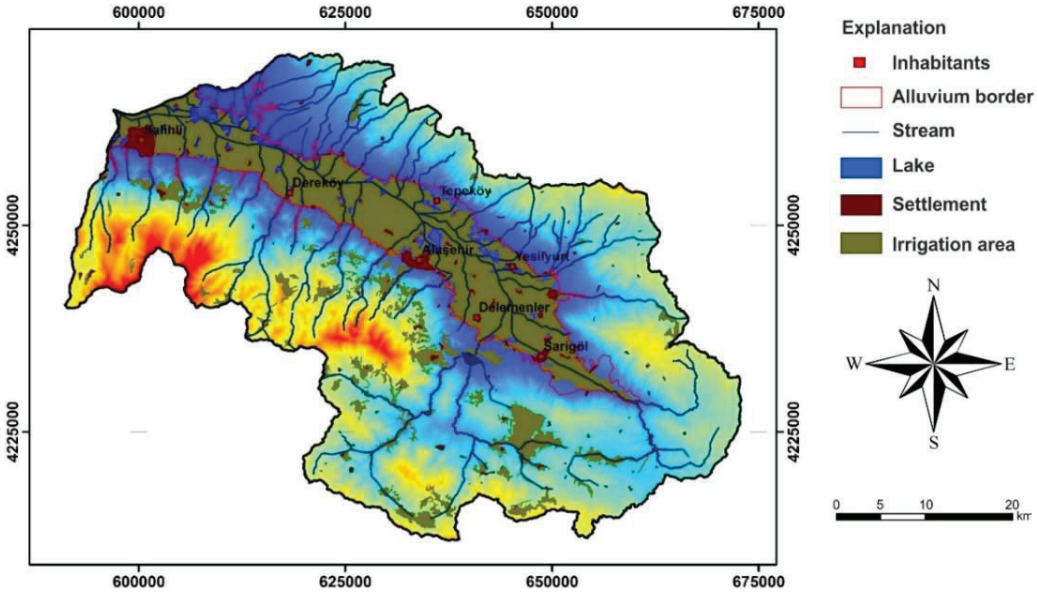

Figure 1.1. Distribution of irrigation areas in the study area

1.4. Aim and Objectives

The aim of this study is to predict groundwater recharge of the alluvium aquifer

using numerical and chemical methods and to determine the mixing mechanism of the geothermal fluid and groundwater in the region. For the purpose of this study, the following research has been completed.

- Twenty-five research wells, ranging in depth from 20 m to 50 m, were done.
- The hydraulic properties of alluvium aquifer were determined by using drilling data.
- Groundwater and rainwater samples were collected for physical and chemical properties of water resources.
- Long-term groundwater level monitoring was done and the meteorological data was collected.
- For groundwater recharge numerical model was used.
- For groundwater recharge chemical methods, using chloride concentrations in groundwater and rainwater samples were measured.
- GIS-based recharge distribution maps were prepared according to alluvium aquifer recharge results obtained from numerical and chemical methods.
- The mixture ratio of geothermal fluid and groundwater resources in the study area was determined.

This study funded by the Scientific and Technological Research Council of Turkey (TÜBİTAK 115Y065).

CHAPTER 2

LITERATURE REVIEW

2.1. Natural Groundwater Recharge

Estimation of groundwater recharge is crucial for the sustainability of aquifers, the management of water resources and the potential water potential in the basin (De Silva, 2015). Recharge estimation is a difficult parameter to determine in areas where the groundwater table is deep and limited by the availability of water on the soil surface due to external conditions such as amount of nutrients, evaporation, precipitation, temperature and climatic factors (De Silva, 2015). Groundwater recharge is important in all groundwater hydrology surveys. Groundwater recharge is becoming a more important issue in the future as the rapidly growing population needs more water and requires more storage of water to save in case of water shortage. Traditional water storage areas are known to be dams. However, the area of dams is steadily declining. In addition, the dams have various disadvantages such as evaporation losses (about 2 m per year in dry and warm climates), potential and structural losses, sediment deposition, ecological and environmental factors (Devine, 1995; Knoppers and van Hulst, 1995; Pearce, 1992). Dams are not suitable for long term water storage. Most of the dams are filled with alluvium finally. This leads to dams are not becoming effective water storage areas. Thus, the importance of groundwater recharge increases. Groundwater recharge and underground storage areas have the advantage of virtually zero evaporation from the aquifer. For this reason, groundwater recharge has become a growing practice in many parts of the world. These aspects of groundwater recharge have also been discussed by (Asano, 1985) at international groundwater recharge symposiums in California and Florida.

Natural recharge of the groundwater is the amount of water reaching the water table by draining down through the vadose zone (Rushton and Ward, 1979). In addition, De Vries and Simmers (2002) define the groundwater recharge as the downward flow of water reaching the water table, which forms the groundwater reservoirs. Groundwater recharge affects the amount of water that can be kept in an aquifer in the long term and is

therefore of great importance in the assessment of any groundwater resources. The amount of water from an aquifer depends primarily on the recovery of groundwater.

Scanlon and Cook (2002) and Delin et al. (2007) have indicated that groundwater recharge is dependent on the application of spatial and temporal scaling. Groundwater recharge is one of the difficult parameters to determine in sustainability studies of groundwater resources due to the many factors involved in the recharge process. Groundwater recharge for water resources includes rainwater from water, irrigation zones or meteorological factors from continuous or intermittent streams that can be arranged with dams. Groundwater is not the dominant water source on earth, but aquifers offer a wide range of possibilities for the storage of groundwater. Therefore, it is expected that the groundwater recharge will play an increasingly important role in the reuse of waters.

2.2. Groundwater Flow Motion

In water basins, the movement of the groundwater is an important factor affecting the water potential and quantity. The water reaches the water table along the soil zones by first filtering the unsaturated zone (vadose zone) and then through the saturated zone. The draining water source can be rainwater and irrigation water. Some of the pores of the unsaturated zone are filled with water and the other part with air. So, the zone on the water table is called the unsaturated zone. The zone below the water table is called the saturated zone because the pores of the soil are completely filled with water. While the motion of the water occurs vertically along the unsaturated zone, the saturated zone can occur both vertically and horizontally. The movement of groundwater on the earth takes place in a hydrological cycle.

2.2.1. Hydrological Cycle

The movement of water between atmosphere, ocean and lakes forms hydrological cycle (Figure 2.1). The water that evaporates from surface waters such as rivers, lakes and oceans return to the earth as precipitation by condensation in the form of water vapor in the atmosphere. However, most of this precipitation does not leach into the ground, some of it is stored along the soil zone and eventually is returned to the atmosphere

through evaporation and transpiration in the leaves of the plant (Alley et al., 2002). This process repeats itself in a hydrological system. The hydrological system is a system that is defined as three-dimensional in space, which is surrounded by certain boundaries, which enters into the system (rainwater and snow) and manages the factors coming out from the system (evaporation, surface flow, transpiration, river flow etc.) (Chow, 1964; Chow et al., 1988). In this system, the role of solar energy is great in the evaporation that takes place in the surface waters and the transpiration processes that take place in the leaves of plants.

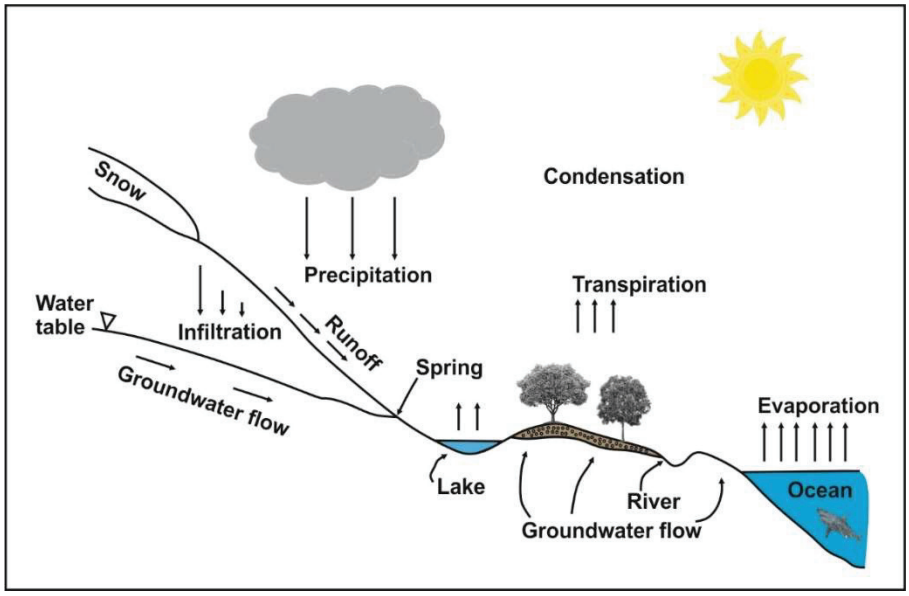

Figure 2.1. Hydrological Cycle
(Source: Todd, 1959)

2.2.2. Saturated Flow

A saturated flow or saturated zone is the area where the pores of the materials forming the underground soil are filled with water. The water in this region forms the groundwater, and the upper part of the region forms the water table. In the hydrologic cycle, surface water is physically and chemically altered as it infiltrates from the unsaturated zone to the saturated zone, resulting in contamination of the groundwater. The increase in the amount of inorganic carbon and the salinity of the groundwater are the most important indicators of contamination. The precipitation waters carry the CO_2

present in the atmosphere over the vadose zone to the groundwater. At the same time, the effective biological processes between plant roots and microorganisms allow for an increase in the amount of CO_2 in the groundwater (Hem, 1970). Therefore, the pH value of the groundwater with increasing amount of CO_2 decreases and the acidity ratio increases. Increasing acidity of groundwater causes pollution by dissolving the rocks in which it interacts. As a result, contamination of groundwater depends on the pH of the water as well as on the physical and chemical properties of the rocks that the groundwater is associated with (Back and Hanshaw, 1965).

In groundwater there is some salt in solution (White et al., 1963). Sometimes water from excessive irrigation or precipitation is drained along the root zone and increases the amount of total dissolved matter, causing the salinity of the groundwater to increase. Since the total amount of dissolved matter increases further towards the depths of the aquifer, it is inevitable that the salinity is higher in the deep. This situation is more likely to occur in areas with artificial recharge and in alluvial rivers.

The vertical movement of water in a homogeneous and saturated environment was expressed by Darcy (1856). The movement of water in the ground was firstly investigated by Darcy (1856) and was called Darcy Law. Darcy (1856) performed this experiment with a vertical test setup. By creating a porous and homogeneous environment in an inclined tube, it can be easily shown that the flow through the inlet and outlet of the tube results in a linear relationship between the water flow rate (Q) and the hydraulic gradient ($\Delta h/L$) and the cross-sectional area of the tube (A) (Figure 2.2).

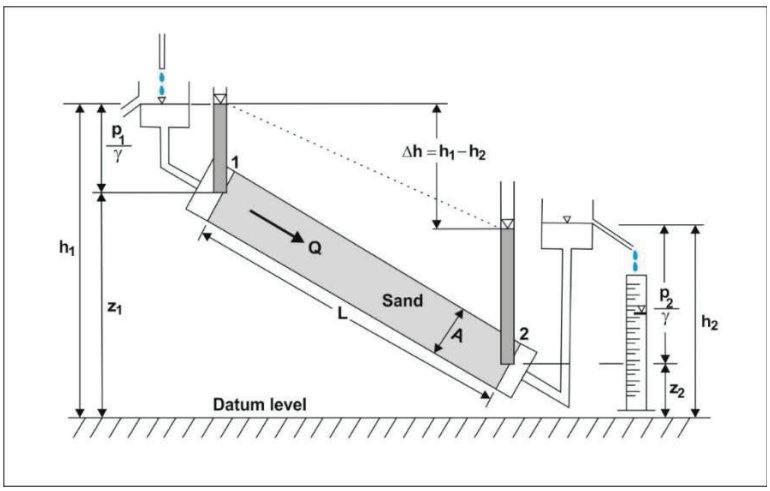

Figure 2.2. Water movement in inclined porous media (Darcy Law)
(Source: Bear and Cheng, 2010)

According to this Darcy's Law can be expressed by the following equation:

$$q = K\frac{\Delta h}{L}A \tag{2.1}$$

Where q is flow rate [L^3 T^{-1}], K is hydraulic conductivity [L T^{-1}], Δh/L is hydraulic gradient [-], A is cross sectional area of soil sample [L^2].

Although Darcy realizes this experiment for porous environments in a simple experimental setup, the Darcy Law with mass conservation equations can be developed more generally for three-dimensional groundwater flows (Figure 2.3).

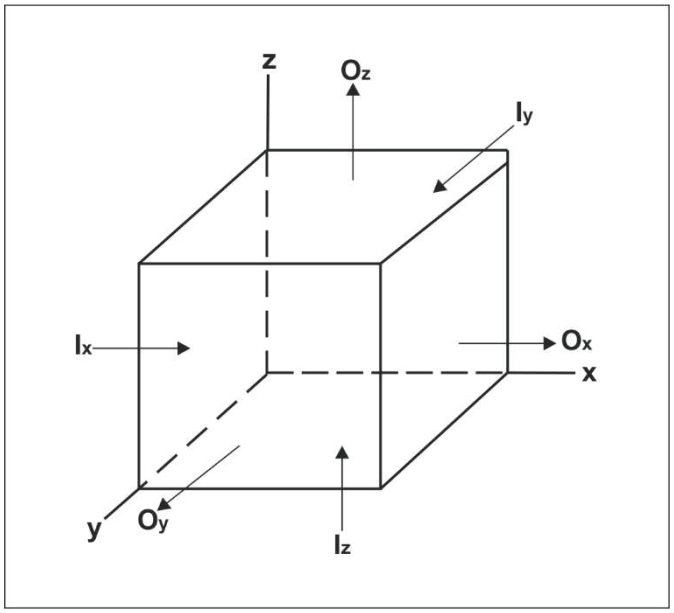

Figure 2.3. Mass conservation for an open system
(Source: Asano, 1985)

Accordingly, the mass conservation equation for an open system with mass inputs and outputs as in Figure 2.3 is expressed as:

$$(I_x+I_y+I_z) - (O_x+O_y+O_z) = \pm\Delta S \tag{2.2}$$

The Darcy's law developed for three-dimensional systems with these mass conservation equations is known as the unsteady-state groundwater flow equation and the

groundwater flow equation for three-dimensional systems is explained by the partial differential equation below.

$$\frac{\partial}{\partial x}\left(K_x \frac{\partial h}{\partial x}\right) + \frac{\partial}{\partial y}\left(K_y \frac{\partial h}{\partial y}\right) + \frac{\partial}{\partial z}\left(K_z \frac{\partial h}{\partial z}\right) = S_s \frac{\partial h}{\partial t} \tag{2.3}$$

Where K_x, K_y and K_z are the hydraulic conductivities along x, y and z axes [L T^{-1}], h is potentiometric head [L], S_s is specific storage for confined aquifer [L^{-1}], t is the time [T]. In Eq. (2.3), $\partial h/\partial t$ will be zero in steady-state conditions where the mass entering and leaving the system is equal and the volume of the system does not change with time. Eq. (2.3) is expressed in terms of the transmissibility of the confined aquifer material with constant thickness by the following partial differential.

$$\frac{\partial^2 h}{\partial x^2} + \frac{\partial^2 h}{\partial y^2} + \frac{\partial^2 h}{\partial z^2} = \frac{S}{T}\frac{\partial h}{\partial t} \tag{2.4}$$

Where T is transmissibility [L^2 T^{-1}].

Eq. (2.4) can also be written for unconfined aquifer. However, Eq. (2.4) has a nonlinear form that cannot be solved for unconfined aquifers (Fancher and Lewis, 1933). Eq. (2.4) can be solved by assuming that unconfined aquifers have small saturated thickness. In this case, Eq. (2.4) can be written by the following partial differential equation:

$$\frac{\partial}{\partial x}\left(K_x b \frac{\partial h}{\partial x}\right) + \frac{\partial}{\partial y}\left(K_y b \frac{\partial h}{\partial y}\right) = S_y \frac{\partial h}{\partial t} \tag{2.5}$$

Where S_y is specific yield of unconfined aquifer [-], b is thickness of unconfined aquifer [L].

2.2.3. Unsaturated Flow

The unsaturated zone forms the portion of the environment that interacts with the air up to the water table. This zone generally consists of three zones such as soil-water

zone, middle zone and capillary zone.

The soil-water zone forms the uppermost layer of the unsaturated zone and is known as the root zone because the vegetation roots of the earth occupy this zone. Due to its close to the earth, it is rich in oxygen and has an effective biological activity. Plant roots rooting in the soil and living species of worms living here form macro pores in the soil. And these plant roots allow the water from precipitation, irrigation or flooding reach the water table through unsaturated zone under the effect of gravity. Most of the evaporation occurs at this zone. In addition, water taken with plant roots is transmitted through atmospheric transpiration through the leaves of plants.

The middle zone is the area between the unsaturated zone and the water table. The infiltration that starts along the soil-water zone continues along the middle zone. The thickness of this zone depends on the depth of the water table. In shallow aquifers, the middle zone is important in deeper aquifers, while the middle zone is not mentioned.

The capillary region is located just above the water table. The term capillarity is not mentioned for the saturated water flows, but for the unsaturated zone, this term is extremely important. Because water molecules have strong gravitational force. These gravitational forces are called cohesion when they are between liquid-liquid molecules and adhesion forces when they are between liquid and solid molecules. The gravitational forces between the water molecules strengthen the withdraw from a water well that opens for pumping or irrigation. The capillary is directly related to the grain size distribution. While the capillary rise is higher in fine grained units, this capillarity is less in coarse grained units.

It has been previously stated that the movement of water in soil intermediate zones is expressed by different differential equations. Accordingly, the Darcy equation (Eq. 2.3) developed for saturated conditions can be expressed in terms of pressure heads (h) in the unsaturated conditions in three dimensions as follows;

$$\frac{\partial}{\partial x}\left[K(\theta)_x \frac{\partial h(\theta)}{\partial x}\right] + \frac{\partial}{\partial y}\left[K(\theta)_y \frac{\partial h(\theta)}{\partial y}\right] + \frac{\partial}{\partial z}\left[K(\theta)_z \frac{\partial h(\theta)}{\partial z}\right] + \frac{\partial}{\partial z}[K(\theta)_z] = \frac{\partial \theta}{\partial t} \qquad (2.6)$$

Where K is hydraulic conductivity [L T^{-1}], θ is water content [-], h is pressure head [L].

2.3. Estimating of Groundwater Recharge

Groundwater recharge estimates can be determined by many different methods.

2.3.1. Numerical Methods

SEEP/W, MODFLOW, SEAWAT and HYDRUS are the most commonly used programs for groundwater recharge and modeling. In this study, HYDRUS-1D program was used.

2.3.1.1. HYDRUS-1D

Numerous numerical programs have been developed for modelling the transport of water, nutrients and chemical elements in soil and groundwater. HYDRUS software programs are the most used modelling programs in these studies (Simunek et al., 2008). There are three different HYDRUS software packages available today such as HYDRUS-1D (Simunek et al., 2005), HYDRUS-2D (Simunek et al., 1999), HYDRUS-2D/3D (Simunek et al., 2006). Despite similar work in all three software, HYDRUS-1D is used for lysimeter, infiltration, one-dimensional problems in soil profile and parcels, HYDRUS-2D and HYDRUS-2D/3D are used to solve two or three-dimensional problems encountered in laboratory and field-scale studies (Simunek et al., 2008).

In general, HYDRUS is a Microsoft Windows based modelling program developed for water flow and dissolution transport analysis in variable saturated porous media. The software package simulates two and three-dimensional movement of water, heat, and multiple solutions in a variable saturated environment. HYDRUS-1D can also be used for the analysis of water and soluble matter in an unsaturated or partially saturated porous medium. HYDRUS can also model flow fields defined by irregular boundaries. The flow field may consist of uniform soils having locale anisotropy. Flow and transmission may occur in a vertical plane, in a horizontal plane, in a three-dimensional region that exhibits radial symmetry about a vertical axis. The water flow region of the model may include boundaries controlled by atmospheric conditions as well as the predicted head and flux boundaries (constant or time varying). The HYDRUS program

numerically solves the Richards equation for a saturated and unsaturated water flow region.

2.3.1.1.1. Governing Equation for HYDRUS-1D

HYDRUS is a computer-based program for numerically solving the Eq. (2.7) developed by Richards (1931) for saturated and unsaturated conditions with transient flow in the soil. The Richards equation is a partial differential equation, and similar equations are used in all HYDRUS model programs (Blonquistet al., 2006). The Richards equation can be solved analytically or numerically using appropriate initial and boundary conditions.

$$\frac{\partial \theta(h)}{\partial t} = \frac{\partial}{\partial z}\left(K(h)\frac{\partial h}{\partial z}\right) + \frac{\partial K(h)}{\partial z} - S(h) \tag{2.7}$$

Where K is hydraulic conductivity [L T^{-1}], θ is water content [-], h is pressure head [L], z is vertical distance [L], t is time [T], S is sink term [L^3 L^{-3} T^{-1}]. The first term explains the effect of capillarity on water movement, while the second term explains the effect of gravity on water movement. As can be seen from the Eq. (2.7), there are two dependent variables: water content and pressure head. These two variables constitute the initial conditions of the Richards equation. The properties of the HYDRUS-1D model program related to soil properties such as water content, pressure head, hydraulic conductivity should be determined.

2.3.2. Chemical Methods

Protecting and sustainability of groundwater is extremely important from a hydrological point of view. Groundwater recharge can be estimated using major-minor anions and isotopes associated with chemical methods. In groundwater recharge studies, the recharge in groundwater basins can be estimated with the help of Chloride Mass Balance method by using chloride ions from major anions.

2.3.2.1. Chloride Mass Balance Method

In areas with high humidity and high temperatures in the world, underground cavities and karstic systems are the areas where significant groundwater recharge occurs (Herczeg et al., 1997). For example, in Europe, where more than 30% of the surface of the terrain is found in karstic systems, most of the drinking water is provided from karst aquifers (Hartmann et al., 2013). Groundwater recharge is a difficult parameter to determine in karstic systems because it involves several variables simultaneously in temporal and spatial scale in water budget studies (Leaney and Herczeg, 1995). So, most researchers have suggested using different techniques in recharge estimation (Alley et al., 2002; De Vries and Simmers, 2002; Scanlon et al., 2002). However, only a few methods can be applied in regional, long-term average recharge estimates. Some of these methods are chloride mass balance method and isotope tracers (Scanlon et al., 2002). Recharge estimates associated with isotope tracers are based on stable and radioactive isotopes. While stable isotopes (^{18}O, ^{2}H) give information about the location of the recharge area and how the groundwater moves during the recharge process, radioactive isotopes (^{3}H, ^{3}He, ^{14}C) provide important information in predicting recharge by aging the groundwater (De Vries and Simmers, 2002; Scanlon et al., 2002). However, recharge estimation using isotope tracers has some disadvantages. Even in developing countries, some scientists have difficulty reaching the laboratories where isotope analysis can be done, and this leads to the loss of data. Therefore, recharge estimation using chemical methods instead of isotope tracers was more favored by researchers. Chloride mass balance method from chemical methods is the most commonly used, simple and low-cost method for predicting groundwater recharge in water budget studies. The chloride mass balance method is usually applied in areas where the groundwater table is close to the surface. The chloride in the pore water begins to condense in the unsaturated region by evaporation and transpiration, and finally reaches the groundwater through horizontal conduction. If vegetation uses water source, chloride may continue evaporation, so the method gives accurate results for groundwater recharge estimation.

The Chloride Mass Balance Method is an alternative method that can be applied to both the vadose zone (Cook et al., 1992; Walker et al., 1991) and the saturated zone (Wood and Sanford, 1995) in the long-term average annual recharge estimates. Chloride Mass Balance Method can be used to estimate the chloride recharge relationship of

groundwater and provide good approaches. When using the Chloride Mass Balance Method, it is recommended that the source of chloride is completely from rainfall and the groundwater is not under the influence of any pollutants (Wood, 2014).

This method is based on the relationship between chloride concentrations in rainwater and chloride concentrations in groundwater samples and can be calculated for the vadose zone by the following equation (Somaratne et al., 2013).

$$R = \frac{([Cl^-]rain \times P)}{[Cl^-]groundwater} \tag{2.8}$$

Where R is the recharge [L T^{-1}], [Cl^-] is the chloride concentrations in rain and groundwater, P is precipitation [L T^{-1}].

2.4. Groundwater Recharge Studies

Grinevskiy and Pozdniakov (2013) studied groundwater recharge estimation using long-term meteorological data with the help of HYDRUS-1D numerical program for a period of 50 years. The study area is located the southwest part of the Moscow Artesian Basin and covers an area of about 49600 km^2. Different soil types and lithological units take place in the study area. During the long winter periods in the basin the temperature varies from 4-5°C on average, so the floor is subjected to intense freezing. At the same time, in the basin which is affected by snow during the winter season, there is a runoff originating from snow water.

In order to estimate the recharge of the groundwater in the basin, the meteorological data (precipitation, evaporation), water content values and hydraulic conductivity values of the inputs of the HYDRUS-1D numerical program are calculated. According to the results of these numerical calculations, researchers have found that the lithological units forming the soil in the basin have importantly changing groundwater recharge values. Researchers have attributed this difference to the fact that there is recharge even in areas where snow is not melting in the basin. In addition, it has been reported that the lithological units forming the basin have different hydraulic conductivity values and are among the factors affecting recharge.

De Silva (2015) estimated the groundwater recharge using HYDRUS-1D numerical model and compared the results of this model with the Water Table Fluctuation (WTF) method to determine the optimal method for the study area. Thirunelvely where is located Jaffna Peninsula in Sri Lanka is the study area. It represents an area where agricultural areas exist and groundwater is used for domestic purposes. At the same time, because study area is a dense agricultural area, the nitrogen fertilizer used by the farmers in the region threatens the quality of the groundwater. The meteorological data such as precipitation, evaporation and temperature were obtained meteorological stations located in the Jaffna Peninsula to estimate the groundwater recharge in the study. Mualem (1976) and Van Genuchten (1980) hydraulic properties are used as another input parameter of the HYDRUS-1D numerical program. Finally, the numerical model is obtained by establishing the initial and boundary conditions of the model.

In the Water Table Fluctuation method (WTF), groundwater level monitoring was performed during January 2007 and December 2008 periods by using groundwater level monitoring devices to note withdrawn and elevations in the water table in a total of 20 wells. As a result, the HYDRUS-1D numerical program is the result that it is more convenient to use the numerical model because it is a program that can be used not only for groundwater flow but also for solving problems such as chemical transport and heat transfer.

Lu et al. (2011) developed a numerical model for predicting groundwater recharge in the Hebei Plain in China. Agricultural areas are the economic development of the study area. Most of the water in the study area is supplied from the groundwater. The growing population in the last few centuries and consequently the increasing agricultural land has significantly increased the use of groundwater and has become a threat to water resources in the study area. The aim of the study is to perform effect of water table on groundwater and to examine recharge values associated with irrigation in the agricultural areas. At the same time, the researchers decided to use the chemical method in addition to the numerical model to decide which method would be more suitable for the region. In order to simulate groundwater recharge, vadose zone hydrological properties and meteorological data were determined. Water content values of the aquifer and groundwater level monitoring were conducted over a 2-year period from 2003 to 2005. According to the results of the numerical model, the researchers obtained different recharge values depending on the depth of the water table and therefore the thickness of

the vadose in different sections of the study area. When comparing these results with the chemical method, they reached the result that the numerical model is more suitable. Finally, researchers mentioned some limitations of the numerical model in their work. In numerical modelling calculations, it has been reported that parameters such as climate data, soil physical and chemical properties should be based on a long cycle.

Luijendijk and Bruggeman (2008) determined the pumping rates from the basin in the Jabal Al Hass region, which is semi-arid climatic in Northwest Syria, and carried out the groundwater recharge using the chloride mass balance method from chemical methods. This area has been selected as the study area since there has been a decrease of about 23 m in water levels due to the increase of agricultural areas in the last 30 years. During June-September 2004, major-minor anion and cation studies were carried out on a total of 44 groundwater samples using groundwater level monitoring methods and water quality methods. In addition, the acidity level of the samples was determined by using the Gran titration method in these wells ranging from 20 to 225 m in depth. In 2001-2002 and 2002-2003, a total of 2 periods of water sampling were carried out to determine the amount of chloride in rainwater. The researchers also calculated the net pumping rates in the basin to determine the return flow from the irrigation. According to the results obtained, the pumping rates have increased twice since 1980. As a result, some authorities have discussed the impact of pumping rates on the sustainability of groundwater, while others have reported that chemical methods alone are not sufficient in groundwater recharge studies.

Anuraga et al. (2006) conducted a groundwater recharge study in Bethamangala, India. The study area covers an area of 177 km^2 and is located in an arid-semi-arid climate region with a maximum temperature of 28°C, which is measured even in December. The most important problem in the study area is that the livelihood of the population constitutes the agricultural areas and accordingly the water resources in the basin are threatened by the water withdrawal. The researchers used the 1-Dimensional SWAP model to perform the recharge study in the region. For this purpose, researchers performed a water level monitoring study for a total of 21 years long period between 1978 and 1999 in the observation wells at 5 different points in the basin. At the same time, hydraulic properties were determined for 6 different types of soil in the study area. According to the results of the simulation, the average recharge value for 6 different soil

types was found to be 155.66 mm/year. As a result, researchers have stated that soil type and agriculture-based irrigation and withdrawal are an important influence on recharge, and that the increase in irrigation areas may decrease recharge values in future periods.

CHAPTER 3

METHODOLOGY

3.1. Study Area

Gediz Basin is one of the most important basins covering about 2% of Turkey. Alaşehir sub-basin, which is a study area, is located in the south-eastern part of Gediz basin and constitutes 15.81% of the basin (Figure 3.1). The Alaşehir sub-basin is 140 km long and 15 km wide between Alaşehir and Salihli in the northwest-southeast direction. The total drainage area of Alaşehir sub-basin is 2710.51 km^2 and the sub-basin has a very wide area. The Büyük Menderes Basin is located to the south of Alaşehir sub-basin. To the north is the upper basin, which is another sub-basin of the Gediz Basin and the drainage area of the Demirköprü Dam. Altitude of the Alaşehir sub-basin, which is typical depression basin ranges from 83 m to 2155 m from the sea level. The upper parts of the basin are surrounded by Bozdağ and Seyran mountains. The study area is the industrial city and the region where agricultural irrigation is made extensively. The water used for agricultural irrigation is provided from the groundwater in the basin, to the Avşar Dam in the west of the basin and from the Derbent Dam in the south.

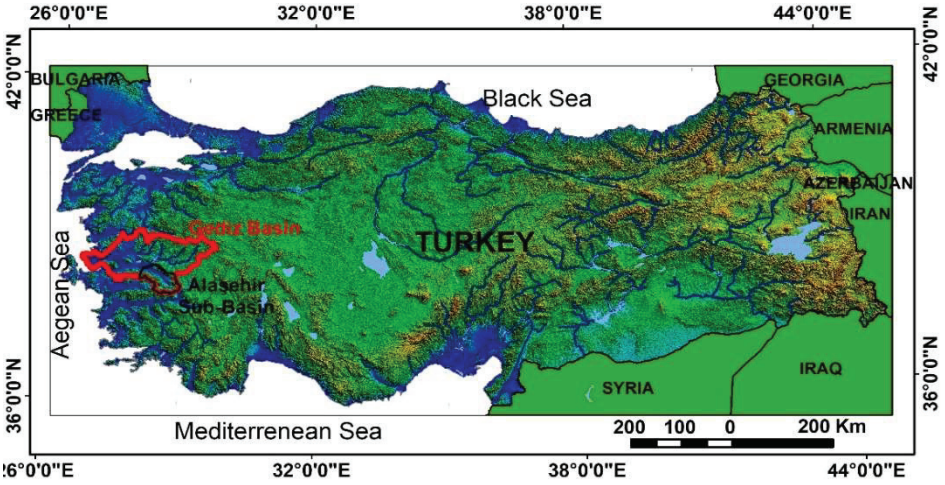

Figure 3.1. Location map of study area

3.2. Research Well

In order to define the alluvium aquifer lithology of the study area, a total depth of 1080 m research wells were drilled at 25 points (SK-1 to SK-25) (Figure 3.2). These drills used to determine the hydraulic properties of the vadose zone. The depth of the research wells ranges from 20 m to 50 m. It has been noted that research wells are far from the pollutant effect in the choice of location. At the same time, it is extremely important that research wells correctly reflect the properties of the alluvium aquifer in the study area. At some points in the drillings, block and gravel soils were encountered and location changes were made. Because, block and gravel soils are easily dispersible units. Although this important point has been noted, block and gravel units were encountered in the wells of SK-6 and SK-9 during drilling. All lithological properties of these well were determined and long-term groundwater level monitoring studies were carried out in the study area.

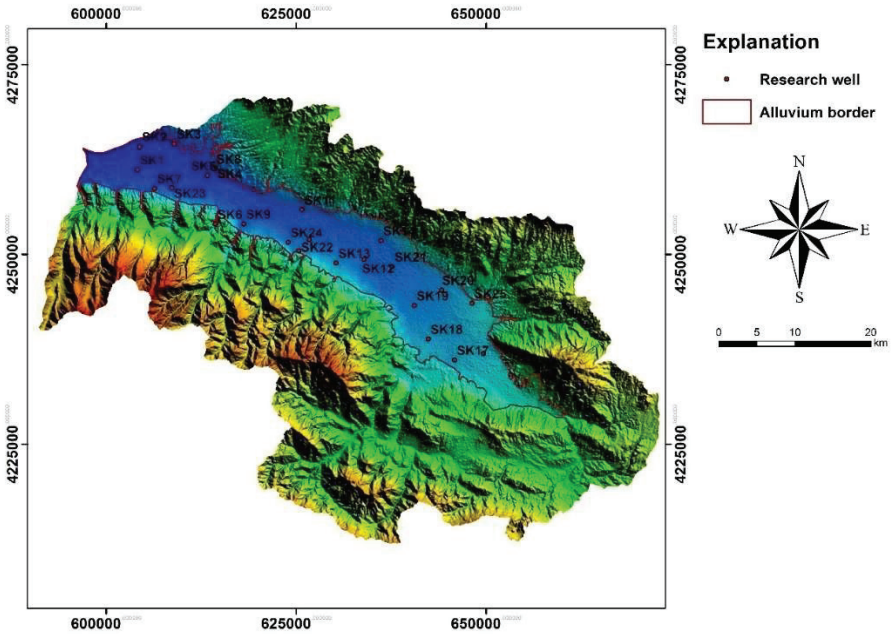

Figure 3.2. Research wells in the study area

3.3. Investigation of Alluvium Aquifer

Characterization of the alluvium aquifer in the study area was carried out by establishing laboratory and field studies.

3.3.1. Laboratory Studies

In the laboratory, soil hydraulic properties of the alluvium aquifer were determined.

3.3.1.1. Water Content and Specific Gravity

Water content experiments are one of the first experiments in the laboratory in core samples taken from research wells. Particularly, in order to find out the amount of water that is infiltrated directly from the precipitation, the results of the water content of the soils are needed. The water content is a parameter that can vary with time because it is indexed to precipitation and can be calculated by Eq. (3.1).

$$\theta = \frac{\theta_{wet} - \theta_{dry}}{\theta_{dry}} \times 100 \tag{3.1}$$

In addition, in the drilling samples in the laboratory, the specific gravity (G_s) of the soil samples was also determined. For this, firstly the dry density (γ_{dry}) values of the samples were calculated using Eq. (3.2), then the specific weights were found using Eq. 3.3.

$$\gamma_{dry} = \frac{\gamma}{(1 + \theta)} \tag{3.2}$$

$$G_s = \frac{(1 + e) \times \gamma_{dry}}{\gamma_{water}} \tag{3.3}$$

Where e is void ratio [-], γ is density [M L^{-3}] (γ_{water} = 1000 kg/m^3). The specific gravity experiment was carried out to check whether the water saturation rates are in contradiction to the natural condition of the soil. To illustrate, it is expected that the percentage of water saturation of a soil below the groundwater level (saturated zone) will be around 100%. However, in case of not obtaining values close to these values as the result of the experiment, the experiments were performed again and progress was made in a controlled

manner. Water content (θ) and specific gravity (G_s) results of the research wells were presented in Appendix A.

3.3.1.2. Porosity

The porosity, which is defined as the total volume ratio of the void volume, can be found with the help of Eq. (3.4). Porosity is one of the properties that reflect the void condition of the soil. The porosity is expressed in decimal or percentage.

$$n = \frac{V_{void}}{V_{total}} \tag{3.4}$$

Where, n is the porosity [-] and V is the volume [L^3]. In the study, porosity value could not be obtained in some depths due to lack of sample or inability to take appropriate sample. To illustrate, porosity could not be determined in gravel units which cannot protect its volume. Therefore, hydraulic parameters such as density, natural mass, void ratio and specific gravity could not be obtained during these depths. Porosity values were calculated in appropriate depths and spatial distribution map of porosity was established. Porosity results of the research wells were presented in Appendix A.

3.3.1.3. Sieve Analysis

The aquifer soil properties affect the permeability, porosity and hydraulic parameters of the aquifer and thus control the recharge rate. In this context, sieve analysis has been carried out in order to classify the soil on the core samples taken from research wells in alluvium aquifer in the study area. The aim here is to determine how the coarse and fine-grained soils of the alluvial material in the study area present variability. With this method, the samples were passed through a series of standard sieve with different size openings in the laboratory and the weight percentages of the grades between the different sizes were determined. In the scope of sieve analysis, 4, 10, 20, 40, 100 and 200 grade sieves were used. There are many soil classification criteria such as the Triangular Classification System (USDA) proposed by today Coduto (1999), the Unified Soil

Classification System (USCS), the Turkish Standard Soil Classification System (TS 1500) and the British Standard Soil Classification System (BS 5930). USCS soil classification criterion, shown in Table 3.1, was used in the soil classification according to the results of the sieve analysis carried out in the laboratory. According to the USCS soil classification given in Table 3.1, the (W) and (P) symbols were used respectively for well graded or poorly graded coarse soils according to grain size distribution. In mixed soil groups such as clayey sand, silty sand, clayey gravel and silty gravel, double symbols such as (SC), (SM), (GC) and (GM) were used respectively.

As can be seen from Table 3.1, No. 4 sieve provides the determination of sand and gravel soils. If the sample remaining on the No. 4 sieve is more than 50%, it is named as gravel soil and less than 50% is called as sandy soil.

No. 200 sieve provides the determination of coarse and fine-grained soils. If the sample remaining on the No. 200 is more than 50%, soil is called coarse-grained soil and less than 50% is called fine-grained soil. In addition, it is expressed as clean gravel (GW-GP) if less than 5% of the remaining sample is in the No. 200, and as gravel with fines (GM-GC) between 5% and 15%. If less than 5% of the sample passing through the No. 200 is called clean sand (SW-SP) and between 5% and 15% is called sand with fines (SM-SC).

Table 3.1. Unified Soil Classification System (USCS) (Source: Standard, 2011)

Major Divisions			Group Symbol	Typical Names
Coarse-Grained Soils More than 50% retained on the 0.075 mm (No. 200) sieve	Gravels 50% or more of course fraction retained on the 4.75 mm (No. 4) sieve	Clean Gravels < %5	GW	Well-graded gravels and gravel-sand mixtures, little or no fines
			GP	Poorly graded gravels and gravel-sand mixtures, little or no fines
		Gravels with Fines > %12	GM	Silty gravels, gravel-sand-silt mixtures
			GC	Clayey gravels, gravel-sand-clay mixtures
	Sands 50% or more of course fraction passes the 4.75 (No. 4) sieve	Clean Sands < %5	SW	Well-graded sands and gravelly sands, little or no fines
			SP	Poorly graded sands and gravelly sands, little or no fines
		Sands with Fines > %12	SM	Silty sands, sand-silt mixtures
			SC	Clayey sands, sand-clay mixtures

(cont. on next page)

Table 3.1. (cont.).

Fine-Grained Soils More than 50% passes the 0.075 mm (No. 200) sieve	Silts and Clays Liquid Limit 50% or less	ML	Inorganic silts, very fine sands, rock four, silty or clayey fine sands
		CL	Inorganic clays of low to medium plasticity, gravelly/sandy/silty/lean clays
		OL	Organic silts and organic silty clays of low plasticity
	Silts and Clays Liquid Limit greater than 50%	MH	Inorganic silts, micaceous or diatomaceous fine sands or silts, elastic silts
		CH	Inorganic clays or high plasticity, fat clays
		OH	Organic clays of medium to high plasticity
Highly Organic Soils		PT	Peat, muck, and other highly organic soils
Prefix: G = Gravel, S = Sand, M = Silt, C = Clay, O = Organic			
Suffix: W = Well Graded, P = Poorly Graded, M = Silty, L = Clay, LL < 50%, H = Clay, LL > 50%			

According to this, sieve analysis was performed with enough core samples and a soil class distribution map was created for the study area.

3.3.2. Field Studies

In the field studies, meteorological data, groundwater monitoring studies and water sampling studies were carried out.

3.3.2.1. Weather Stations

Three weather stations were installed Yeşilova (MT-1), Alhan (MT-2) and Çavuşlar (MT-3) regions (Figure 3.3). The meteorological data such as the amount of precipitation, wind direction and speed, humidity, air temperature were measured from these stations. All three stations have a data bank that records data every one hour and was set to measure the same parameters at the same time intervals. Stations belonging to the General Directorate of State Hydraulic Works (DSİ) and the General Directorate of Meteorology, which are located in the basin, were taken into consideration in the location selection of the stations. The weather stations were positioned at high points such as the house roof and the top of the shack so that they are not damaged. All three weather stations represent the nearby research well.

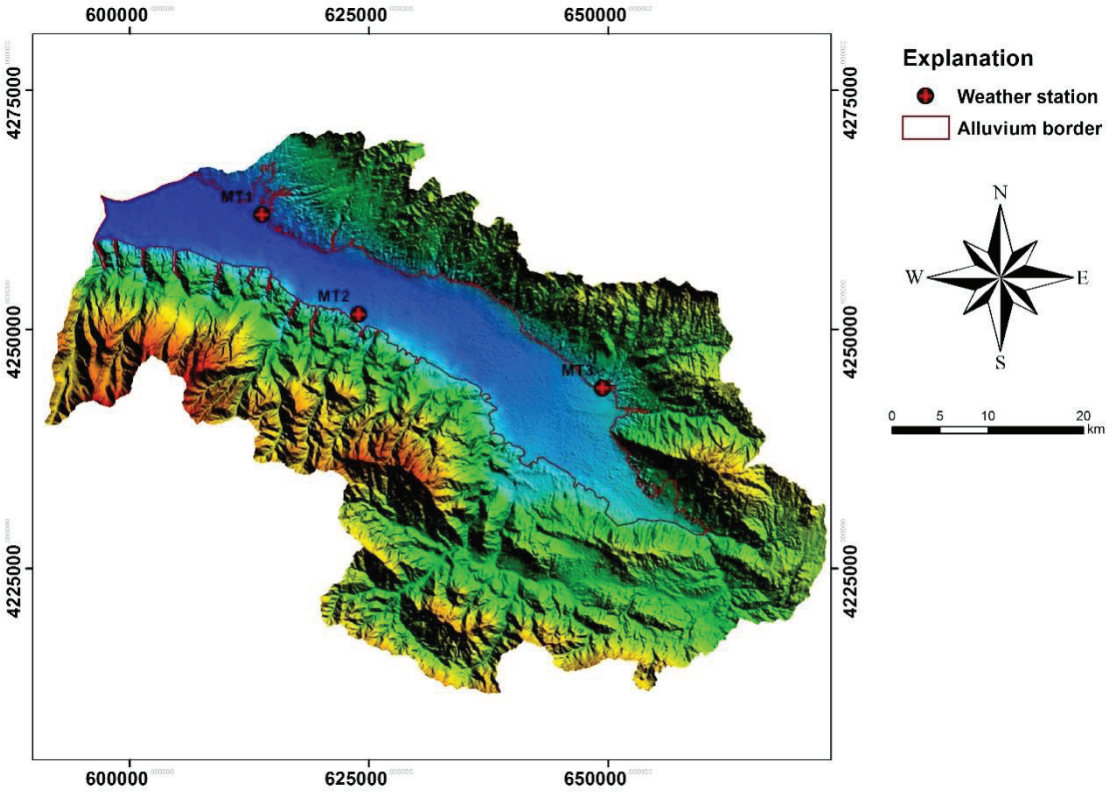

Figure 3.3. Location of weather stations

From July 16, 2016 to July 31, 2017, meteorological data were collected from these weather stations on a regular basis for one year. The daily temperature and precipitation change graphics for all three weather stations are presented in Figure 3.4 to Figure 3.6. At the same time, using Thornthwaite method, potential evapotranspiration (PET), actual evapotranspiration and runoff values of Alaşehir sub-basin were determined by using monthly average temperature values obtained from weather stations.

3.3.2.1.1. Thornthwaite Method

The Thornthwaite method is one of the methods developed to determine the amount of evaporation in drainage basins. This method is based on empirical methods derived from precipitation for many drainage basins and potential evaporation values can be found with Eq. (3.5) (Thornthwaite, 1948).

$$PET = 1.6 \times (10T/I)^{a} \tag{3.5}$$

$$a = 6.7 \times 10^{-7} \times I^3 - 7.7 \times 10^{-5} \times I^2 + 1.8 \times 10^{-2} \times I + 0.49 \quad (3.6)$$

Where T is monthly mean temperature (°C), I is the heat index value at the given average temperature, a is the exponent defined as the function of the heat index. Thornthwaite (1948) noted that a long-term meteorological data is needed in this method, which is widely used in climate classification of any region. Monthly mean temperature values for the Alaşehir sub-basin were monitored from data obtained from meteorological stations for one year (Figure 3.4 to Figure 3.6). The heat index values corresponding to the obtained average monthly temperature values were obtained from the Thornthwaite heat index table (Table 3.2).

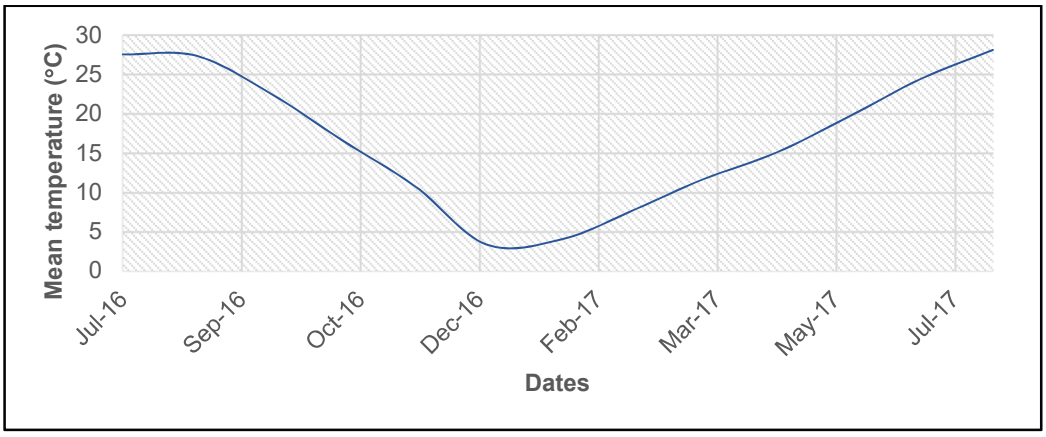

Figure 3.4. Monthly mean temperature change graph of Yeşilova (MT-1) weather station for one year

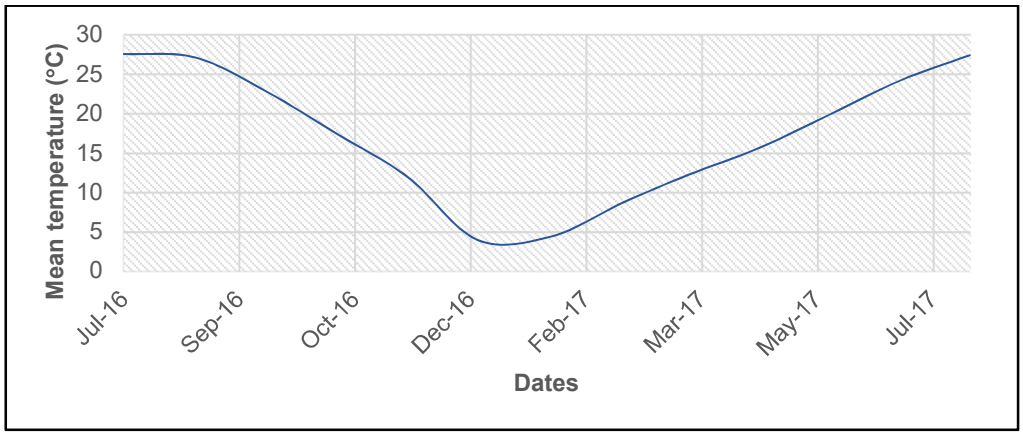

Figure 3.5. Monthly mean temperature change graph of Alhan (MT-2) weather station for one year

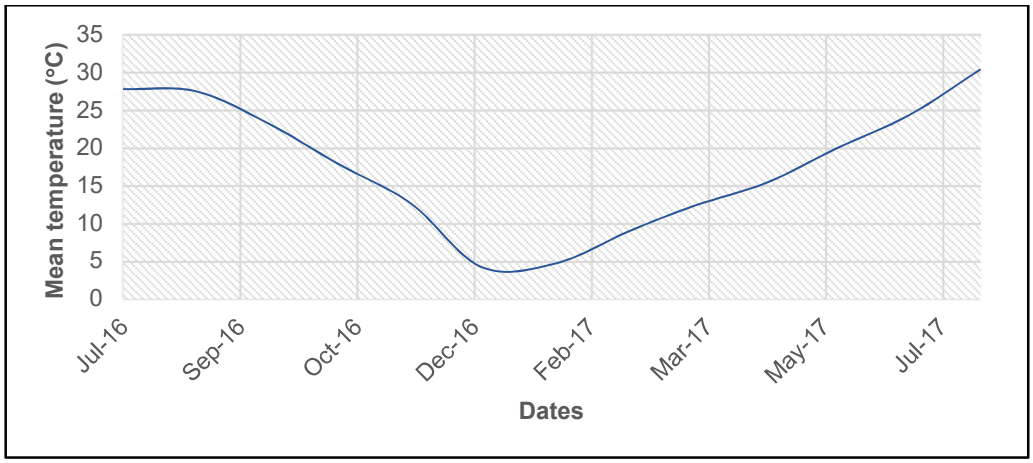

Figure 3.6. Monthly mean temperature change graph of Çavuşlar (MT-3) weather station for one year

The heat index values corresponding to the average monthly temperature values are presented in Table 3.3. Sunshine periods for the Alaşehir sub-basin were obtained from the Ministry of Energy and Natural Resources website (E.İ.E, 2017). The monthly average temperature values in Table 3.3 are average values obtained from all three meteorological stations.

Table 3.2. Heat index values calculated by Thornthwaite (Source: Thornthwaite, 1948)

Temperature (°C)	0	0.1	0.2	0.3	0.4	0.5	0.6	0.7	0.8	0.9
0	0	0	0.01	0.01	0.02	0.03	0.04	0.05	0.06	0.07
5	1.00	1.03	1.06	1.09	1.12	1.16	1.19	1.22	1.25	1.28
10	2.86	2.90	2.94	2.99	3.03	3.07	3.12	3.16	3.21	3.25
15	5.28	5.33	5.38	5.44	5.49	5.55	5.60	5.65	5.71	5.76
20	8.16	8.22	8.28	8.34	8.41	8.47	8.53	8.59	8.66	8.72
25	11.44	11.50	11.57	11.64	11.71	11.78	11.85	11.92	11.99	12.06
30	15.07	15.15	15.22	15.3	15.38	15.45	15.53	15.61	15.68	15.76
35	19.03	19.11	19.20	19.28	19.36	19.44	19.53	19.61	19.69	19.78
40	23.30	23.38	23.47	23.56	23.65	23.74	23.83	23.92	24.00	24.09

These values were then multiplied by the latitude correction coefficient according to the sunshine hours and the geographical latitude of the study area, and the potential

evapotranspiration values for the Alaşehir sub-basin were calculated. From this, actual evapotranspiration and runoff values were obtained for the study area.

Table 3.3. Monthly mean temperature and heat index values of the Alaşehir sub-basin

Months	Mean Temperature (°C)	Heat Index (I)	Sunshine Hours (h)	Latitude Correction
January	4.4	0.82	4.6	0.85
February	8.5	2.23	5.45	0.84
March	12	3.76	6.57	1.03
April	15.4	5.49	7.62	1.10
May	19.8	8.03	9.49	1.23
June	24.4	11.02	11.32	1.24
July	27.6	13.28	11.77	1.25
August	27.3	13.07	11.06	1.17
September	22.9	10.01	9.26	1.04
October	17.3	6.55	7.11	0.96
November	11.7	3.62	5.22	0.84
December	3.8	0.66	3.94	0.83

3.3.2.2. Groundwater Monitoring

Groundwater levels are affected by many factors such as precipitation, evaporation, irrigation and pumping. The changes in groundwater level are one of the most important parameters reflecting the properties of alluvium aquifer. Long-term monitoring of groundwater level changes is needed in studies on the sustainability of water resources such as recharge of groundwater. For this purpose, groundwater level monitoring methods were carried out in the research wells of the study area using both level recorders called diver and manually (Figure 3.7). Thirteen data loggers and two barometric air pressure recorders (Baro diver) were installed in the research wells. Baro divers were placed in Piyadeler and Taytan wells. The Baro diver is a device that gives its own water head and air pressure as a total pressure value in cm-H_2O. In this study, the Baro diver was compensated with diver (data logger) and used to find hydraulic head.

The salinity and temperature values in the groundwater were measured in the field with the Hach-Lange HQ40D multi-parameter probe.

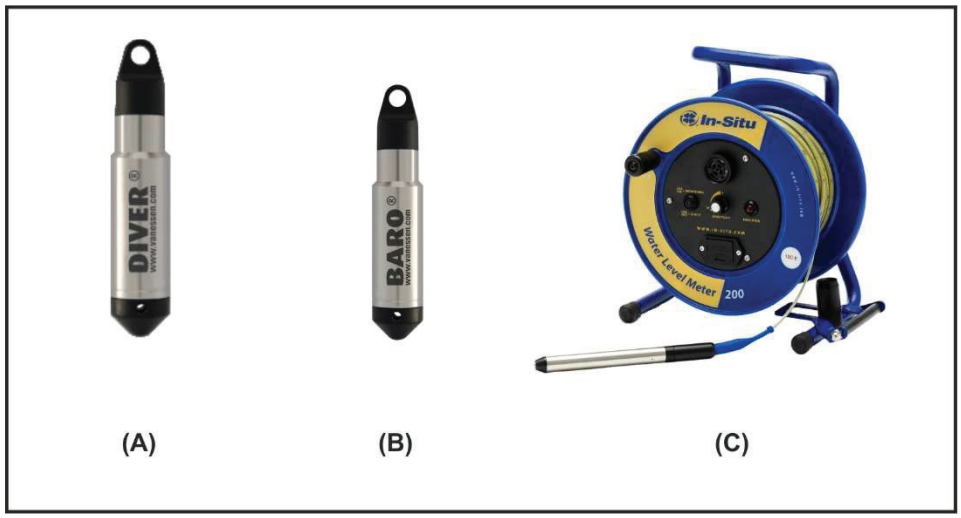

Figure 3.7. Groundwater level monitoring devices. (A) Diver (data logger), (B) Baro diver, (C) Water level meter (manual meter)

3.3.2.3. Hydraulic Conductivity

Hydraulic conductivity is a measure of the water transmission capacity of soils. Hydraulic conductivity is a parameter that can be determined in the laboratory and in the field. Permeability tests in the laboratory are carried out with constant level permeability tests on coarse grained soils, while falling level permeability tests are applied on fine grained units such as sand and clay. In the field, hydraulic conductivity can be calculated from pumping test (withdrawal water from soil) and borehole tests (sending water to soil). In this study, hydraulic conductivity values were obtained by borehole tests in the field.

3.3.2.3.1. Borehole Test

A falling level permeability test was performed by using sealing elements in boreholes opened in the field. The application of the falling level permeability test is schematically shown in Figure 3.8. Sealing elements were used in the research wells each having a diameter of 89 mm.

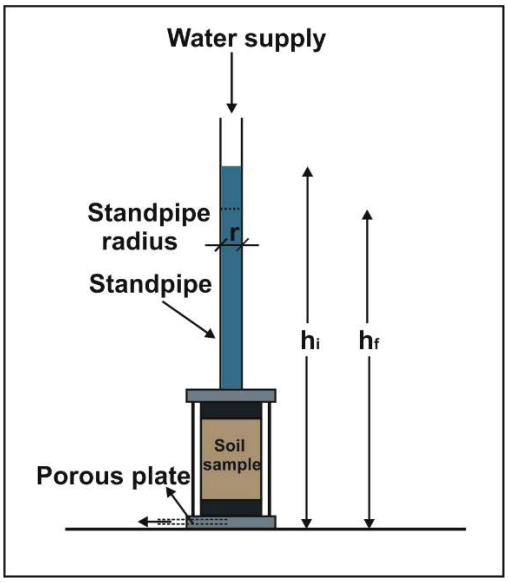

Figure 3.8. Schematic representation of falling level permeability test

With 1 min, 5 min and 10 min time intervals, clean water was sent at 1.67×10^{-5} m^3/s, 4.3×10^{-6} m^3/s and 2.8×10^{-6} m^3/s, respectively. Subsequently, the descents of the water levels were recorded, depending on the time in the wells. The water heights at the beginning and end of the experiment were determined after the steady flow was obtained. According to the obtained data, the hydraulic conductivity values for units belonging to the vadose zone in each well were calculated using Eq. (3.7). Then, the permeability values of the lithological units in the vadose zone for 1 min, 5 min and 10 min time intervals were obtained. Finally, the averages of the permeability values were taken for these time intervals.

$$K = \frac{q}{5.5 \times r \times \Delta h} \tag{3.7}$$

Where q is the constant flow rate [$L^3\ T^{-1}$], r is the inner radius of standpipe [L], Δh is the difference in water levels [L] ($h_f - h_i$). In the study area, different soil groups were obtained in the vertical direction and it is represented in Figure 3.9 schematically. In this context, the vertical permeability values in the vadose zone for each research well were determined using Eq. (3.8) for the hydraulic conductivity values of the research wells in the study area.

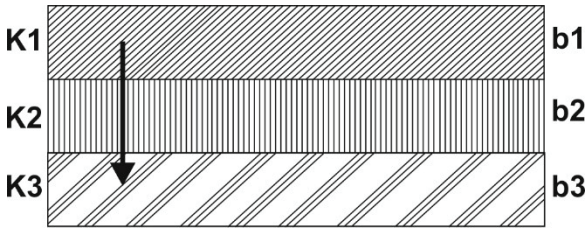

Figure 3.9. Schematic representation of different soil groups in the vertical direction

$$K_v = \frac{b_1 + b_2 + b_3}{\sum_{m=1}^{n} \frac{b_m}{K_m}} \tag{3.8}$$

Where K_v is the vertical permeability value [L T^{-1}], b is the thickness of lithological units in the vadose zone [L]. Based on these values, the permeability distribution map for the study area was established.

3.3.2.4. Water Sampling

The physical and chemical properties of the groundwater samples were measured in the wells.

Physical parameters such as water temperature, pH and electrical conductivity were determined in the area. The measurements were done with the Hach-Lange HQ40D multi-parameter probe. The probes used were cleaned by washing with pure water before and after each measurement to avoid interference between measuring points.

In order to determine the chemical parameters, water sampling studies were carried out in May 2017 and September 2017 respectively, in order to represent the wet and dry periods from the research wells. In addition, rainwater was taken from the Hacıaliler, Alaşehir and Alhan villages and attention has been paid to ensuring that the sampling was done correctly so that the water samples can accurately reflect the quality conditions at the points where they are taken. During water sampling, 100, 250 and 1000 ml volumes of high density polyethylene (HDPE) sampling bottles with leak-proof lids were used. Sample bottles were washed at least twice with the waters to be sampled before filling. All samples were filled with no air in the bottles. Hydrochloric acid (HCI) was added to prevent the minerals from sticking to the bottle before the bottles were closed.

The samples were stored at +4°C in a refrigerator. 250 ml for basic anions and cations, 100 ml leak-proof HDPE bottles for heavy metals were used. Heavy metals analysis was done in international laboratory (ALS Chemex-Canada). Major anion and cation were measured in Dokuz Eylül University. The results of major anion and cation evaluated both in the Piper and Wilcox diagrams and the dominant water types in the study area were determined. In addition, by using chloride concentration results, groundwater recharge values were obtained for the wet and dry period by Chloride Mass Balance Method.

CHAPTER 4

RESULTS AND DISCUSSIONS

4.1. Hydraulic Parameters of Alluvium Aquifer

In this section, alluvium aquifer soil hydraulic properties such as water content, porosity, soil classification and hydraulic conductivity are mentioned.

4.1.1. Water Content Values

The samples obtained from the drillings in 25 research wells within the study area were subjected to the water content test in the laboratory. The water content values were calculated with the help of Eq. (3.1) in every 0.5 meters in the samples taken from the research wells. In addition to the porosity, the specific gravity and natural mass of the samples were also determined using Eq. (3.3). Water contents, specific gravity and natural mass values were not calculated and/or very low water content values were obtained at depths where the soil consist of gravel and blocks of coarse-grained materials. Suitable samples could not be obtained in order to be able determine the hydraulic parameters from the research wells SK-24 and SK-25 in the field and other hydraulic parameters including water content could not be determined in these wells thereof. The results of the water content obtained during the well depth for all research wells are given in Appendix A. Since the SK-6 and SK-9 wells were wells opened to the side of the river, gravel and block sized coarse grains were found during drilling and average water content values in these wells were found as 6.72% and 3.50% during vadose zone, respectively. The reason for the low water content in these wells is that they have scattered samples that cannot protect the volume. In general, it is observed that the water content of the coarse-grained materials (GC, GM, SC and SM) in the alluvium aquifer in the study area is lower than the fine-grained materials (CL, ML). It is also seen that water content values are variable in time and depth due to being indexed to precipitation (Appendix A). In this context, the water content distribution map was not prepared because the spatial interpretation is not very meaningful in water content.

4.1.2. Porosity Values

The porosity values of the samples taken from the research wells were calculated using Eq. (3.4). In determining the porosity values, a calculation was made at every 0.5 m depth at which the porosity can be calculated as values in water content and the porosity results for all research wells were given in Appendix A. Porosity values of SK-6, SK-8, SK-9, SK-15, SK-16, SK-22, SK-23, SK-24 and SK-25 were not determined because of not obtaining appropriate samples for porosity experiment with drilling. In order to create porosity distribution map in the remaining wells, arithmetic mean porosity values were calculated during well depth (Table 4.1). Finally, a porosity distribution map was established using alluvium aquifer arithmetic mean porosity values (Figure 4.1).

Table 4.1. The mean porosity values of the research wells

Well ID	x	y	z	Depth (m)	Location	Mean porosity
SK-1	604121	4261160	88	30	Karaoğlanlı	0.38
SK-2	604422	4264194	101	30	Taytan	0.45
SK-3	608939	4264553	97	50	Durasallı	0.39
SK-4	614316	4261311	121	50	YeşilovaTepe	0.43
SK-5	613324	4260377	105	30	YeşilovaMera	0.41
SK-7	606376	4258683	131	50	Kabazlı	0.35
SK-10	626711	4251955	148	50	Piyadeler	0.36
SK-11	625770	4255886	125	50	Toygarlı	0.47
SK-12	633947	4249342	143	50	Baklacı	0.4
SK-13	630254	4248858	101	50	Akkeçili	0.39
SK-14	636158	4251807	148	50	Tepeköy	0.46
SK-17	645856	4236078	188	50	Ahmetağa	0.42
SK-18	642390	4238848	195	50	Haceli	0.38
SK-19	640552	4243264	170	50	Sobran	0.46
SK-20	644149	4245284	170	50	Yeşilyurt	0.43
SK-21	637643	4248393	145	50	Ilgın	0.44

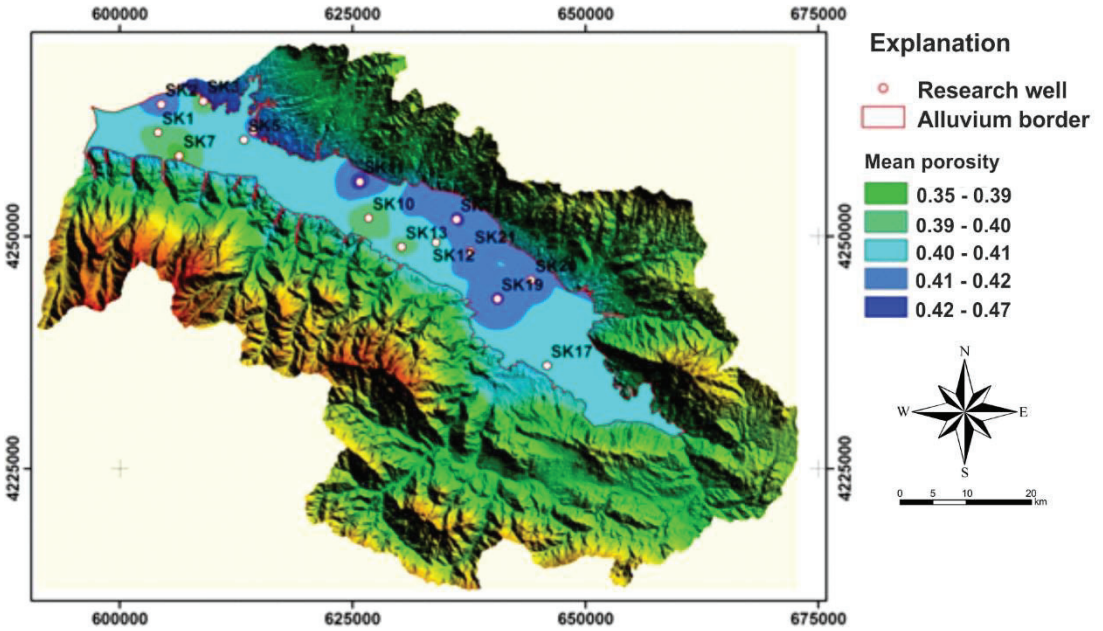

Figure 4.1. Alluvium aquifer mean porosity distribution map

According to the mean porosity distribution map of the alluvium aquifer, especially the northeastern part of the area, porosity values of the soils of fine sand and clay levels are change between 0.41 and 0.47. The porosity values of the alluvium aquifer are generally found to be in the range of 0.40 (Figure 4.1). The porosity distribution map created indicates the mean of the porosities obtained from the drilling. According to the vertically changing soil class, porosity values vary. Figure 4.1 shows that north of the study area has high porosity.

4.1.3. Soil Classification

Sieve analyses were performed in the laboratory from the samples that can be taken as appropriate samples from the research wells. USCS soil classification criterion was used to evaluate the soil classification of the study area (Table 3.1). According to the sieve analysis results, different soil groups were obtained at different depths along the depth of the research wells (Appendix A). This situation makes it difficult to form an alluvium aquifer soil classification distribution map. For this, it was generally considered that the handling of the dominant soil group along the depth of the well will be a more accurate approach to the evaluation. Prior to the generation of the soil classification distribution map, dominant soils were determined at the total depth of the research wells

and dominant soil groups were established for each well (Table 4.2). According to the results obtained, a soil classification distribution map of the alluvium aquifer was prepared (Figure 4.2).

Table 4.2. Dominant soil class values of research wells

Well ID	x	y	z	Depth (m)	Location	Dominant soil
SK-1	604121	4261160	88	30	Karaoğlanlı	GC-SC
SK-2	604422	4264194	101	30	Taytan	SC
SK-3	608939	4264553	97	50	Durasallı	CL-SC
SK-4	614316	4261311	121	50	Yeşilova Tepe	CL-ML
SK-5	613324	4260377	105	30	Yeşilova Mera	GC-ML
SK-7	606376	4258683	131	50	Kabazlı	GC-SC
SK-8	614192	4261269	115	50	Hacılı	GC
SK-10	626711	4251955	148	50	Piyadeler	SC
SK-11	625770	4255886	125	50	Toygarlı	SC-CL
SK-12	633947	4249342	143	50	Baklacı	CL
SK-13	630254	4248858	101	50	Akkeçili	GC
SK-14	636158	4251807	148	50	Tepeköy	SC-CL
SK-17	645856	4236078	188	50	Ahmetağa	SC
SK-18	642390	4238848	195	50	Haceli	GP
SK-19	640552	4243264	170	50	Sobran	CL
SK-20	644149	4245284	170	50	Yeşilyurt	SC
SK-21	637643	4248393	145	50	Ilgın	SC
SK-22	625345	4250473	171	50	Piyadeler	GC-GP
SK-23	608633	4258773	117	50	Yeşilkavak	GP

According to the general geological structure and sediment transport mechanism of the study area, it is observed that generally the regions near to the high topography areas are dominated by coarse grained soils, whereas those with flat or low topography are dominated by fine grained soils (Figure 4.2). In the south eastern part where the

topography has lower slope, it is seen that fine sandy soils predominate, whereas in the western part of the area and high slope areas it is seen that the gravel sized soils dominate. It is clear that in the central parts of the area fine grained soils dominate (Figure 4.2). This distribution also coincides with the permeability distribution values of the aquifer material. Soil class distribution map is extremely important for the investigation of the characterization of the aquifer and the groundwater recharge.

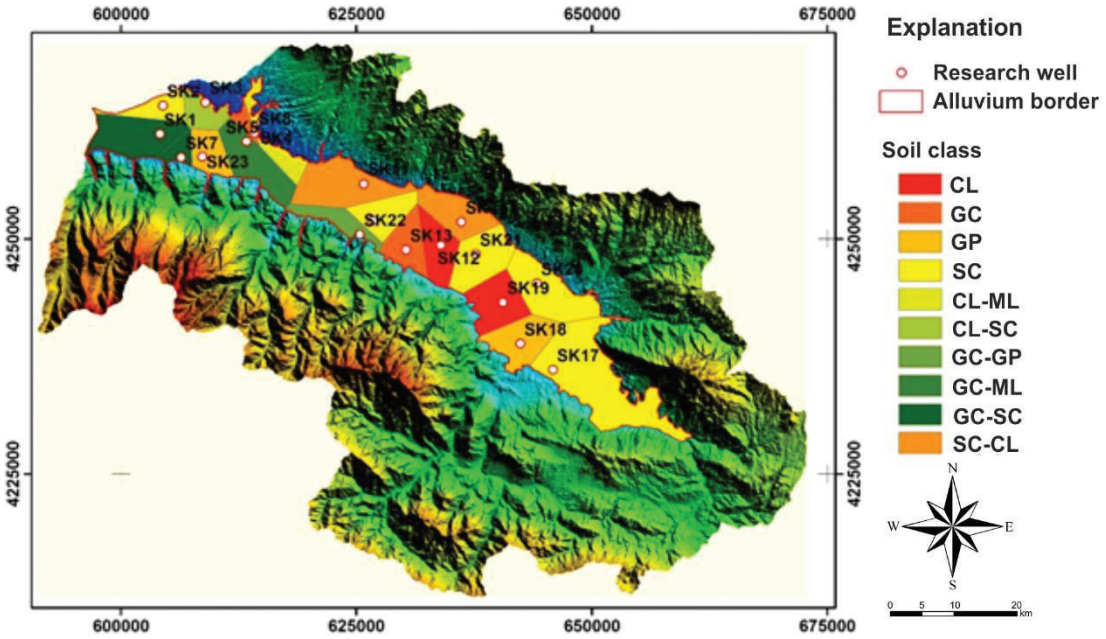

Figure 4.2. Alluvium aquifer soil class distribution map

4.1.4. Hydraulic Conductivity Values

Hydraulic conductivity values for the lithological units of the vadose zone in the alluvium aquifer were calculated using Eq. (3.7). However, it was thought that the formation of the permeability distribution map with these hydraulic conductivity values will be difficult by this way. For this, the vertical permeability values of each research well were determined using Eq. (3.8) and the results obtained are presented in Table 4.3.

The calculated hydraulic conductivity values for the research wells in the study area range from 1.39×10^{-6} m/s to 1.62×10^{-5} m/s (Table 4.3). It was seen that the calculated hydraulic conductivity values are low and close to each other. This is due to the fact that

the soil groups are dominated by fine-grained soils at different depths and the alluvium in the region is highly heterogeneous.

Table 4.3. Vertical permeability values of research wells

Well ID	x	y	z	Depth (m)	Location	K_v (m/s)
SK-1	604121	4261160	88	30	Karaoğlanlı	8.67×10^{-6}
SK-2	604422	4264194	101	30	Taytan	1.62×10^{-5}
SK-3	608939	4264553	97	50	Durasallı	9.39×10^{-6}
SK-4	614316	4261311	121	50	Yeşilova Tepe	4.18×10^{-6}
SK-5	613324	4260377	105	30	Yeşilova Mera	1.39×10^{-6}
SK-7	606376	4258683	131	50	Kabazlı	1.95×10^{-6}
SK-8	614192	4261269	115	50	Hacılı	1.80×10^{-6}
SK-10	626711	4251955	148	50	Piyadeler	2.15×10^{-6}
SK-11	625770	4255886	125	50	Toygarlı	2.72×10^{-6}
SK-12	633947	4249342	143	50	Baklacı	2.18×10^{-6}
SK-13	630254	4248858	101	50	Akkeçili	4.08×10^{-6}
SK-14	636158	4251807	148	50	Tepeköy	2.87×10^{-6}
SK-17	645856	4236078	188	50	Ahmetağa	3.90×10^{-6}
SK-18	642390	4238848	195	50	Haceli	4.39×10^{-6}
SK-19	640552	4243264	170	50	Sobran	4.70×10^{-6}
SK-20	644149	4245284	170	50	Yeşilyurt	9.94×10^{-6}
SK-21	637643	4248393	145	50	Ilgın	1.15×10^{-5}
SK-22	625345	4250473	171	50	Piyadeler	2.04×10^{-6}
SK-23	608633	4258773	117	50	Yeşilkavak	1.48×10^{-5}

The soil group (GW, SW) where the ratio of clay and silt was low was not found. According to the soil class distribution map, it is seen that fine-grained soil groups such as GC, SC, which are dominant in the study area or under 49% of the soil class, are dominant in the study area. Therefore, the low and medium permeability values of the obtained hydraulic conductivities confirm these results. In this context, the hydraulic

conductivity values of alluvial materials were also consistent with the permeability ranges prepared by Canik (1998) (Table 4.4).

Table 4.4. The permeability table (Source: Canik, 1998)

Material	Hydraulic conductivity (m/s)
Uniform gravel block	$0.4\text{-}4\times10^{-3}$
Well grained gravel-aggregate	$4\times10^{-3}\text{-}4\times10^{-5}$
Less clayey sand	$7\times10^{-4}\text{-}7\times10^{-6}$
Clayey sand	$7\times10^{-6}\text{-}7\times10^{-8}$
Silty, clayey sand	$7\times10^{-6}\text{-}7\times10^{-8}$
Compressed silt	$7\times10^{-8}\text{-}7\times10^{-10}$
Compressed clay	$<10^{-9}$
Bituminous Materials	$4\times10^{-5}\text{-}4\times10^{-8}$
Portland Cement	$<10^{-10}$

Vertical permeability values in Table 4.3 of research wells were converted to meter/day to obtain a spatial distribution map. The permeability values are ranging from 0.12 to 1.40 m/din the study area. Higher permeability values are obtained in the west part of the basin. (Figure 4.3)

As a result, when the soil class distribution map and permeability distribution map are examined, it is seen that both soil class distribution and hydraulic conductivity do not offer very different values due to the absence of a very different permeable soil group in the study area.

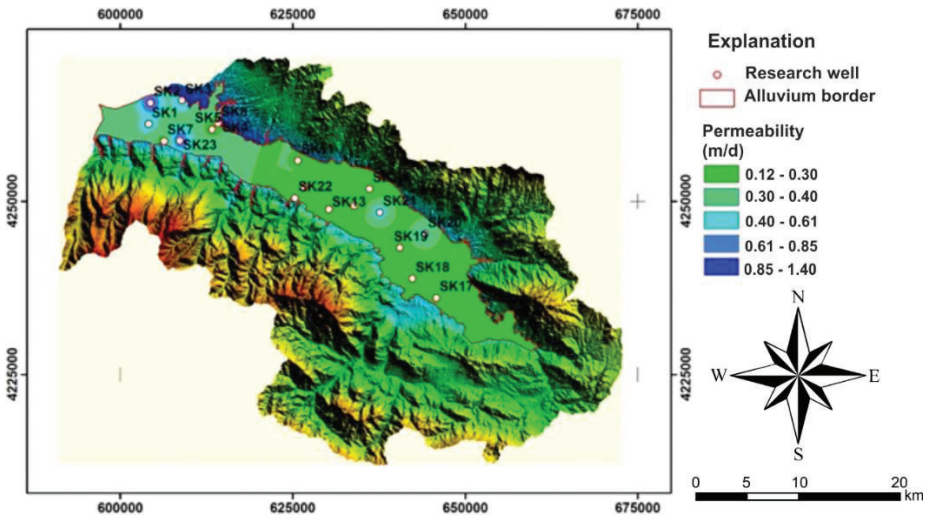

Figure 4.3. Hydraulic conductivity values of alluvium aquifer in vadose zone

4.2. Meteorological Characteristics

One-year long-term meteorological monitoring studies were carried out at the weather stations located at three different locations in the study area. Accordingly, daily temperature and rainfall change graphs for meteorological stations were presented in Figure 4.4, Figure 4.5 and Figure 4.6.

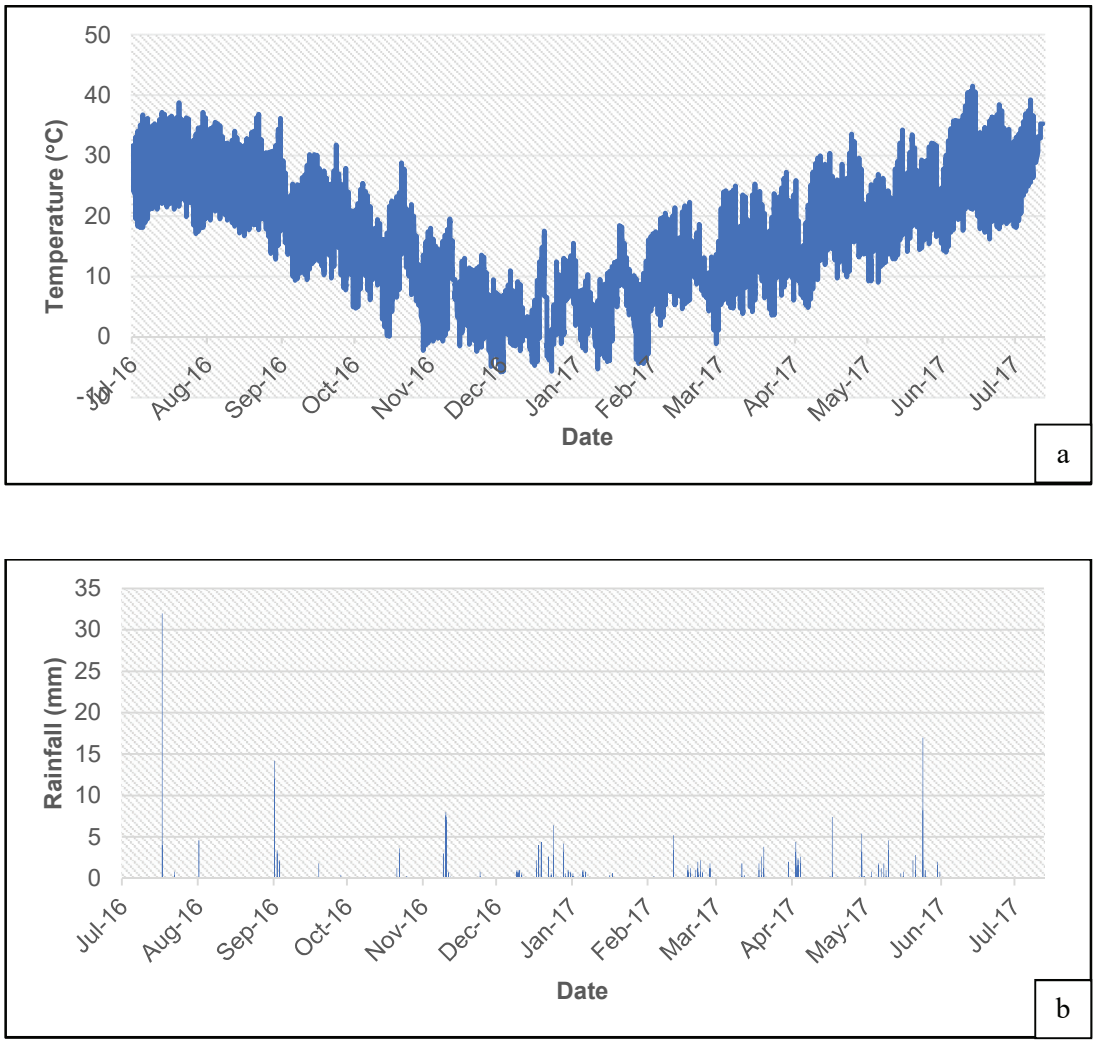

Figure 4.4. Daily temperature (a) and rainfall change (b) graphs of the Yeşilova (MT-1) weather station

The highest temperature recorded by the Yeşilova (MT-1) weather station was 41.6°C in July 2017, while the lowest temperature was measured as -5.9°C in December 2016 (Figure 4.4a).

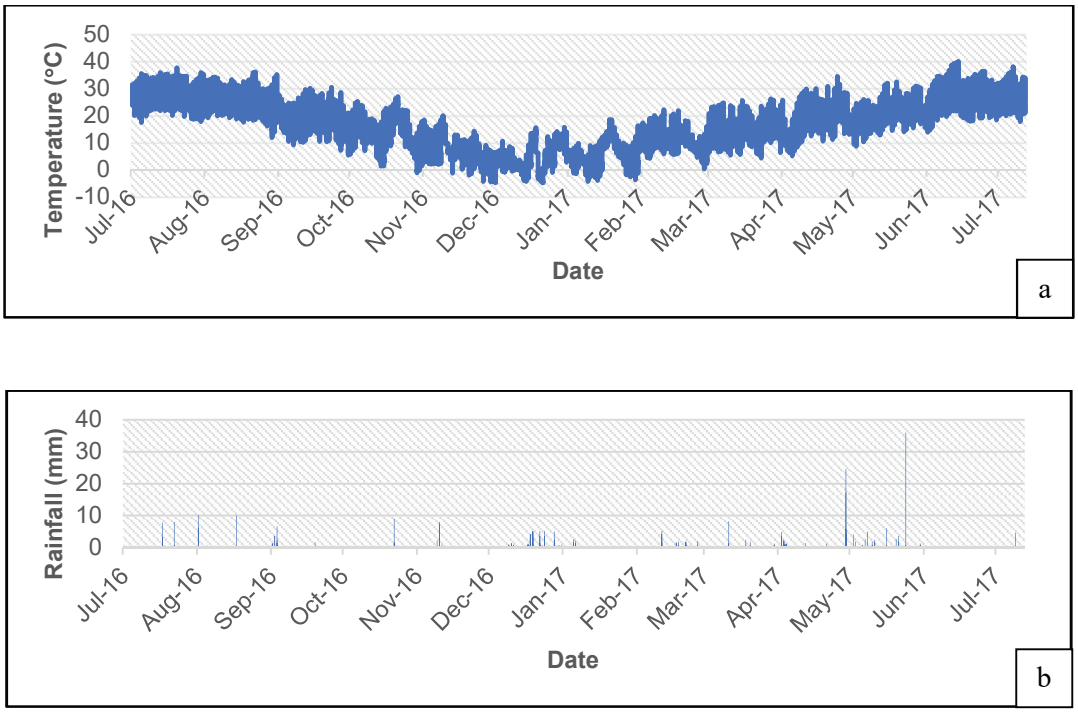

Figure 4.5. Daily temperature (a) and rainfall change (b) graphs of the Alhan (MT-2) weather station

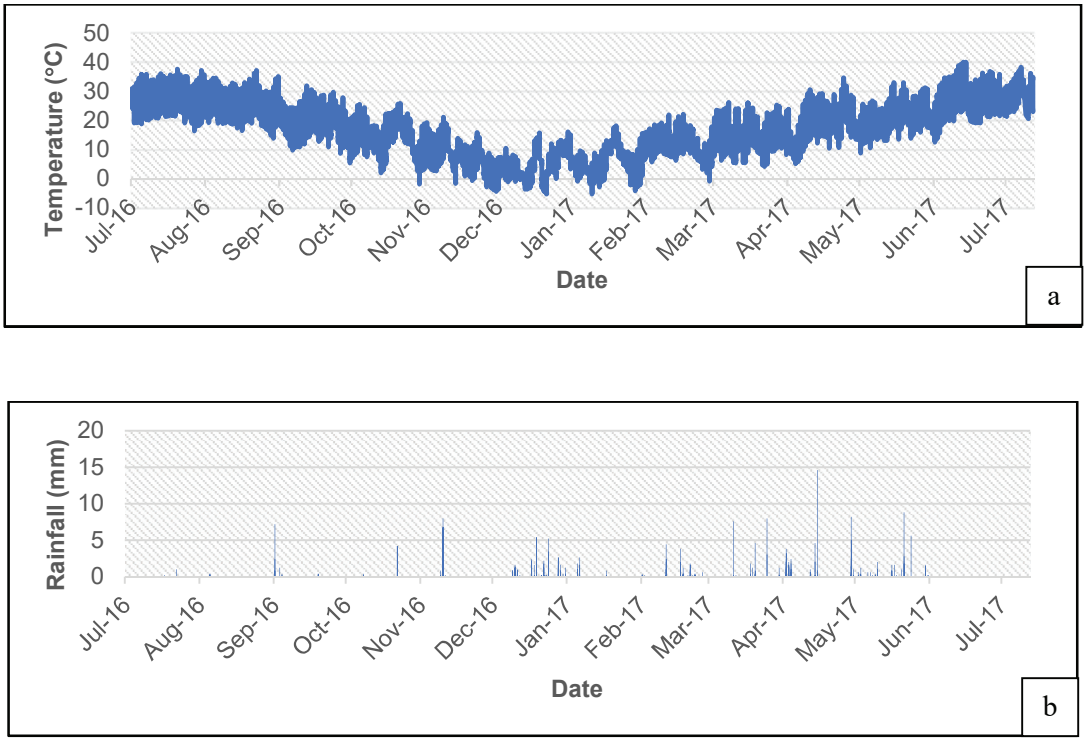

Figure 4.6. Daily temperature (a) and rainfall change (b) graphs of the Çavuşlar (MT-3) weather station

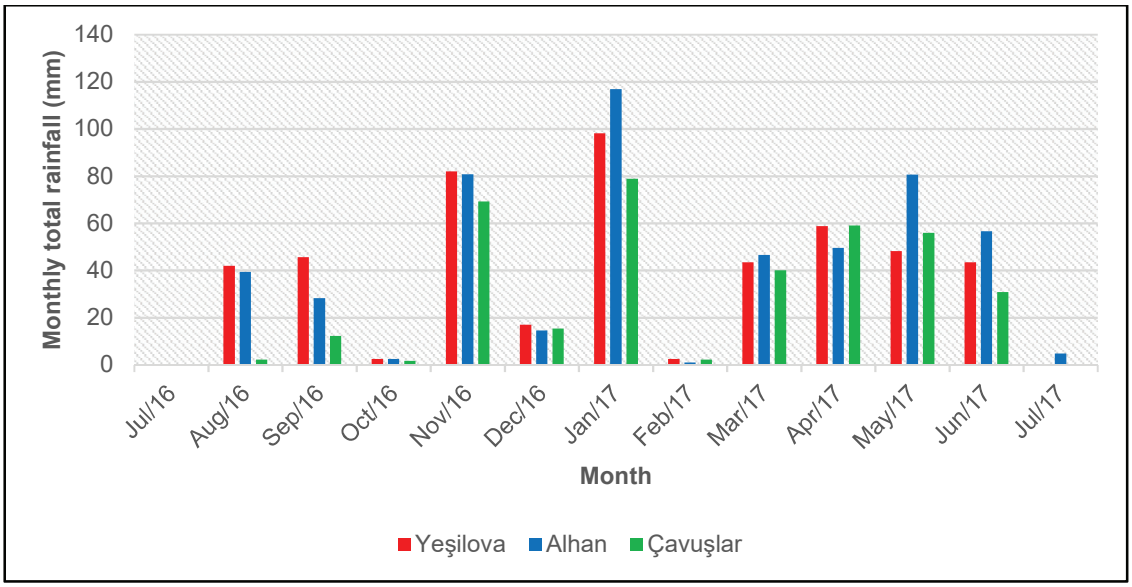

Figure 4.7. Monthly total rainfall graph measured for the Alaşehir sub-basin

The highest temperature recorded by the Alhan (MT-2) weather station was 40.1°C in July 2017, while the lowest temperature was measured as -4.9°C in December 2016 and January 2017 (Figure 4.5a).

The highest temperature recorded by the Çavuşlar (MT-3) weather station was 40.2°C in July 2017, while the lowest temperature was measured as -5.2°C in January 2017 (Figure 4.6a).

Accordingly, there is a similarity between daily temperature change and rainfall graphs recorded at all three weather stations. When the daily temperature change graphs recorded by the weather stations of Yeşilova (MT-1), Alhan (MT-2) and Çavuşlar (MT-3) is dealt, the lowest temperatures measured for the Alaşehir sub-basin are between November 2016 and March 2017 (Figure 4.4a to Figure 4.6a). From daily rainfall change graphs, monthly total rainfall graph was prepared for the Alaşehir sub-basin. Accordingly, the wet period for the Alaşehir sub-basin appears to be between September 2016 and May 2017 (Figure 4.7).

The mean minimum and maximum temperature measured for the study area from the three weather stations were obtained as 5.8°C and 30.05°C, respectively.

Using the daily temperature from the weather stations, the potential evapotranspiration values for the basin were first determined by the Thornthwaite method and then the actual evapotranspiration and runoff values were obtained. Total annual

runoff and total potential-actual evapotranspiration graph prepared according to data of Alaşehir weather stations were given in Figure 4.8.

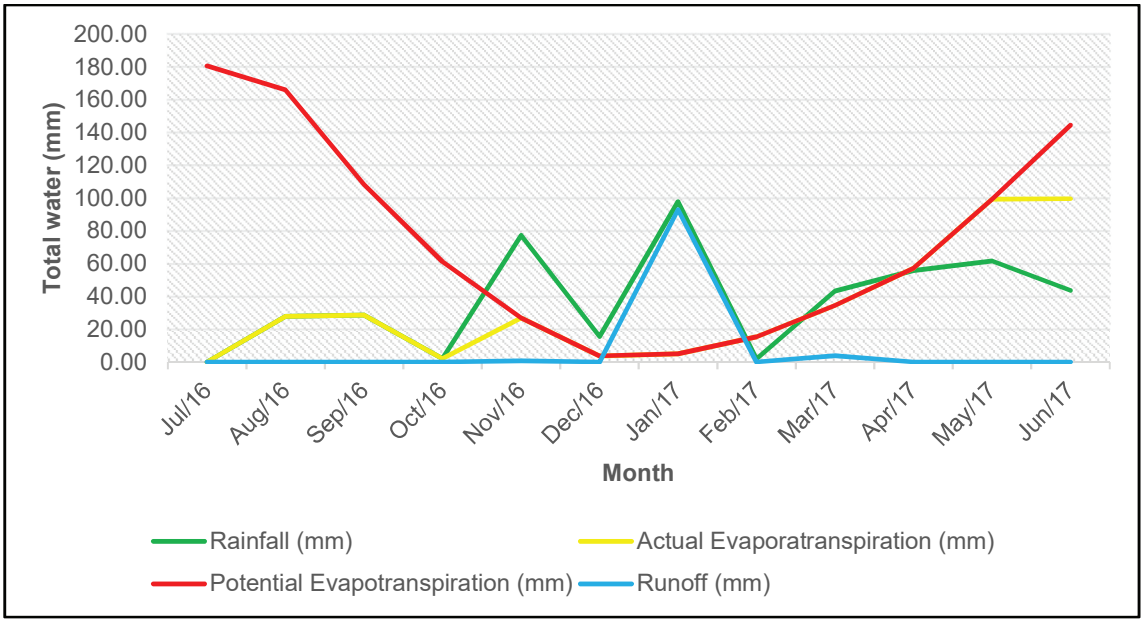

Figure 4.8. Monthly total rainfall, potential and actual evapotranspiration graph of Alaşehir sub-basin

Potential evapotranspiration (PET) refers to the evaporation that occurs when there is maximum humidity in the environment. Accordingly, as can be seen from Figure 4.8, the potential evapotranspiration values with the increasing humidity amounts in summer in Alasehir sub-basin are the highest levels. Actual evapotranspiration is measured to be less than the potential evapotranspiration values because it is limited only to soil moisture (Figure 4.8). The actual evapotranspiration value recorded for the study area for a total of one year is 400.62 mm/year.

Runoff is expressed as water lost from the surface when rainfall is higher than potential evapotranspiration. When considered in Figure 4.8, the potential evapotranspiration values in the Alaşehir sub-basin are well above the rainfall for a one-year period. Thus, the total annual potential evapotranspiration is measured as 902.92 mm/year, while the total annual rainfall is measured as 457 mm/year. Accordingly, in the months when the potential evapotranspiration was above the rainfall, runoff was recorded as 0 mm (Figure 4.8). For Alaşehir sub-basin, runoff is 0.66 mm in November 2016, 93 mm in January 2017 and 3.88 mm in March 2017 and total runoff was obtained as 97.54

mm/year. When noted, these months are months when the rainfall is much more than the potential evapotranspiration.

According to the data obtained from weather stations, it was concluded that the study area is the continental transition characteristic from the inner Aegean and Mediterranean climate. The annual mean temperature value in the Alaşehir sub-basin was measured as 16.25°C. When the temperature change graphs of the Alaşehir sub-basin are examined, it is seen that the mean temperature value is much higher than the annual mean temperature value. The fact that the long-term mean temperature is higher than the annual mean temperature indicates that the basin has an arid period. In addition, the fact that the high evaporation values in the study area are higher than the rainfall is evidence that the Alaşehir sub-basin is located in an arid climate region.

In the basin, where the climate is generally temperate, summer is quite hot and arid. The rainfall is particularly prevalent in spring and summer. Especially in the Aegean region including the study area, meteorological data reveal that the decrease of precipitation and the increase of evaporation amounts are influenced by the climate change of the region. This decrease in rainfall will continue to affect surface and groundwater resources in the region negatively.

4.3. Groundwater Level Monitoring

The data from the level recorders in the research wells need to be converted to a hydraulic head unit in order to better interpret withdrawal and water rise due to the water withdrawal and rainfall in the study area. The data required for this process is only provided by the Baro diver, which measures the air pressure. These devices located outside the well only measure the air pressure. Hydraulic head was found by compensating two Baro Divers and data loggers. In order to understand the effect of rainfall in the basin to the groundwater, hydraulic head graphs are plotted against the rainfall data obtained from the weather stations.

The dataloggers located in the research wells in the study area were adjusted to receive data at intervals of one hour as well as at weather stations and were regularly taken data from these devices every month for a period of approximately 1.5 years from 26 January 2017 until 8 June 2018. The purpose of receiving monthly data is to prevent the loss of data. Hydraulic head graphs obtained from diver data show only the data from

the wet period, September 2017 to May 2018 (Appendix B). Here, it is aimed to understand the effect of rainfall on the alluvium aquifer, as well as the effect of the irrigation attraction, which started in the basin in spring, on the aquifer.

Groundwater level changes obtained manually from research wells are given in Table 4.5. The graphs of the hydraulic head obtained from the data loggers are given in Appendix B.

Manually measured groundwater level monitoring results for 2017 and 2018 coincide with the measured decrease in rainfall (Table 4.5). It is observed that the decrease in rainfall is reflected in the groundwater level as a lack of recharge. Moreover, the presence of an arid clime in the region causes an increase in demand for groundwater. This situation increases the withdrawal in the basin. The fact that the occupancy rates of the dams located in the region are very low is the result of the effects of the lack of rainfall in the region and especially in the Aegean region.

In general, it is expected that the hydraulic head of the wells after rainfall will increase. However, according to the hydraulic head graphs obtained from data loggers, SK-2, SK-3 and SK-7 wells did not provide significant changes in rainfall (Appendix B). The main reason for this is that SK-2, SK-3 and SK-7 were located in regions where clayey sand and clay-based soils are present according to distribution of alluvium materials. In this context, it is observed that there is no permeable soil to allow the rainfall to reach the groundwater level, and therefore, SK-2, SK-3 and SK-7 wells do not react to the rainfall.

When the hydraulic head graphs of the SK-11, SK-12, SK-13 and SK-17 wells were considered, the highest rainfall values were recorded after May. On the other hand, water levels are expected to rise along with the rainfall. However, although the highest rainfall values were recorded after May in these wells, water levels reduced due to the water withdrawal.

On the other hand, it is observed that the hydraulic head data obtained from the other monitoring points reacts to the rise in rainfall in the wet period.

The shortage of precipitation, which is the main source of recharge for both surface water and groundwater, is directly reflected in groundwater recharge in the study area. In addition, the low level of occupancy rates in the dams in the region is seen as the effects of lack of precipitation in the Aegean region. As can be seen from the groundwater level measurements, this downward trend is continuing.

Table 4.5. Groundwater level measurements obtained from manual meter in research wells

Well ID	Water level (m), 2017												Water level (m), 2018					
	January	February	March	April	May	June	July	August	September	October	November	December	January	February	March	April	May	June
SK-1	4.14	4.08	3.95	6.05	4.00	4.10	3.90	3.95	4.28	6.10	5.93	5.74	5.79	5.12	5.00	5.76	5.97	6.01
SK-2	2.23	2.09	2.06	2.24	2.23	2.57	2.70	2.57	2.58	2.57	2.55	2.38	3.29	2.85	2.50	2.81	3.22	3.34
SK-3	4.30	4.09	4.24	4.36	4.48	4.72	5.00	4.12	4.40	4.68	4.71	4.64	4.75	4.70	4.78	5.60	5.53	6.98
SK-4	35.12	34.89	38.58	33.74	31.40	41.99	35.43	36.23	36.35	36.28	36.04	40.99	42.23	41.36	40.85	41.56	40.07	42.27
SK-5	3.25	3.17	2.93	3.30	3.10	3.14	3.84	3.57	3.94	4.05	4.13	3.24	3.29	3.17	3.24	3.25	3.19	3.45
SK-6	2.81	2.80	2.78	2.75	2.80	2.74	2.66	2.80	2.83	2.91	2.97	2.85	2.92	2.90	2.95	3.73	3.70	3.68
SK-7	25.80	25.50	24.80	29.97	29.70	29.33	31.37	32.12	32.17	32.05	32.09	32.09	31.88	31.60	31.34	31.00	31.36	34.30
SK-8	3.78	3.76	3.73	3.70	3.37	3.57	4.20	4.42	4.54	4.40	4.28	4.28	4.10	4.00	4.08	4.30	4.27	5.98
SK-9	21.50	21.60	21.29	21.50	21.90	21.74	22.87	24.00	23.60	23.49	23.20	22.74	22.44	22.12	21.71	20.92	20.92	22.59
SK-10	27.52	26.45	23.50	19.15	27.90	29.57	32.78	32.40	31.67	31.04	30.46	29.38	28.78	25.69	25.13	28.86	27.42	29.35
SK-11	10.26	9.82	10.07	11.68	10.40	10.44	16.90	14.33	13.53	12.39	11.80	11.24	10.84	10.75	10.56	11.65	12.80	16.24
SK-12	10.34	9.60	9.17	9.15	10.50	9.70	10.23	10.61	10.60	10.58	10.39	10.27	10.35	10.14	9.78	9.80	10.21	10.29
SK-13	23.80	23.10	22.95	23.18	23.54	23.52	24.44	25.00	25.22	25.17	24.97	24.59	24.48	24.50	24.54	24.60	25.00	25.98
SK-14	25.80	25.52	25.29	25.80	26.79	26.22	28.60	28.09	28.18	28.10	27.85	25.36	25.12	25.15	27.22	27.51	27.71	28.24
SK-17	16.56	15.85	15.88	16.93	16.90	23.70	25.94	22.58	22.79	21.56	20.48	18.36	18.25	18.18	18.09	18.20	18.65	19.01
SK-18	37.85	37.79	37.83	37.88	34.48	32.75	33.47	33.58	33.64	33.69	33.01	32.47	32.39	32.18	32.10	31.95	32.00	32.89
SK-19	16.44	15.12	17.85	17.99	18.86	19.00	19.16	19.30	19.15	19.10	18.99	18.90	18.32	18.21	18.20	18.05	18.30	19.21
SK-20	19.82	19.01	18.90	18.78	18.40	18.42	18.87	19.00	19.11	19.05	19.14	19.04	19.20	18.85	18.74	18.69	19.27	19.88
SK-21	25.87	25.79	25.74	26.00	26.04	26.87	26.95	26.91	26.98	26.21	25.94	25.15	25.09	25.00	24.87	24.98	25.36	26.91
SK-22	32.44	31.89	31.84	32.10	32.14	32.70	32.78	32.81	32.88	31.04	30.91	30.55	30.19	30.10	30.24	30.36	31.16	32.04
SK-23	11.20	11.15	10.53	10.51	10.01	10.00	10.36	10.41	10.57	10.51	10.48	10.32	10.21	10.10	10.27	10.56	11.14	11.20

4.4. Characteristic of Groundwater in the Study Area

Water samples were collected in wet (May 2017) and dry seasons (September 2017) for to determine the physical and chemical properties of the groundwater. In addition, rainwater samples were collected from three different regions; Hacıaliler (YM-1), Alasehir (YM-2) and Alhan (YM-3) villages to determine chloride recharge values.

4.4.1. Physical Properties

The physical properties of the water samples were determined by Hach-Lange HQ40D multi-parameter probe in field study. For this purpose, physicochemical parameters such as water temperature, pH and electrical conductivity were measured. The results of the physical analyses of water samples for May 2017 (wet period) and September 2017 (dry period) were given in Table 4.6. Sampling campaign was not carried out in SK-15, SK-16, SK-17, SK-18, SK-21, SK-22, SK-23, SK-24 and SK-25 in both periods. Also, no water samples were taken from the SK-9 and SK-12 wells for the dry period. For this reason, the physical parameters of these wells were not determined. In addition, rainwater samples were taken in Hacıaliler (YM-1), Alaşehir (YM-2) and Alhan villages (YM-3) during wet period and their physical properties are given in Table 4.6.

Table 4.6. Physical properties of groundwater and rainwater samples in the study area

Well ID	pH		T (°C)		Electrical Conductivity (µS/cm)	
	Wet period (May 2017)	Dry period (September 2017)	Wet period (May 2017)	Dry period (September 2017)	Wet period (May 2017)	Dry period (September 2017)
SK-1	7.53	7.6	19.3	21.1	329	672
SK-2	6.67	7.6	19.4	21.8	1138	1265
SK-3	7.02	7.8	19	21.8	1086	989
SK-4	7.54	7.7	19.3	26.4	1525	1087

(Cont. on next page)

Table 4.6 (cont.).

SK-5	7.12	7.4	19.5	21.5	1961	1135
SK-6	6.57	7.2	22.2	25.1	4340	4480
SK-7	7.55	7.8	24	22.9	571	517
SK-8	7.26	7.8	22.3	23.7	1198	1063
SK-9	6.91	-	24.8	-	770	-
SK-10	7.58	7.9	23.2	21.9	964	708
SK-11	6.52	7.3	21.5	21.4	1727	2030
SK-12	6.85	-	21.9	-	7910	-
SK-13	7.18	7.4	21.3	22.7	884	898
SK-14	7.92	7.6	21.6	21	972	962
SK-19	7.52	7.6	20.4	21.2	965	951
SK-20	7.00	7.7	23.1	21.3	881	874
YM-1	7.67	-	22.1	-	108.3	-
YM-2	7.55	-	19.7	-	177.7	-
YM-3	7.75	-	19	-	225	-

- not measured

4.4.1.1. pH

pH is an important parameter used to determine the water-rock interaction. The solubility of many minerals depends on the pH of the environment. In this respect, pH determines the manner of occurrence in water of metal and solute material concentration. Decreasing the pH increases the solubility of the metals.

The pH values of the groundwater samples analyzed from the study area for the wet and dry period vary between 6.52 and 7.92 (Table 4.6). The pH values of the rainwater samples from three different places ranged from 7.55 to 7.75 (Table 4.6).

These results indicate that the groundwaters in the wells show slightly alkaline properties. Accordingly, the pH values of the waters are within the limits of the Regulation Concerning Water Intended for Human Consumption (İTASHY, 2013) (Table 4.7). Therefore, groundwater is compatible with drinking water standards in terms of pH values in the study area.

Table 4.7. Regulation Concerning Water Intended for Human Consumption criteria (Source: İTASHY, 2013)

Parameter	Parametric Value	Unit
pH	≤ 9.5-6.5≤	pH Units
Electrical Conductivity (EC)	2500	µS/cm at 20°C
Nitrate (NO_3)	50	mg/L
Nitrite (NO_2)	0.50	mg/L
Ammonium (NH_4)	0.50	mg/L
Aluminum (Al)	200	µg/L
Antimony (Sb)	5.0	µg/L
Arsenic (As)	10	µg/L
Boron (B)	1	mg/L
Chromium (Cr)	50	µg/L
Copper (Cu)	2	mg/L
Chloride (Cl)	250	mg/L
Iron (Fe)	200	µg/L
Manganese (Mn)	50	µg/L
Sulfate (SO_4)	250	mg/L
Sodium (Na)	200	mg/L
Fluoride (F)	1.5	mg/L
Lead (Pb)	10	µg/L
Mercury (Hg)	1.0	µg/L
Nickel (Ni)	20	µg/L

4.4.1.2. Temperature Distributions of Groundwater

Geothermal resources have been used for power generation and direct use in Alaşehir sub-basin. Therefore, temperature of site is very critical. It can be seen that groundwater resources of some site have been affected by geothermal fluid. All monitoring wells data was used to prepared temperature distribution maps of the study area. Groundwater temperature distribution maps were performed both wet and dry period which is given in Table 4.9 (Figure 4.9a and Figure 4.9b). The result show that the groundwater temperature is range from 19°C to 24.8°C in May 2017 and range from 21°C and 26.4°C in September 2017.

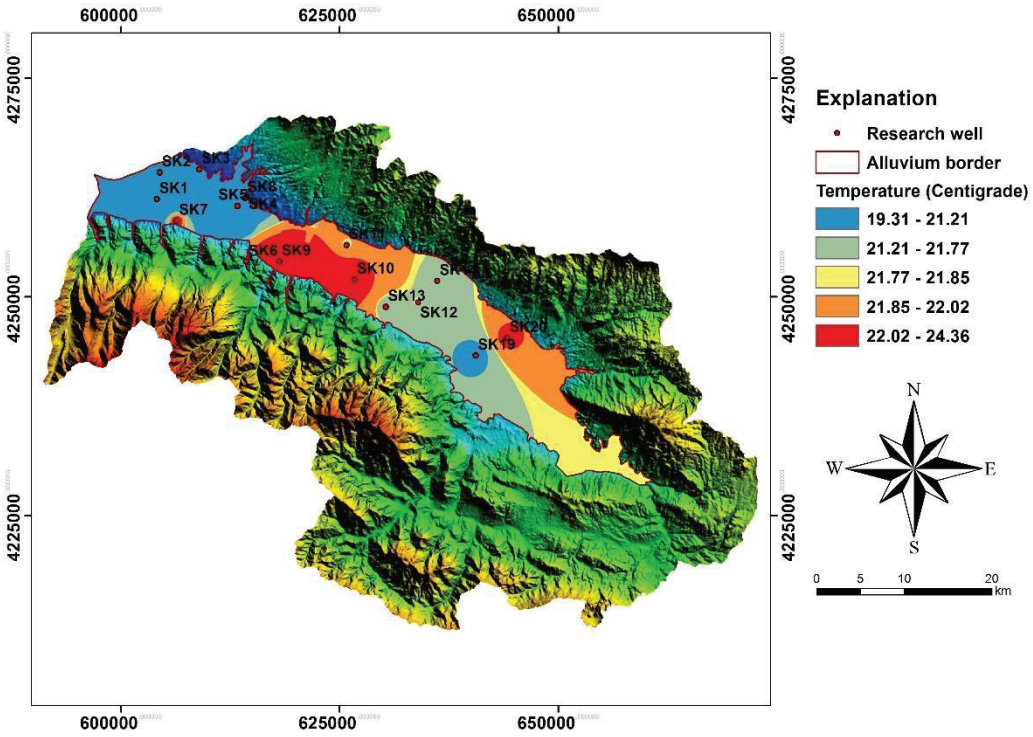

(a) Wet period

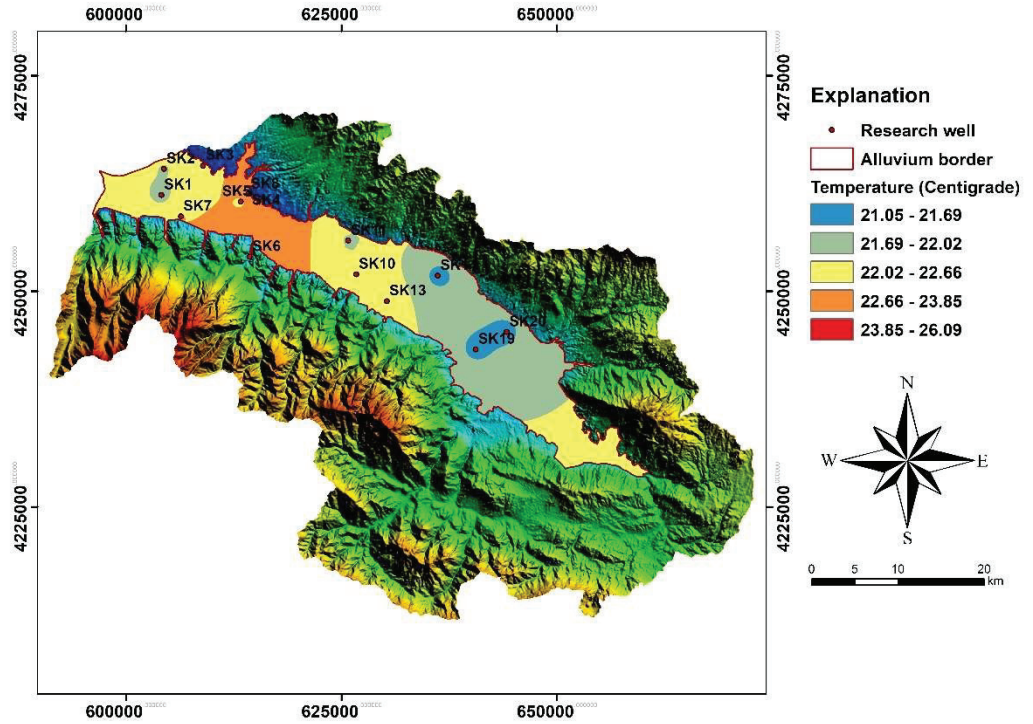

(b) Dry period

Figure 4.9. Groundwater temperature distribution map

(a) Wet period, (b) Dry period

The highest temperature was measured in the SK-6 well in both periods. This well has been affected by geothermal fluid. This region has some deep drill for geothermal energy. One of the drills was blowout on May 18, 2012. In particular, thermal pollution began to increase in the alluvium aquifer by geothermal fluid intrusion after the blowout accident (Rabet et al., 2017).

4.4.1.3. Electrical Conductivity

Electrical Conductivity (EC) provides very important data on water in the study area. Electrical conductivity, which is the total concentration of ions contained in groundwater depends on the type and solubility of rocks, climatic conditions and precipitation conditions in the region. At the same time, electrical conductivity significantly controls the irrigation and drinking properties of groundwater.

The electrical conductivity values of the groundwater for wet and dry period is range from 329 μS/cm to 7910 μS/cm. According to the analyzed results, the electrical conductivity values for the wet period (May 2017) ranged from 329 μS/cm to 7910 μS/cm, while the electrical conductivity values for the dry period (September 2017) ranged from 517 μS/cm to 4480 μS/cm.

The electrical conductivity distribution maps for the research wells for both periods are given in Figure 4.10a and Figure 4.10b. The highest electrical conductivity value for the wet period (May 2017) was measured in wells SK-6 and SK-12. The reason for the high electrical conductivity value in the SK-6 well is thought to be related to the geothermal system and increased water circulation in the wet period. On the other hand, the reason for the high electrical conductivity in the SK-12 well is the clayey levels within the alluvium units. The highest electrical conductivity value for the dry period (September 2017) was found in the well of SK-6. Low EC values were measured in the SK-1 well and in the west part of the study area. The electrical conductivity values of rainwater are between 177.7 μS/cm and 225 μS/cm.

The highest temperature and electrical conductivity values were obtained in wells close to the Alhan region between Kabazlı (SK-7) and Akkeçili (SK-13). The groundwaters of this region have been affected by geothermal fluid. As result, the wells except SK-6 and SK-12 conform to the usable water class in terms of irrigation due to the fact that the study area is used as dense agricultural area (Table 4.7).

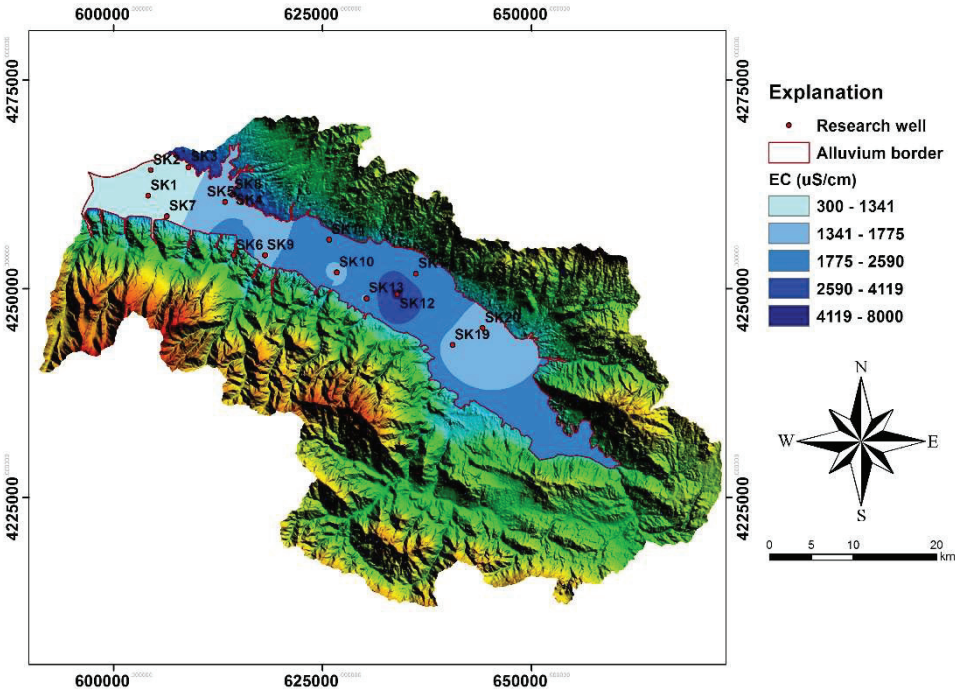

(a) Wet period

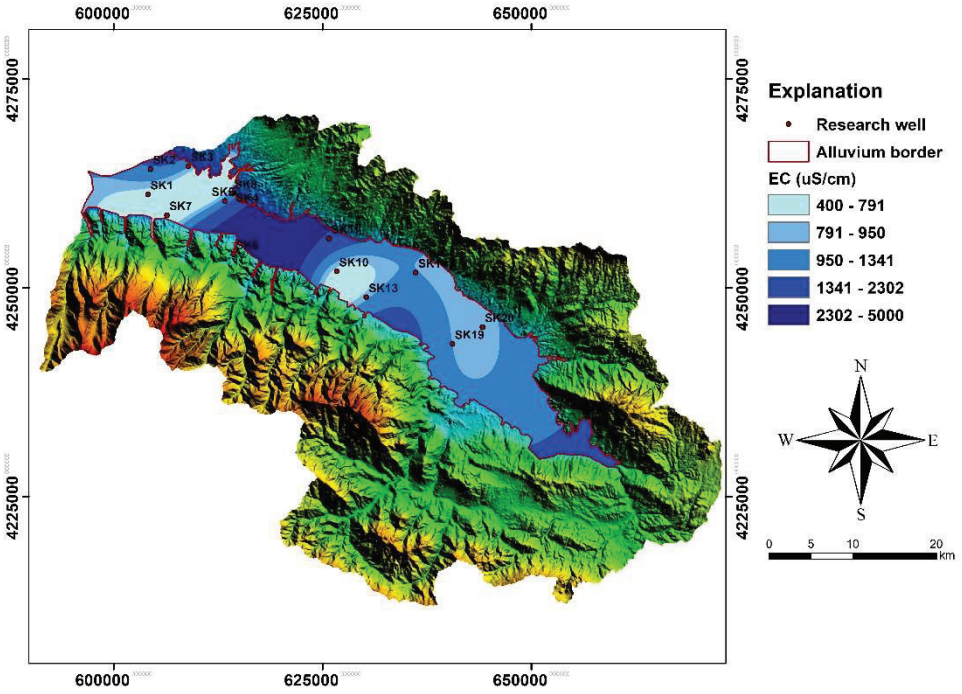

(b) Dry period

Figure 4.10. Groundwater Electrical Conductivity (EC) distribution map
(a) Wet period, (b) Dry period

4.4.2. Chemical Properties

4.4.2.1. Major Anions and Cations

Major anions (SO_4^{2-}, HCO_3^-, CO_3^-, Cl^-) and cations (Ca^{2+}, Mg^{2+}, Na^+, K^+) in water samples were analyzed by ion chromatography, carbonate and bicarbonate ions were analyzed by titrimetric method in Dokuz Eylül University laboratory. The chemical analysis results of the rainwater and groundwater samples belonging to wet and dry period are given in Table 4.8. Water types distribution map of groundwater and rainwater samples are presented in Figure 4.11.

The result show that the dominant cation ions in the alluvium aquifer are sodium and calcium, while the dominant anions are sulphate and bicarbonate. Considering the major anion-cation changes in wet and dry periods, similar distributions were obtained in both periods. While the amount of sodium in groundwater is decreasing towards south east of basin, the amount of sulphate is increased (Figure 4.11a and Figure 4.11b). The reason for the increase of sulphate amount is in grape production used agricultural chemicals that mixed into the groundwater. The east part of the study area is a region where agricultural land is concentrated.

In the Wilcox diagram, the risk of sodium and salinity in groundwater samples and rainwater samples were compared. SK-6 well has a very high sodium and salinity risk during both wet and dry period (Figure 4.12a and Figure 4.12b). Low sodium and salinity values were measured in the samples taken from the rainwater. According to the Wilcox diagrams, when the sodium hazard of the groundwater samples in the study area is examined, the Sodium hazard of the groundwater samples is low. When the salinity hazard of the groundwater samples in the study area is examined, the salinity hazard of the groundwater is high (Figure 4.12a and Figure 4.12b).

According to chemical analysis results, Piper diagrams of water samples of groundwater and rainwater belonging to wet and dry period were obtained. As can be seen in the Piper diagrams, similarity in water chemistry of the wet and dry periods was obtained. Ca-Mg-HCO_3, Na-HCO_3 and Na-Ca-Mg-HCO_3 water types are dominant in the study area (Figure 4.13a and Figure 4.13b). According to Piper diagrams, a significant portion of the water resources are enriched in Ca-Mg-HCO_3 ions. SK-2, SK-3 and SK-4 exhibit mixed water type characteristics whereas SK-5 and SK-6 wells have Na-HCO_3 water type in wet period. The SK-5 well provides the Na-Ca-Mg-HCO_3 water type in the

dry period (Figure 4.13b). SK-6 provides different types of water from other wells in both periods due to the geothermal fluid intrusion (Figure 4.13). The increase in electrical conductivity and temperature is the best example to this.

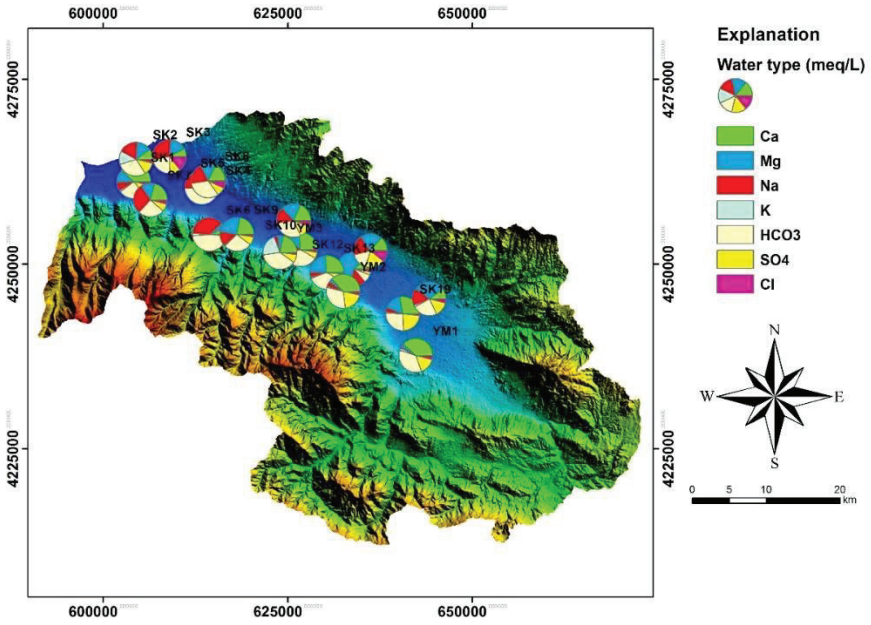

(a) Wet period

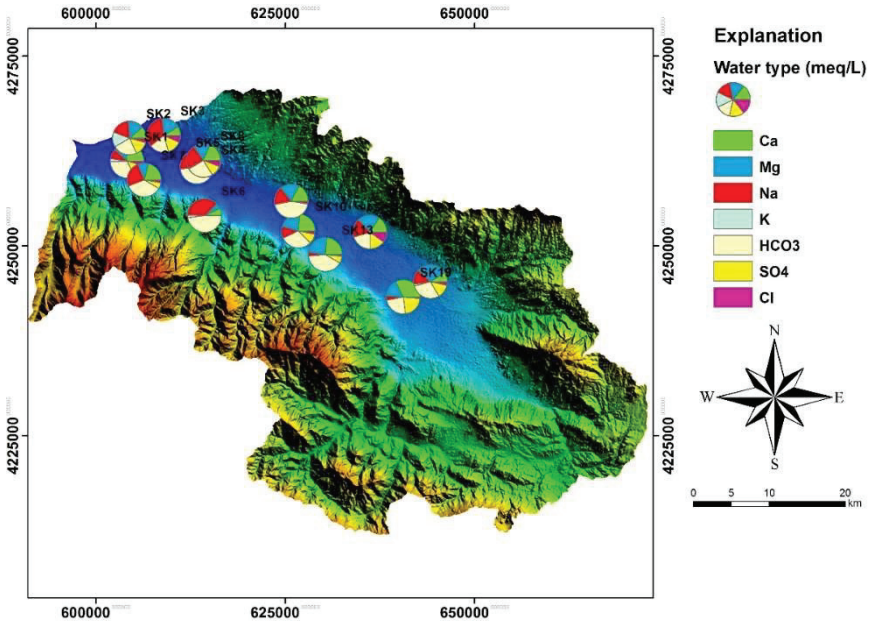

(b) Dry period

Figure 4.11. Major anion-cation distribution map of groundwater and rainwater
(a) Wet period, (b) Dry period

Table 4.8. Chemical analysis results of groundwater and rainwater in the wet and dry period

Well ID	Wet period								Dry period							
	Ca^{2+} (mg/l)	Mg^{2+} (mg/l)	Na^{+} (mg/l)	K^{+} (mg/l)	SO_4^{2-} (mg/l)	HCO_3^{-} (mg/l)	CO_3^{-} (mg/l)	Cl^{-} (mg/l)	Ca^{2+} (mg/l)	Mg^{2+} (mg/l)	Na^{+} (mg/l)	K^{+} (mg/l)	SO_4^{2-} (mg/l)	HCO_3^{-} (mg/l)	CO_3^{-} (mg/l)	Cl^{-} (mg/l)
SK-1	56.70	10.71	13.91	3.80	36	115.90	*	10	92.92	21.34	35.73	18.93	114	320.90	*	25
SK-2	56.12	47.91	116.52	140.81	165	501.60	*	35	67.17	53.50	125.87	163.95	202	435	42.01	43
SK-3	44.33	54.77	188.61	4.22	135	396.60	*	142	38.89	48.37	176.89	2.93	148	259.90	58.21	52
SK-4	68.65	74.56	257.06	6.59	185	396.60	55.21	209	59.17	51.88	167.30	6.30	88	375.20	21	123
SK-5	73.84	47.09	543.43	14.05	41	1687	*	53	116.01	52.36	151	8.04	111	746.80	*	39
SK-6	175.20	99	1231	154	4	4228	*	54.1	193.40	98	1226	154	3	4213	*	30
SK-7	49.75	18.83	78.02	2.62	41	184.30	56.41	17	56.14	17.02	74.51	2.52	37	295.30	18	12
SK-8	109.16	54.59	140.97	11.08	121	610.20	*	74	100.17	51.55	139.95	10.49	134	413.70	55.81	54
SK-9	77.35	54.14	54.38	7.22	68	293.50	40.21	15	-	-	-	-	-	-	-	-
SK-10	144.84	38.81	93.58	17.23	77	619.90	*	25	94.27	53.70	52.51	6.22	90	378.90	13.20	21
SK-11	206.05	125.57	195.17	10.01	346	1022	*	105	221.66	142.15	255.74	7.44	26	1732	*	58
SK-12	581.80	1805	871	33	378	1233	*	250	-	-	-	-	-	-	-	-
SK-13	142.11	77.75	27.98	13.44	90	593.70	*	15	116.75	74.16	19.76	9.25	80	615	*	15
SK-14	66.46	62.30	109.52	7.87	222	247.10	37.21	92	86.10	69.50	111.86	8.32	194	346.60	*	95
SK-19	154.79	55.89	27.3	11.20	302	450.90	*	18	192.66	60.59	27.82	11.4	306	439.30	*	16
SK-20	44.28	82.38	85.53	16.67	149	330.10	55.81	33	42	83.03	77.98	15.82	148	421	24	29
YM-1	17.04	0.85	0.77	1.75	17	48.20	*	3	-	-	-	-	-	-	-	-
YM-2	29.15	1.69	4.26	2.05	37	74.44	*	5	-	-	-	-	-	-	-	-
YM-3	35.21	5.53	6.52	67.72	30	187.30	*	6	-	-	-	-	-	-	-	-

* no data; - not measured

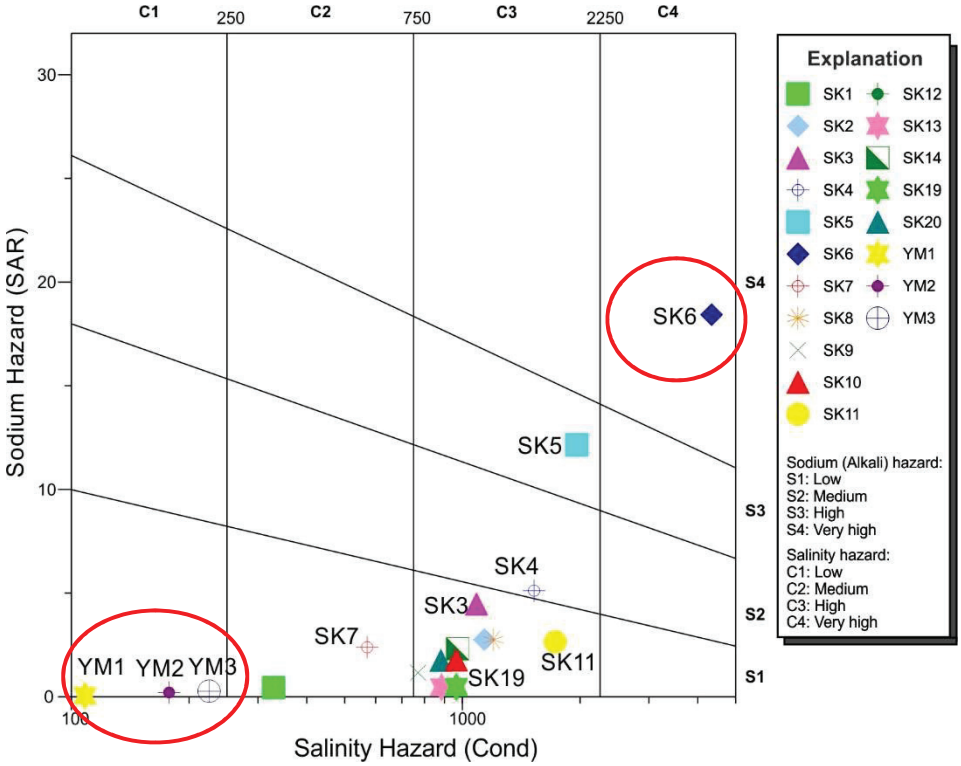

(a) Wet period

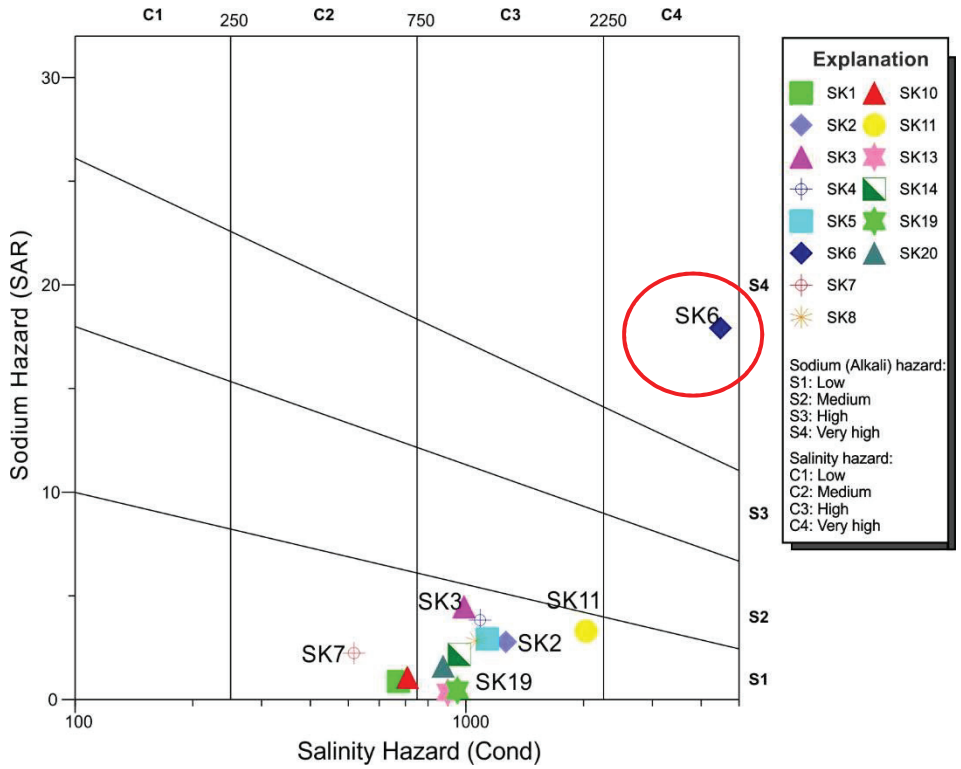

(b) Dry period

Figure 4.12. Wilcox diagrams of groundwater and rainwater

(a) Wet period, (b) Dry period

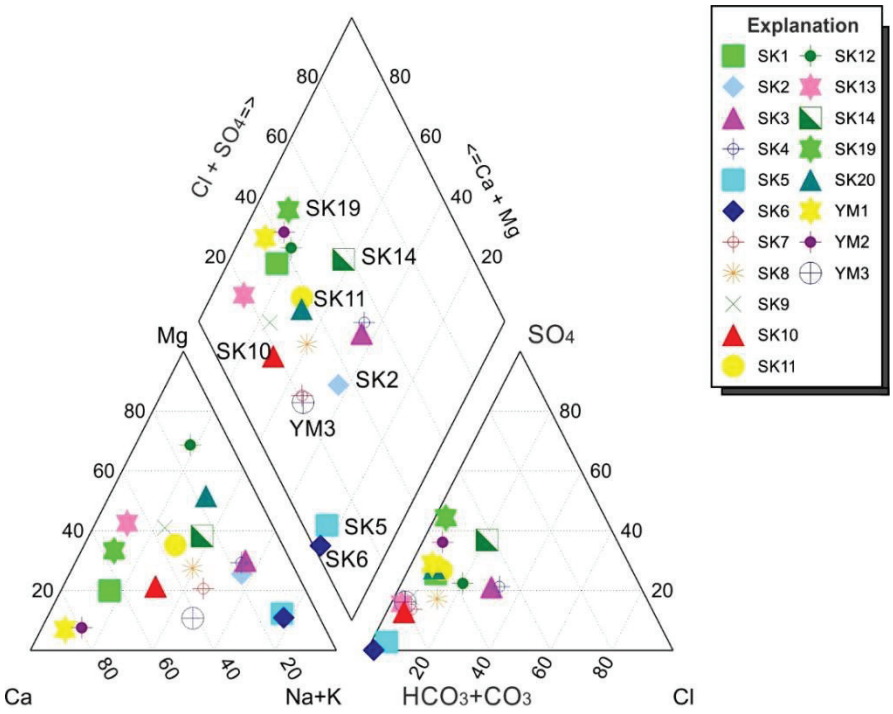

(a) Wet period

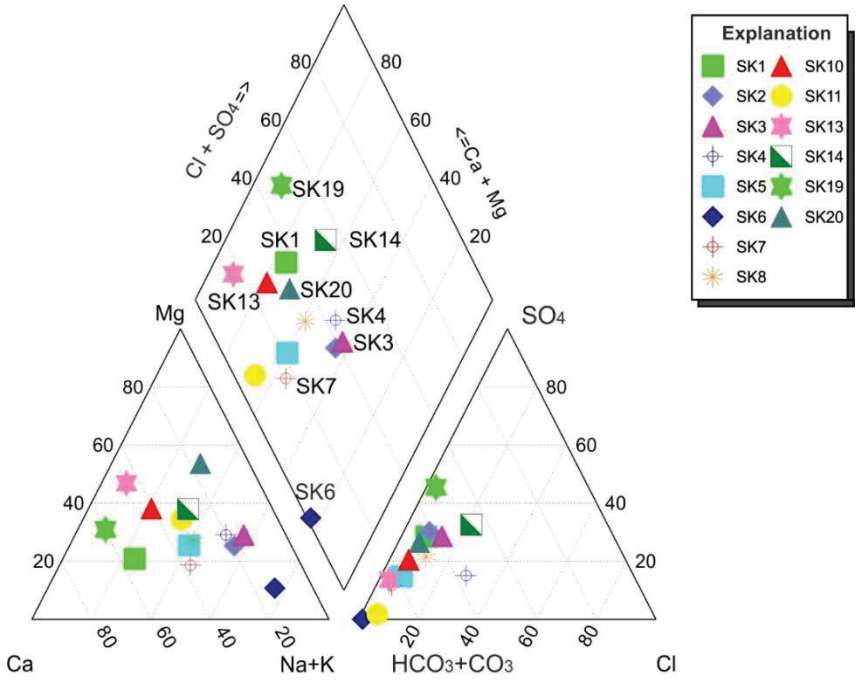

(b) Dry period

Figure 4.13. Piper diagrams of groundwater and rainwater

(a) Wet period, (b) Dry period

4.4.2.2. Trace Elements

Boron (B) and Bromide (Br^-) found in trace amounts in groundwater are the most important elements used to determine pollutant properties. In particular, Bromide is present in trace amounts in coastal aquifers as a result of seawater intrusion or in areas where the industry is located. High Boron values in groundwater in irrigation areas cause the plants to dry out and thus reduce agricultural yields.

Boron (B) and Bromide (Br^-) analyses were carried out for groundwater in the wet and dry period. The obtained results are presented in Table 4.9.

Table 4.9. Trace element results of groundwater in the study area

Well ID	Wet period		Dry period	
	B (mg/l)	Br^- (mg/l)	B (mg/l)	Br^- (mg/l)
SK-1	0.02	0.02	0.09	0.08
SK-2	0.88	0.11	1.18	0.13
SK-3	0.75	0.66	0.67	0.15
SK-4	0.94	0.77	0.57	0.49
SK-5	6.43	0.27	1.78	0.23
SK-6	21.94	-	22.52	-
SK-7	0.11	0.06	0.11	0.05
SK-8	4.77	0.16	4.47	0.23
SK-9	0.19	0.05	-	-
SK-10	3.10	0.08	0.26	0.06
SK-11	1.90	0.33	2.21	0.27
SK-12	0.88	-	-	-
SK-13	0.05	0.03	0.05	0.05
SK-14	0.20	0.38	0.23	0.39
SK-19	0.04	0.04	0.04	0.04
SK-20	0.39	0.09	0.41	0.09

- not measured

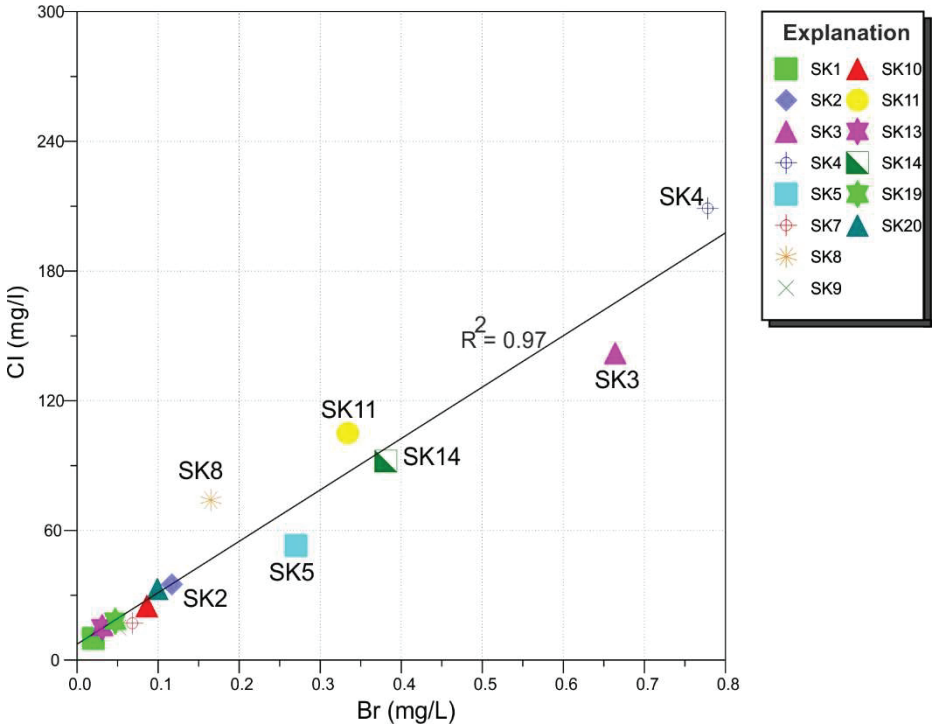

(a) Wet period

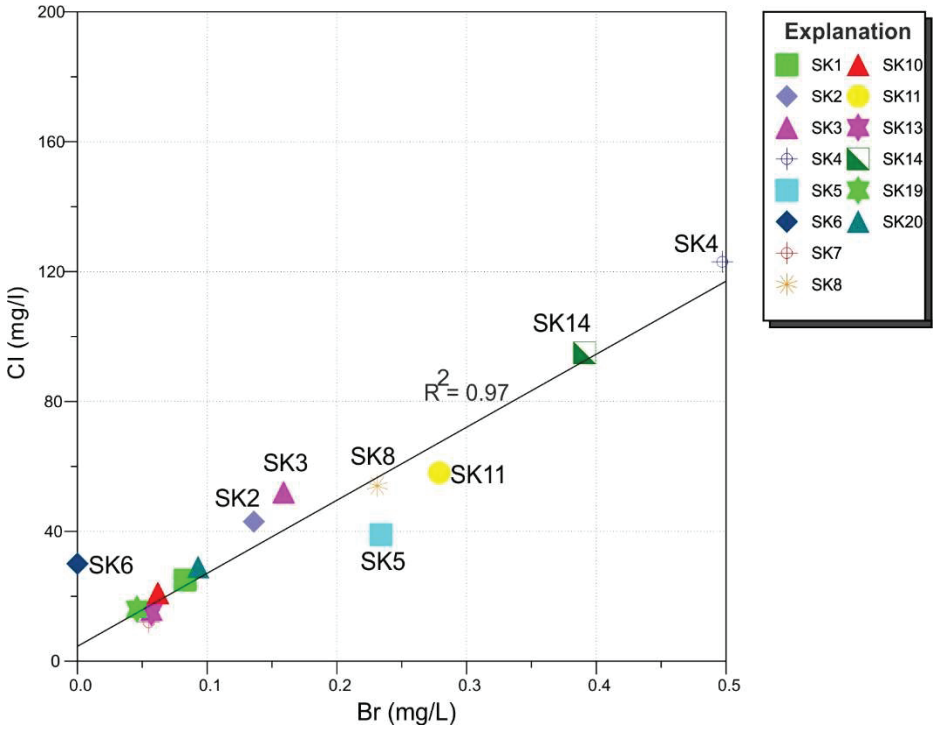

(b) Dry period

Figure 4.14. Chloride and Bromide relation of groundwater

(a) Wet period, (b) Dry period

Boron (B) values are between 0.02 mg/l and 21.94 mg/l in the wet period and between 0.04 mg/l and 22.52 mg/l for the dry period. According to these results, in the wet period, the Boron values in the SK-5, SK-6, SK-8, SK-10 and SK-11 wells remained out of Regulation Concerning Water Intended for Human Consumption criteria for both periods (İTASHY, 2013) (Table 4.7). In particular, high Boron values were measured in the SK-6 well in both periods. In the remaining wells, Boron values are within the limits of the Regulation Concerning Water Intended for Human Consumption (İTASHY, 2013).

Bromide (Br^-) values ranged from 0.02 mg/l to 0.77 mg/l in the wet period and 0.04 mg/l to 0.49 mg/l in the dry period. The lowest Bromide values were measured in the SK-1 well at both wet and dry periods.

The relationship between Chloride and Bromine gives important information about the mixing mechanism of groundwater and geothermal system. A linear relationship was observed between Chloride and Bromide for the wet and dry period correlations and the correlation coefficient was 0.97 (Figure 4.14). The high correlation coefficient obtained in the diagrams between Chloride and Bromide indicates that the alluvium aquifer is affected by the geothermal system in the study area.

4.5. Alluvium Aquifer Recharge Values

In this study, two different methods, numerical and chemical methods, were used to estimate the groundwater recharge of alluvium aquifer. In the following section, numerical model results are mentioned.

4.5.1. HYDRUS-1D Model Results

4.5.1.1. Soil Water Retention Curve Equations

HYDRUS-1D allows the use of 5 different analytical models for hydraulic features. These are vanGenuchten, Brooks and Corey, Vogeland Cislerova, Kosugi, and Durner. The hydraulic features of vanGenuchten (1980) were chosen in this study because hydraulic properties are generally described using the pore size distribution model of Mualem (1976) together with the water retention function defined by vanGenuchten (1980).

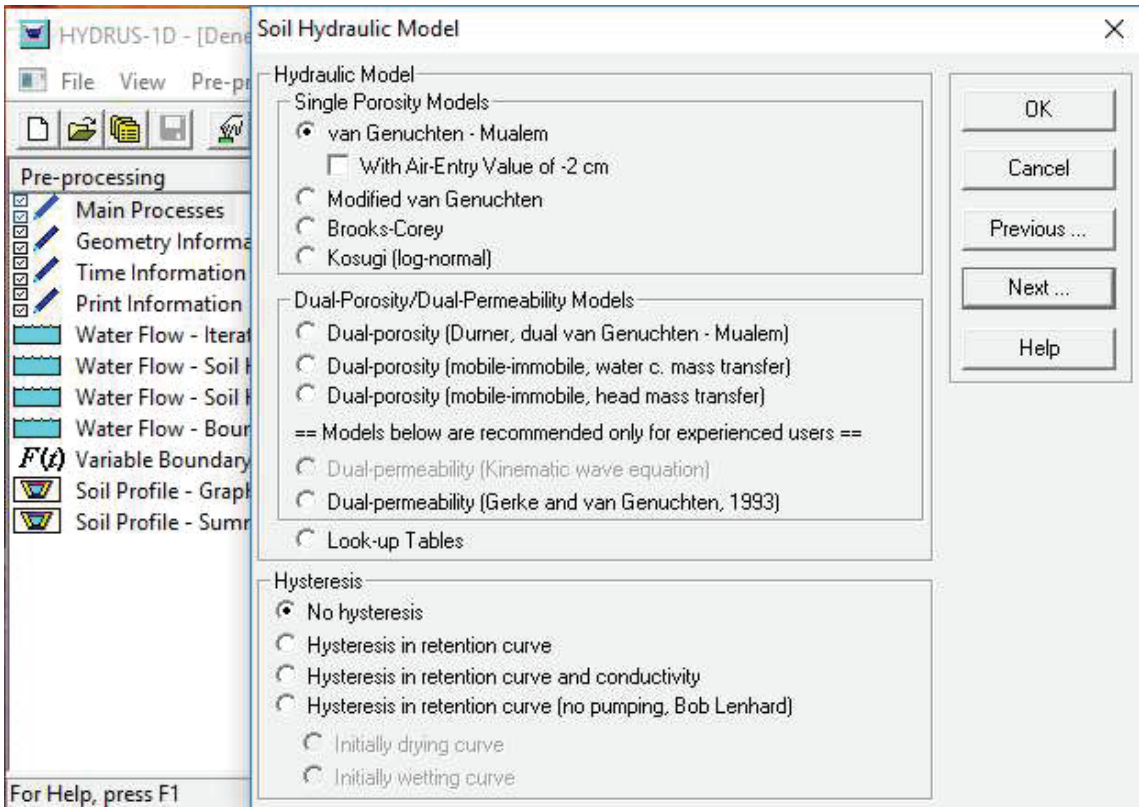

Figure 4.15. HYDRUS-1D Hydraulic Model

The most widely used water retention function developed by vanGenuchten (1980);

$$S_e(h) = \frac{1}{\left[1 + (-\alpha h)^n\right]^m} \tag{4.1}$$

Where Se (h) is the soil water saturation, α [L^{-1}], n [-] and m [-] are auxiliary parameters. Here, it is written as Se (h) instead of Se to emphasize that the effective saturation is a function of the pressure head.

$$\theta(h) = \frac{\theta_s - \theta_r}{\left[1 + (-\alpha h)^n\right]^m} + \theta_r \tag{4.2}$$

Where θ is the water content [-], θ_s is the saturated water content [-], θ_r is the residual water content [-], n, α is parameter and $m = 1 - \frac{1}{n}$.

$$K(h) = K_s S_e^l \left[1 - \left(1 - S_e^{1/m}\right)^m\right]^2 \quad (4.3)$$

Where K(h) is hydraulic conductivity in the matric potential (m) (pressure head), K_s is hydraulic conductivity in saturated conditions, S_e is effective water content, *l* is parameter describing the pore structure of soil.

As can be seen, the above equations have 6 independent parameters; θ_r, θ_s, α, n, m and *l*. The pore connection parameter *l* in the hydraulic conductivity function is estimated to be about 0.5 on average for most soils (Mualem, 1976). The recommended vanGenuchten parameters for 12 different soil types are given in Table 4.10.

Table 4.10. vanGenuchten hydraulic parameters for 12 different soil types

Soil type	θ_r [L^3 L^{-3}]	θ_s [L^3 L^{-3}]	α [cm^{-1}]	n [-]
Sand	0.053	0.375	0.035	3.18
Loamy Sand	0.049	0.0390	0.035	1.75
Sandy Loam	0.039	0.387	0.027	1.45
Loam	0.061	0.399	0.011	1.47
Silt	0.05	0.489	0.007	1.68
Silty Loam	0.065	0.439	0.005	1.66
Sandy Clay Loam	0.063	0.384	0.021	1.33
Clay Loam	0.079	0.442	0.016	1.41
Silty Clay Loam	0.09	0.482	0.008	1.52
Sandy Clay	0.117	0.385	0.033	1.21
Silty Clay	0.111	0.481	0.016	1.32
Clay	0.098	0.459	0.015	1.25

4.5.1.2. Hysteresis in Soil Water Retention Curve

Soil water retention curves are often drawn from the high water content to the lower water content, called the moisture release curve or drying curve. When the soil sample has been re-saturated after drying, the matric potential (the pressure head in the unsaturated zone) may not be the same. In the soil water retention curves, the wetting

curve is usually drawn below the drying curve (Figure 4.16). This situation is known as Hysteresis. In the HYDRUS-1D software program, it is assumed that the value of θr, θ_s and n remain constant in dry and wet conditions in order to determine the hysteresis (Simunek et al., 2008). Only the α parameter changes (Anlauf et al., 2012). For this reason, no hysteresis option was selected in HYDRUS-1D under soil hydraulic properties parameter (Figure 4.16).

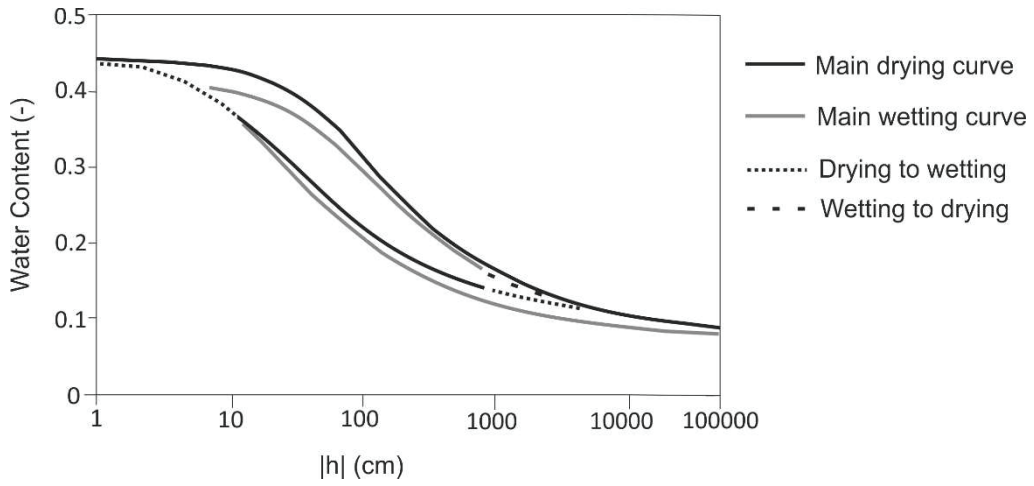

Figure 4.16. Main drying and wetting soil water retention curves are not the same because of hysteresis

4.5.1.3. HYDRUS-1D Model Simulation

In this section, infiltration model simulation for the SK-1 well is mentioned. The model results of the remaining research wells are given in Appendix D. In the HYDRUS-1D model, first, the depth of the soil layer in vadose zone (5 m), the axis of the water movement and the number of materials were entered, the length unit was determined as meters and the time period was selected as year. Profile discretization has been made by dividing into 101 nodes for one research well. A vertical cross section depicting the vertical discretization of the flow domain is shown in Figure 4.17.

The red, blue and green colors in Figure 4.17 represent the lithological units in the flow domain. Each grid interval is 0.5 meters. In the HYDRUS-1D program, number of time variable boundary records was selected as 12 for one year period. The wide array of time scales required to efficiently simulates the flow pathways is the most important

problem of the modeling. Therefore, unsaturated flow numerically requires small time steps in the order of seconds to describe the vertical movement of moisture in the unsaturated domain where as the groundwater flow can be run with time steps in the order of days. In the areas where the converge error can be given numerically, the number of iterations was increased and/or the time steps were reduced in the HYDRUS-1D.

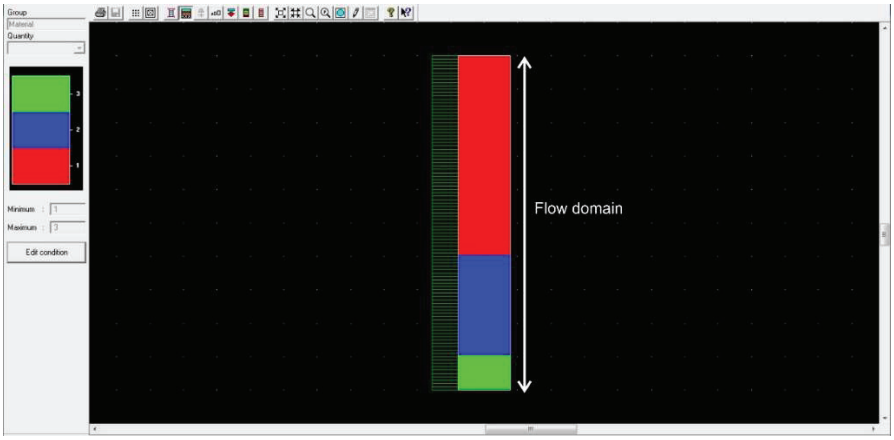

Figure 4.17. Flow domain discretization of SK-1

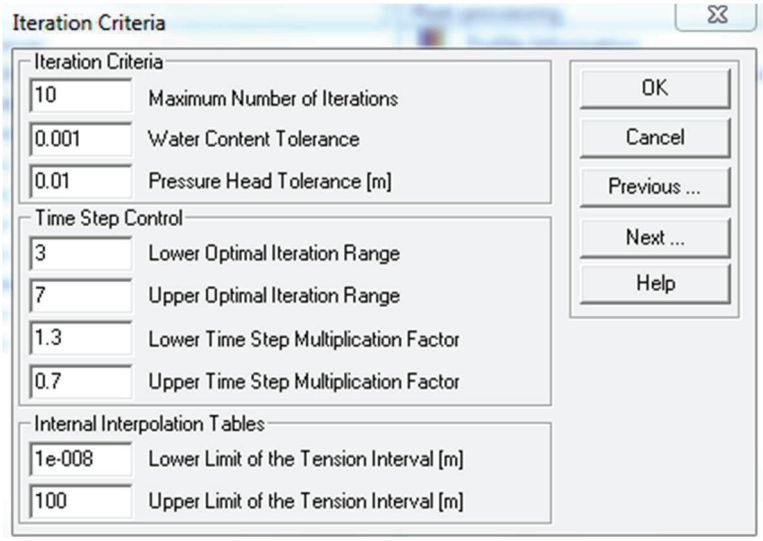

Figure 4.18. HYDRUS-1D iteration criteria dialog window

In the HYDRUS-1D program, the iteration criteria dialog window contains information related to the iterative process that is used to solve the Richards equation. The iterative process continues until a satisfactory degree of convergence is obtained. The

recommended value of iteration criteria is given in Figure 4.18. After the discretization, the soil hydraulic parameters given in Table 4.11 were entered along the depth of the well. vanGenuchten parameters are given in Table 4.12.

Table 4.11. Soil Hydraulic parameters of SK-1

Well ID	Permeability (K) (m/s)	Soil Water Content (θ) (%)	Soil Layer Depth (m)
SK-1	7×10^{-6}	0.2762	3
	1.6×10^{-5}	0.1593	1.5
	9.19×10^{-6}	0.0624	0.5

Table 4.12. vanGenuchten Parameters of SK-1

Well ID	θ_r	θ_s	α (1/m)	n	l
SK-1	0.045	0.43	14.5	2.68	0.5
	0.034	0.46	1.6	1.37	0.5
	0.034	0.46	1.6	1.37	0.5

Finally, weather station data obtained from field studies were assigned to the program and the model was created separately for each research well, selecting appropriate initial and boundary conditions. Weather station data is given in Table 4.13.

Table 4.13. Weather Data for the Alaşehir sub-basin

Months	Rainfall (mm)	Actual Evapotranspiration (mm)	Potential Evapotranspiration (mm)	Runoff (mm)
Jul-16	0.00	0.00	180.68	0.00
Aug-16	27.87	27.87	165.91	0.00
Sep-16	28.67	28.67	108.40	0.00
Oct-16	2.13	2.13	61.22	0.00
Nov-16	77.33	27.00	27.00	0.66
Dec-16	15.67	3.72	3.72	0.00

(cont. on next page)

Table 4.13 (cont.).

Jan-17	97.93	4.93	4.93	93.00
Feb-17	1.87	15.43	15.43	0.00
Mar-17	43.33	34.61	34.61	3.88
Apr-17	55.80	57.22	57.22	0.00
May-17	61.60	99.37	99.37	0.00
Jun-17	43.70	99.67	144.43	0.00

4.5.1.4. Initial and Boundary Condition

4.5.1.4.1. Initial Condition

The HYDRUS-1D is a Windows-based software program that can solve the groundwater flow equations numerically. The solving of groundwater flow equations depends primarily on the formation of appropriate initial and boundary conditions. As can be seen from Eq. (2.7), HYDRUS-1D allows the use of two different initial conditions such as water content and pressure head. The initial conditions of the model can be expressed in terms of water content and pressure head as follows;

$$\theta(z,t) = \theta_i(z,0), \tag{4.4}$$

$$h(z,t) = h_i(z,0), \tag{4.5}$$

Where θ_i [-] and h_i [L] represent water content and pressure head, respectively. Accordingly, water content values of the vadose zone determined in the laboratory were used in the study as initial condition (Eq. 4.4).

4.5.1.4.2. Boundary Condition

4.5.1.4.2.1. Atmospheric Boundary Condition with Surface Runoff

The atmospheric boundary condition with surface runoff is one of the system-dependent boundary conditions of the HYDRUS-1D program, which represents the soil-

air interface exposed to atmospheric conditions. In atmospheric boundary condition with surface runoff, the potential flow is completely controlled by meteorological conditions such as precipitation and evaporation along this interface. The soil surface boundary conditions may vary from the predicted flow to the predicted head conditions. This occurs when the precipitation exceeds the infiltration capacity of the soil. On the other hand, it causes the rainwater to accumulate on the soil layer depending on o soil conditions. In this case, the infiltration rate is controlled by the precipitation rate instead of the soil infiltration capacity (Neuman et al., 1974).

4.5.1.4.2.2. Free Drainage

This boundary condition can be applied if there is groundwater below the flow domain. Free drainage boundary condition cannot be used for the edges of the flow domain. For this purpose, the bottom of the flow domain was selected as free drainage boundary condition (Figure 4.19).

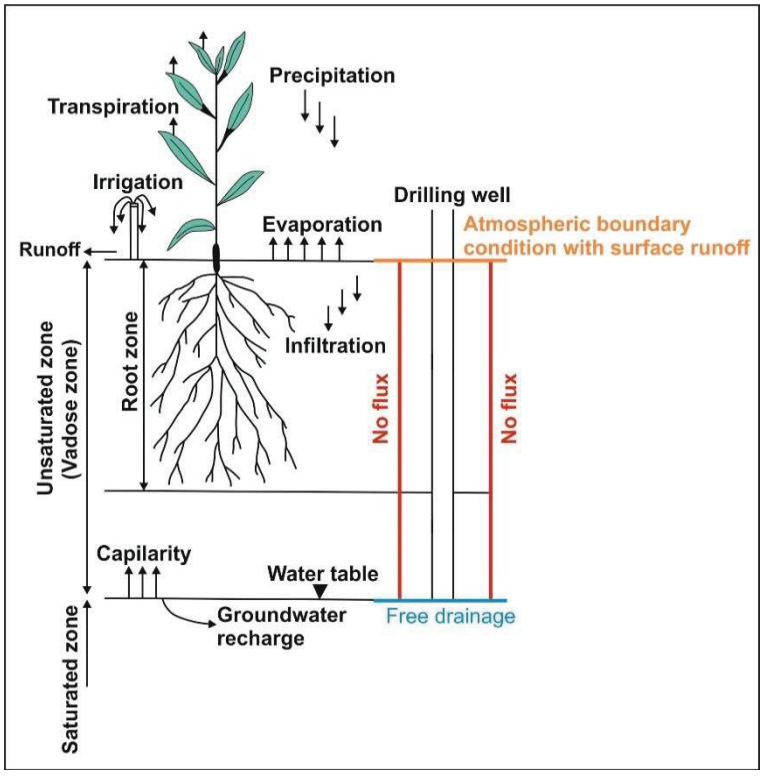

Figure 4.19. Schematic representation of model boundary conditions

4.5.1.5. HYDRUS-1D Recharge Values

The following assumptions have been made regarding the model whose upper and lower boundaries are determined.

- The infiltration only takes place in the vertical direction for vadose zone
- No flux from lateral boundary

The recharge values of the research wells obtained for the study area according to the HYDRUS-1D model are presented in Table 4.14 and all recharge graphs for the model are given in Appendix C.

Table 4.14. Groundwater recharge values of research wells

Well ID	Location	Recharge (m/year)	Recharge (mm/year)
SK-1	Karaoğlanlı	0.034832	34.83
SK-2	Taytan	0.021783	21.78
SK-3	Durasallı	0.060552	60.55
SK-4	YeşilovaTepe	0.060045	60.04
SK-5	YeşilovaMera	0.022264	22.26
SK-7	Kabazlı	0.062007	62.00
SK-8	Hacılı	0.052719	52.71
SK-10	Piyadeler	0.036315	36.31
SK-11	Toygarlı	0.036284	36.28
SK-12	Baklacı	0.034362	34.36
SK-13	Akkeçili	0.037306	37.30
SK-14	Tepeköy	0.036329	36.32
SK-17	Ahmetağa	0.036662	36.66
SK-18	Haceli	0.068521	68.52
SK-19	Sobran	0.034228	34.22
SK-20	Yeşilyurt	0.036294	36.29
SK-21	Ilgın	0.038805	38.80
SK-22	Piyadeler	0.062595	62.59
SK-23	Yeşilkavak	0.046808	46.80
	Mean		43.09

The recharge value of 19 research wells is range from 21.78 mm/year to 68.52 mm/year, and the mean value of the recharge was obtained 43.09 mm/year (Table 4.14). This value accounts for 10% of the precipitation rate handled in the HYDRUS-1D program. About 10% recharge value represents the recharge coefficient for the study area.

In order to be able to interpret how recharge values are distributed within the basin in the modelling study, a spatial distribution map of point recharge values was prepared (Figure 4.20).

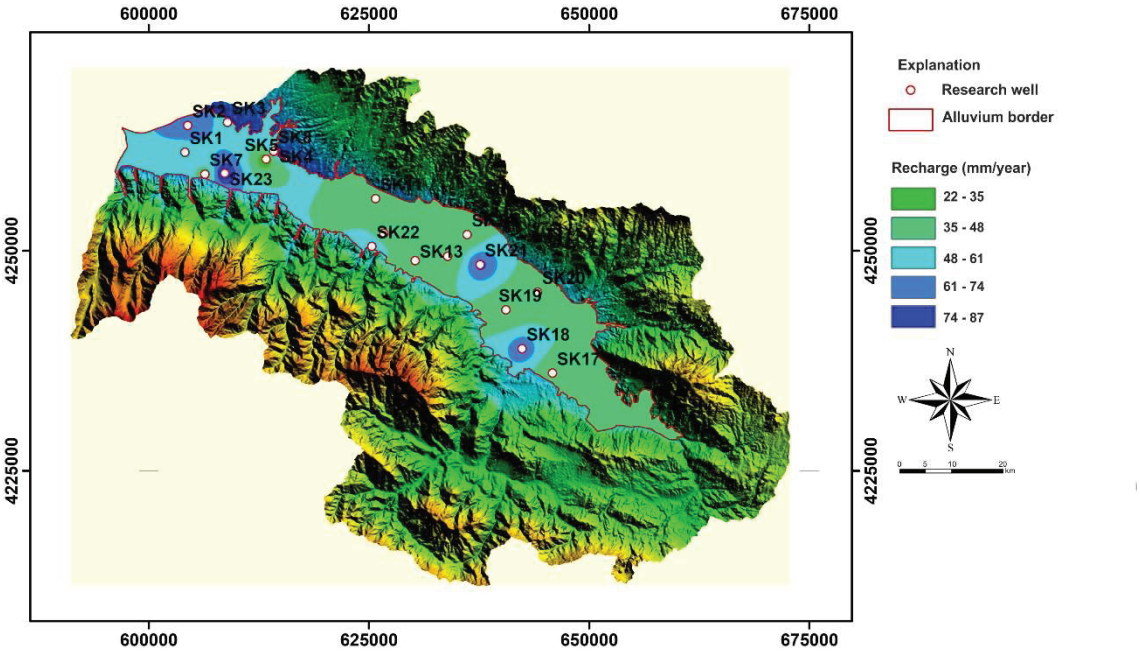

Figure 4.20. Alaşehir sub-basin recharge values distribution map created according to HYDRUS-1D model

The obtained HYDRUS-1D point recharge values do not reflect recharge in permeable stream beds and coastal alluvial fans. As shown in Figure 4.20, higher recharge values were obtained in the west part of the basin, while lower recharge values were obtained in the east of the basin. The highest recharge values were obtained in SK-3, SK-4, SK-7, SK-18 and SK-22 wells. It is thought that the most important factor here is the soil class in the unsaturated zone. When the SK-18 and SK-17 wells were compared, the presence of some gravel units in the well of SK-18 was directly increased recharge value (Figure 4.20).

The west part of the basin contains some gravel units compared to east parts. Therefore, higher recharge values were obtained in the west part of the study area (Figure 4.20). Recharge values obtained from the HYDRUS model yielded results consistent with alluvium aquifer hydraulic conductivity distribution map. It has been concluded that in the basin where the hydraulic conductivity increases, the recharge values increase. Therefore, the recharge mechanism of the alluvium aquifer is controlled by soil class and hydraulic conductivity values.

In the HYDRUS model, the value of water mass on the surface to vertical infiltration is considered. Rainwater is retained as water content when passing through unsaturated zone. So, in the basin, when the soil exceeds the moisture content, the infiltration starts.

4.5.1.6. Model Calibration and Validation

Model calibration is generally defined as the process of tuning a model for a particular problem by manipulating the input parameters (e.g., soil hydraulic parameters) and initial or boundary conditions within reasonable ranges until the simulated model results closely match the observed variables. In the HYDRUS-1D, inverse modeling is a form of model calibration. Inverse modeling requires a set of observed data, such as measured water contents or pressure heads. In model calibration, the objective is usually to obtain better model predictions. The HYDRUS models have an inverse modeling capability (Figure 4.21).

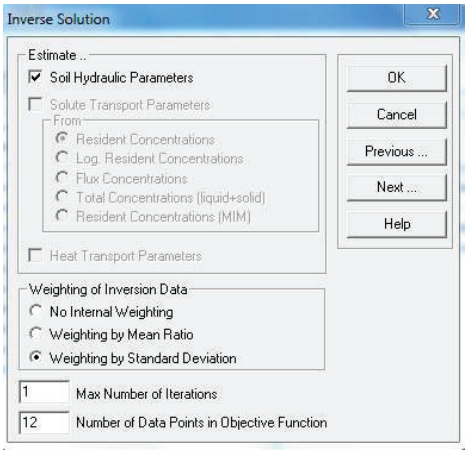

Figure 4.21. Inverse solution window in the parameter optimization

The measured data to be used in the objective function were entered in the data for inverse solution window. In objective function, number of data points were set to 12. It represents months for one year period (Figure 4.21).

In this study, monthly mean observed water contents from soil moisture sensor located in Hacılı region and SK-2 well were used to calibrate the HYDRUS-1D model for one year (Figure 4.22). In Figure 4.22, Type was set to a value of 2 for all water content measurements. In this case, X is time, Y is the observed data and Position is the observation node corresponding to where the water content is measured. When iType(i)=2, iPos(i)=0 represents the average water content of the entire transport domain. The observed and predicted water content after running HYDRUS-1D are shown in Figure 4.23. The final model simulation was a good fit to the observed water content and predicted water content (Figure 4.23).

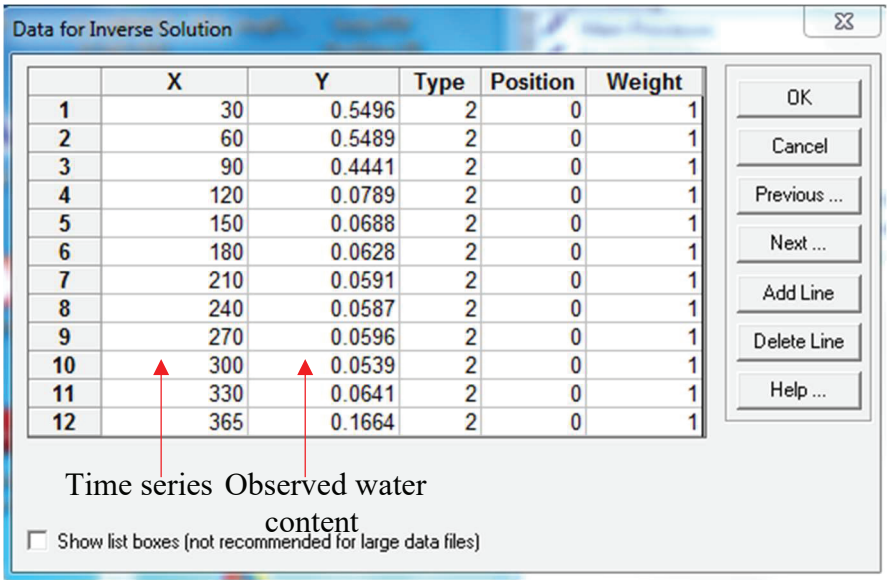

Figure 4.22. Data window in inverse solution

In this study, monthly mean observed water contents from soil moisture sensor located in Hacılı region and SK-2 well were used to calibrate the HYDRUS-1D model for one year (Figure 4.22). In Figure 4.22, Type was set to a value of 2 for all water content measurements. In this case, X is time, Y is the observed data and Position is the observation node corresponding to where the water content is measured. When iType(i)=2, iPos(i)=0 represents the average water content of the entire transport domain. The observed and predicted water content after running HYDRUS-1D are shown in

Figure 4.23. The final model simulation was a good fit to the observed water content and predicted water content (Figure 4.23).

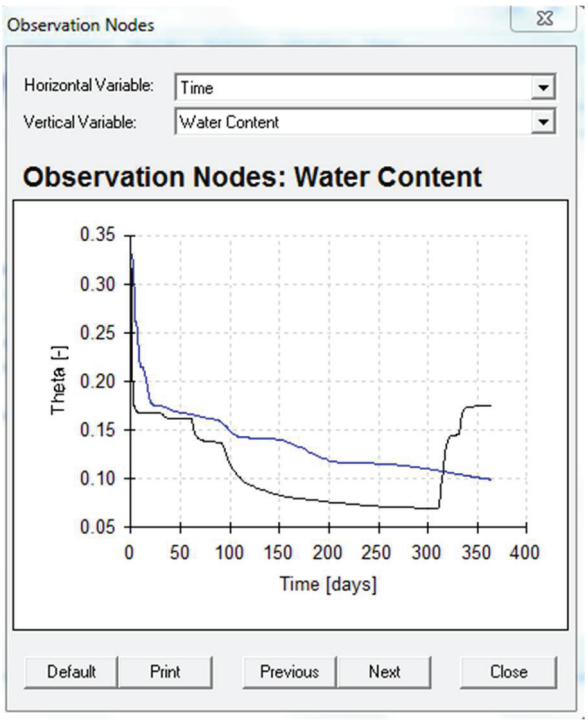

Figure 4.23. Observed (black curve) and predicted (blue curve) water content in the parameter optimization

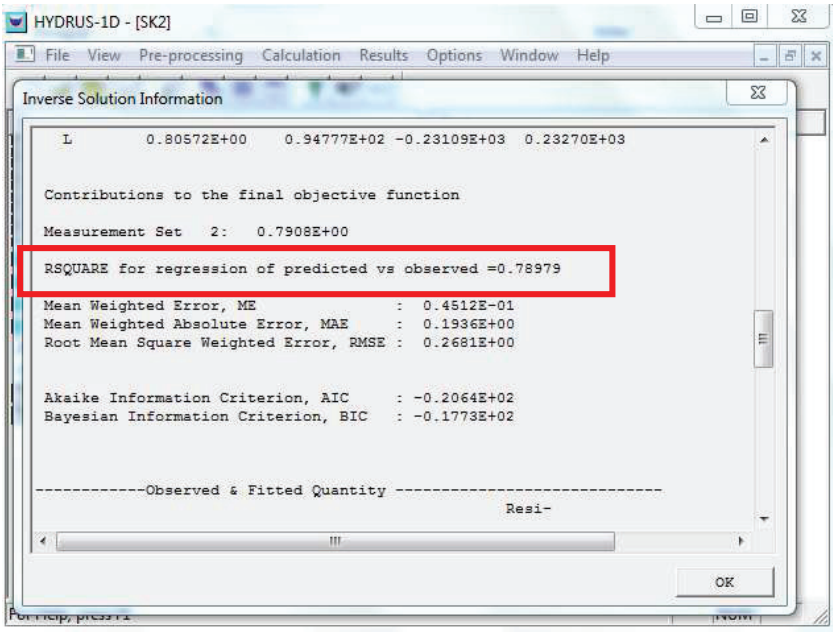

Figure 4.24. Iteration results from the parameter optimization

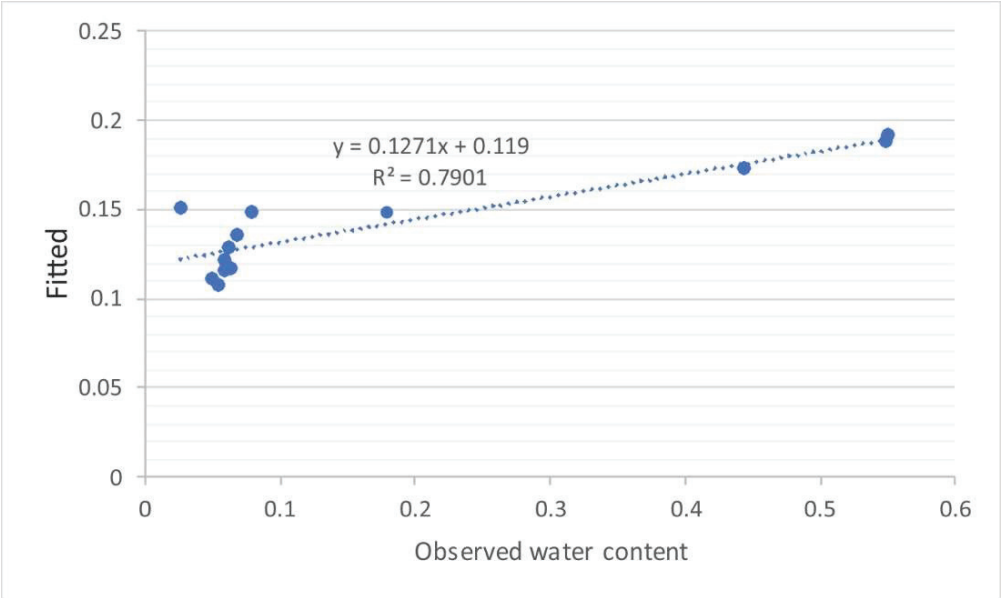

Figure 4.25. R^2 for regression of predicted and observed

The agreement between predicted and observed moisture data was evaluated by the coefficient of determination (R^2), the Nash-Sutcliffe model efficiency coefficient (NSE) and the root mean square error (RMSE). In this study, R^2 was used for model calibration. R^2 describes the proportion of the variance in measured data explained by the model. R^2 ranges from 0 to 1, with values greater than 0.5 considered to be acceptable (Moriasi et al., 2007).

As illustrated in Figure 4.25, a good agreement between modeled and observed soil moisture content as indicated by high R^2 which was found 0.79.

Based on these results, the limitations of the HYDRUS-1D model are given following.

- Core drilling and laboratory tests are needed for the HYDRUS-1D model.
- HYDRUS-1D model can only be modeled using research drilling data. For this reason, it is a more expensive method than the Chloride Mass Balance Method.
- HYDRUS-1D models only the vertical flow as a point.
- For point-based uses; the model only gives surface infiltration and does not take into account the lateral recharge of the aquifer.
- HYDRUS-1D can be used in regional or natural groundwater recharge studies rather than aquifer based studies.

4.5.2. Chemical Method Results

Groundwater recharge can also be estimated by chemical methods. Chloride Mass Balance Method results used in this study are given in detail below.

4.5.2.1. Chloride Mass Balance Method

The amounts of chloride recharge in the wells were calculated using Eq. (2.8) and the results are presented in Table 4.15.

Table 4.15. Alaşehir sub-basin wet and dry period chloride concentrations and chloride recharge values

Well ID	Coordinate			Chloride Concentration (mg/l)			
	x	y	z	Wet Period	Dry Period	Mean Cl^- concentration	Recharge (mm/year)
SK-1	604121	4261160	88	10	25	17.50	130.57
SK-2	604422	4264194	101	35	43	39.00	58.59
SK-3	608939	4264553	97	142	52	97.00	23.56
SK-4	614316	4261311	121	209	123	166.00	13.77
SK-5	613324	4260377	105	53	39	46.00	49.67
SK-6	614345	4253994	211	54.1	30	42.05	54.34
SK-7	606376	4258683	131	17	12	14.50	157.59
SK-8	614192	4261269	115	74	54	64.00	35.70
SK-9	618086	4254018	143	15		15.00	152.33
SK-10	626711	4251955	148	25	21	23.00	99.35
SK-11	625770	4255886	125	105	58	81.50	28.04
SK-12	633947	4249342	143	250		250.00	9.14
SK-13	630254	4248858	101	15	15	15.00	152.33
SK-14	636158	4251807	148	92	95	93.50	24.44
SK-19	640552	4243264	170	18	16	17.00	134.41
SK-20	644149	4245284	170	33	29	31.00	73.71
Mean							74.85
Recharge (%)							16.38

As shown in Table 4.15, in the wells where the chloride concentration of the groundwater increased, the amount of recharge decreased. The mean recharge value in the Alaşehir sub-basin was found as 16.38% according to the Chloride Mass Balance Method. In the study area, 5 mg/l was used for rainwater chloride concentrations, which is the average of three rainwater samples taken during the wet period. According to this, when 457 mm/year rainfall rate measured from weather stations for the study area is used, infiltration rate was found as 16.38% (Table 4.15). As can be seen from Table 4.15, the chloride recharge value is higher than the HYDRUS-1D model. This is because, in the Chloride Mass Balance Method, lateral recharge values in the basin are also taken into account. Especially the west part of the study area is where there are dense river drainage networks. Therefore, in the west part of the study area there is a high lateral recharge. However, the HYDRUS-1D model does not take into account the lateral recharge values in the recharge estimation studies.

In order to better interpret the amount of chloride recharge in the Alaşehir sub-basin, chloride recharge distribution map was obtained (Figure 4.26).

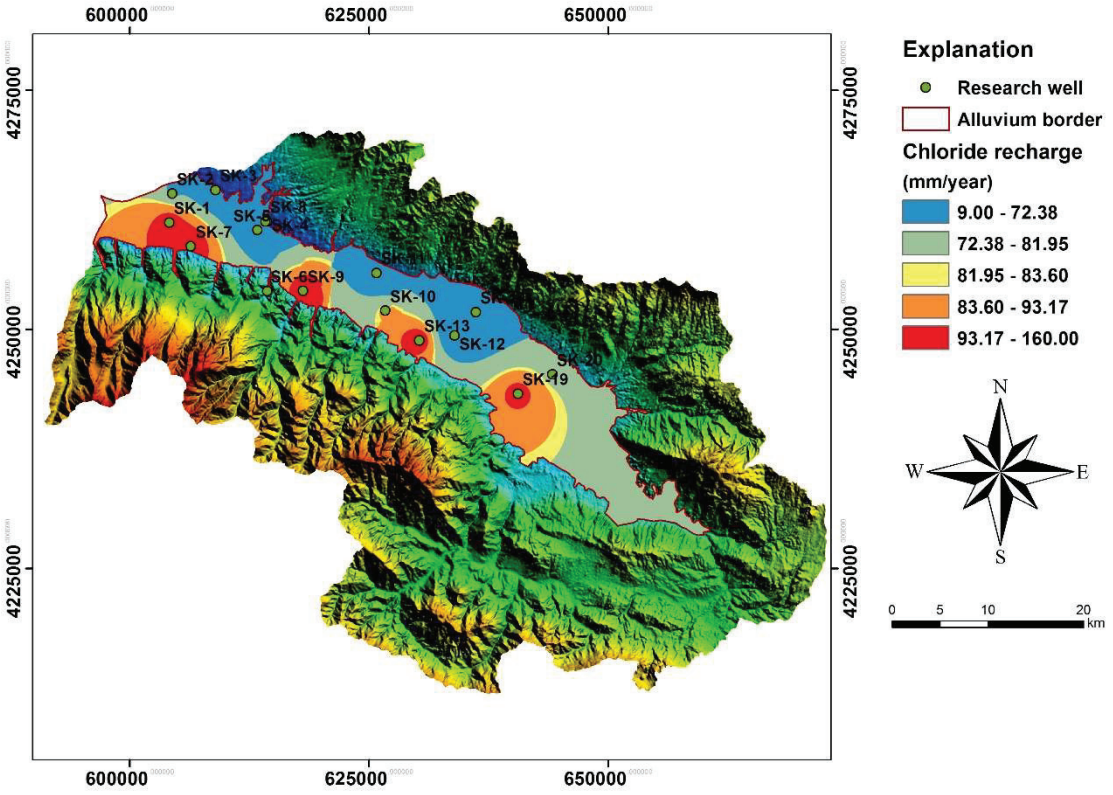

Figure 4.26. Chloride recharge distribution map for the Alaşehir sub-basin.

The distribution map of recharge indicated that high recharge values were obtained in the south-eastern and south-western regions of the study area (Figure 4.26).

As a result, when using this method, the mean rainwater chloride concentration should be determined by rainwater sampling during wet period. If the Chloride Mass Balance Method is applied quickly and economically, results can be achieved that can be used as an approach to the amount of recharge.

4.6. Mixing Mechanism of Groundwater and Geothermal System

The distribution map of groundwater and geothermal wells available in the basin was established in order to interpret the mixing mechanism of groundwater and geothermal fluid in the study area (Figure 4.27).

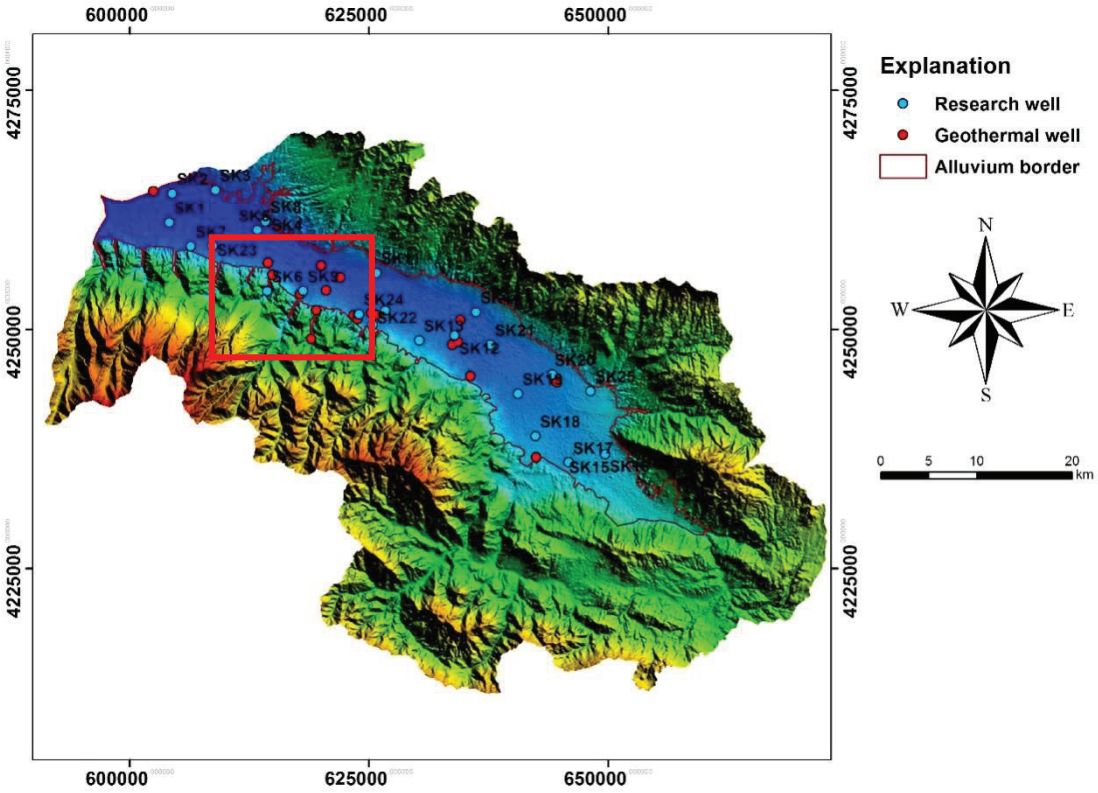

Figure 4.27. Distribution map of research wells and geothermal wells in the study area

As can be seen from Figure 4.27, the geothermal wells in the basin are concentrated in the Göbekli, Çağlayan and Piyadeler villages located in the middle part.

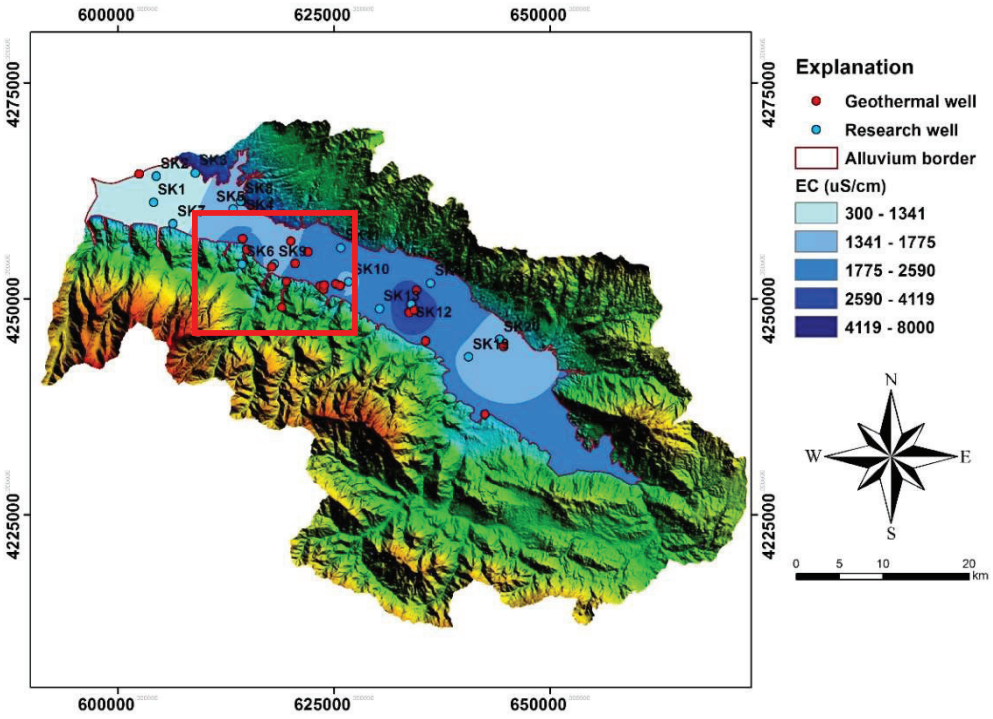

(a) Wet period

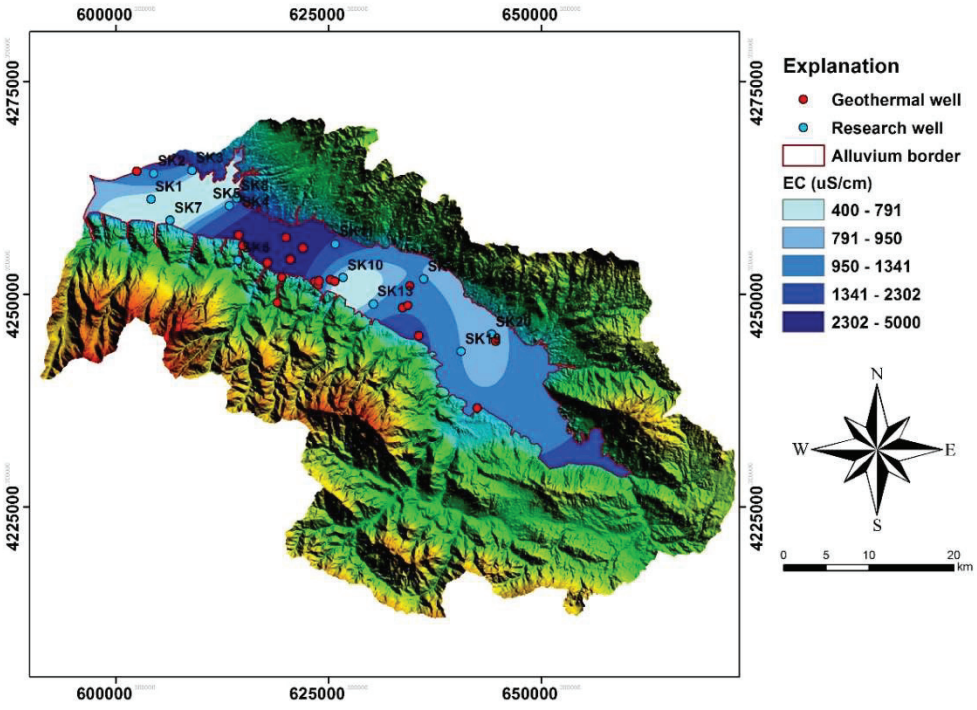

(b) Dry period

Figure 4.28. EC distribution maps of groundwater and geothermal wells in the study area. (a) Wet period, (b) Dry period

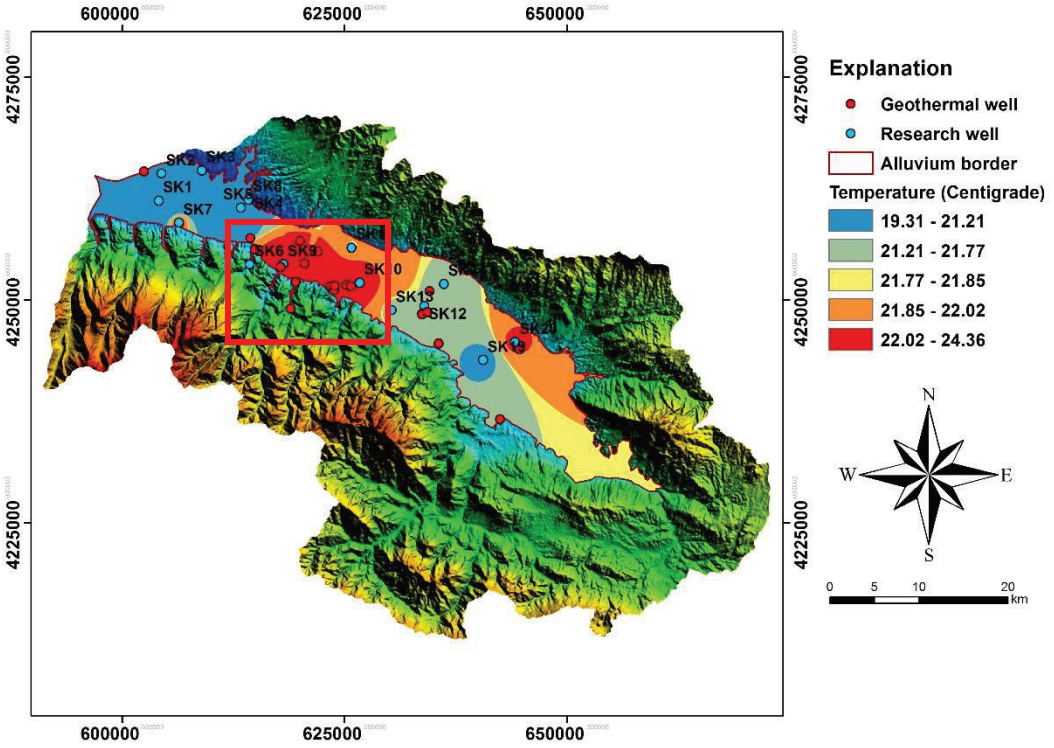

(a) Wet period

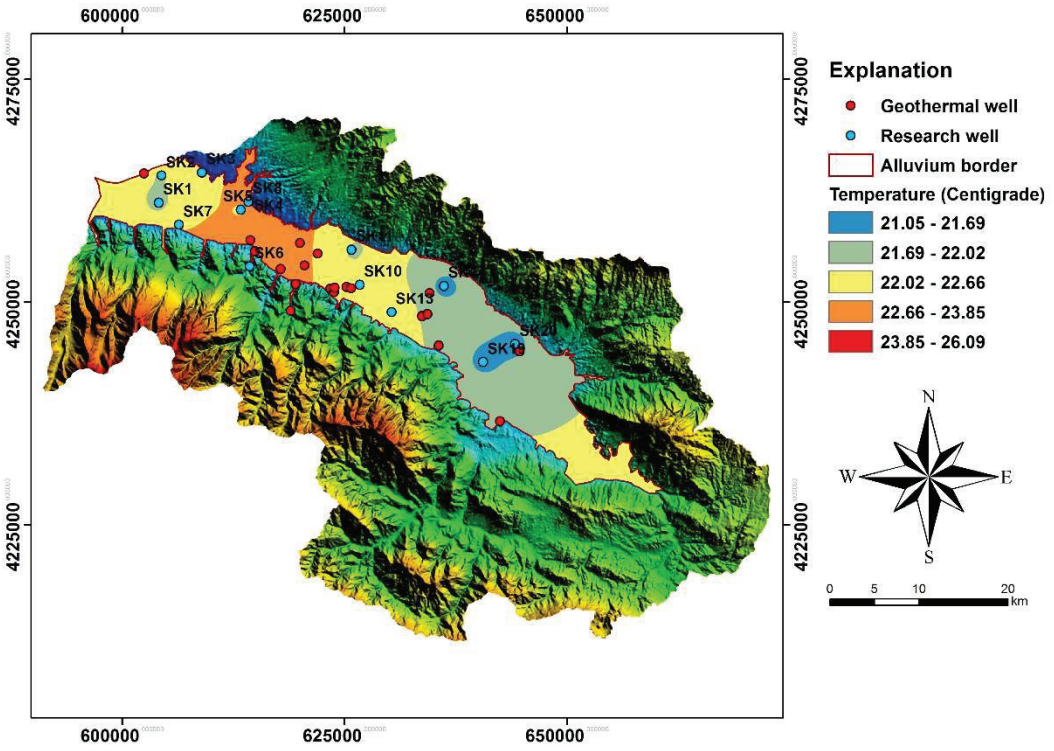

(b) Dry period

Figure 4.29. Temperature distribution maps of groundwater and geothermal wells in the study area. (a) Wet period, (b) Dry period

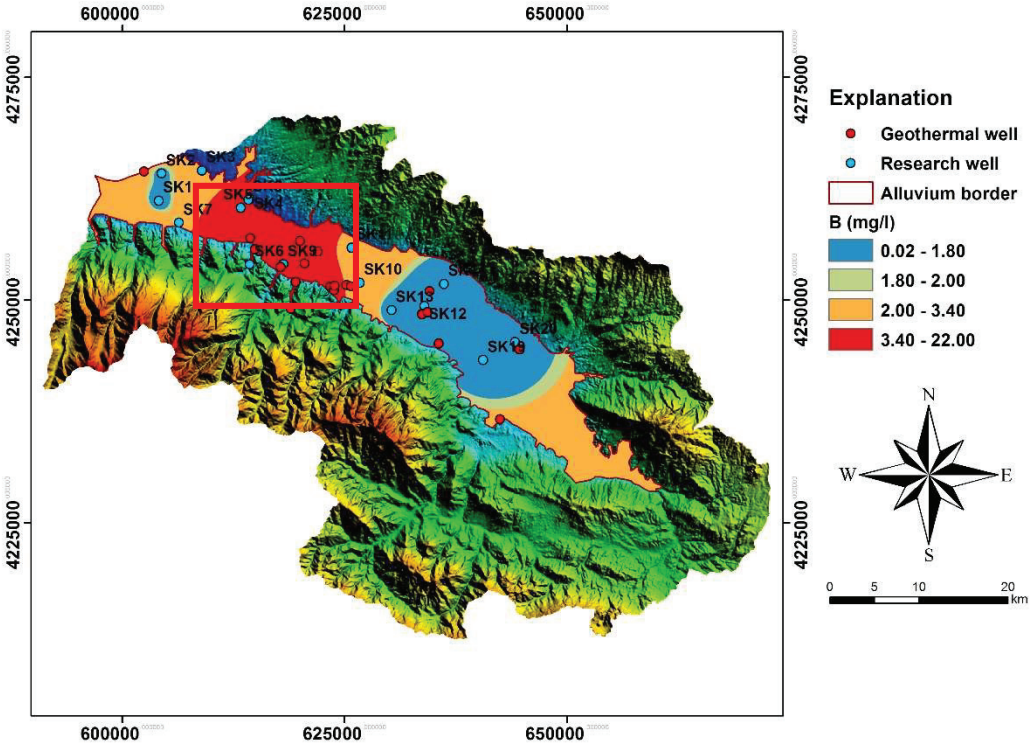

(a) Wet period

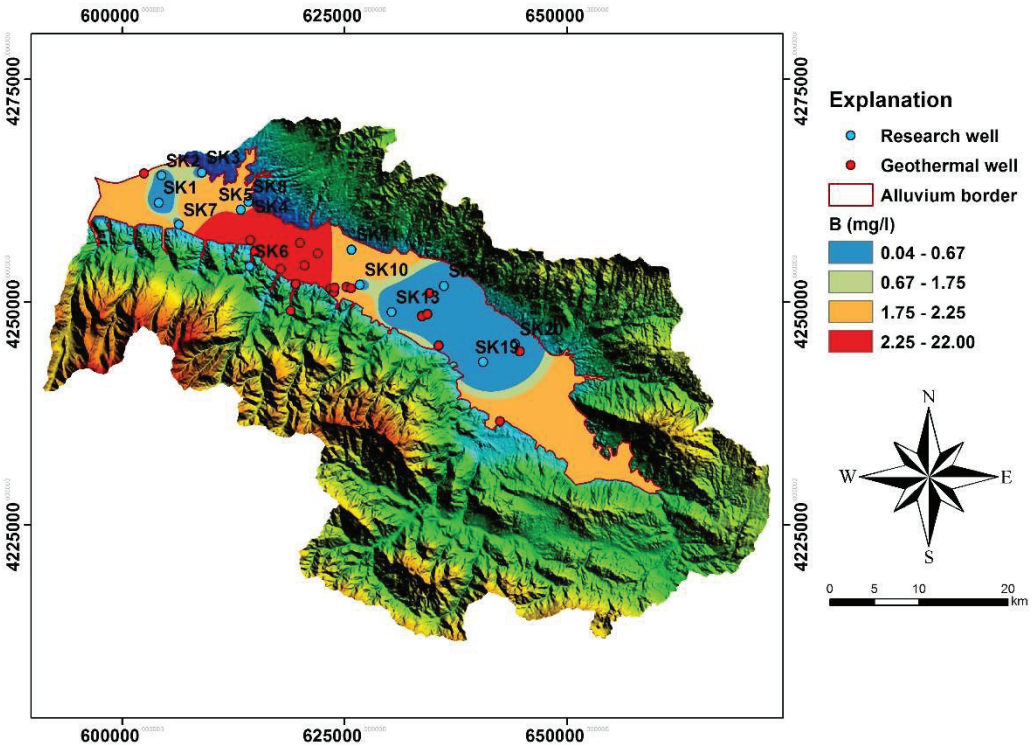

(b) Dry period

Figure 4.30. Boron distribution maps of groundwater and geothermal wells in the study area. (a) Wet period, (b) Dry period

Electrical Conductivity (EC), temperature and Boron distribution maps were prepared for wet and dry period in order to determine the analysis effect of geothermal fluid on groundwater resources. Parameters of geothermal wells were not included in the interpolation when EC, temperature and Boron distribution maps were created.

EC distribution map show that the highest EC values in the wet and dry period are areas where the geothermal application is intensive. The lowest EC values were recorded in the SK-1 well and in the western part of the area. This is because the SK-1 well is not affected by the geothermal fluid in the basin (Figure 4.28a and Figure 4.28b).

The distribution map temperature show that the high temperature values are obtained in SK-6 well in both periods and it means the well affected by geothermal fluid (Figure 4.29a and Figure 4.29b).

Boron is an important indicator and gives important information about the mixing mechanism of geothermal fluid and groundwater. The Boron distribution maps show that SK-6 has high concentration in both periods. Boron exceeds groundwater limits (Figure 4.30a and Figure 4.30b).

In order to determine the mixing mechanism of groundwater and geothermal fluid in the study area, KLM-2 geothermal well studied by Rabet (2014) in the same region was taken as a reference well. The location of this well with the research wells in the region is given in Figure 4.31.

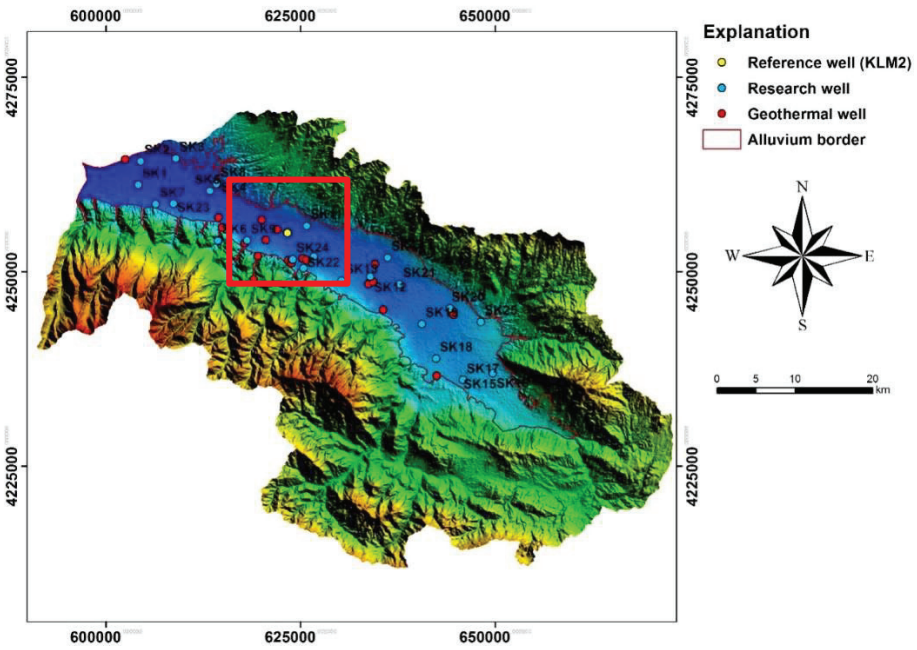

Figure 4.31. Research wells, geothermal wells belonging to private companies in the Alaşehir sub-basin and location map of reference geothermal well

Table 4.16. The physical and chemical properties of KLM-2 geothermal well (Source: Rabet, 2014)

Parameter	Value
pH	8.72
T (°C)	100
EC (μS/cm)	2860
Ca^{2+} (mg/l)	7.2
Mg^{2+} (mg/l)	1
Na^{+} (mg/l)	1006
K^{+} (mg/l)	53
SO_4^{2-} (mg/l)	52
HCO_3^{-} (mg/l)	1450.46
CO_3^{-}(mg/l)	54.12
Cl^{-} (mg/l)	1747.82
B (mg/l)	127.62

$$C_1 \times Y_1 + C_2 \times Y_2 = M \times R \quad (4.1)$$

Where C_1 is Boron value in the research well (mg/l), C_2 is Boron value in the geothermal well (mg/l), Y_1 and Y_2 are mixing ratio, M is mixture amount (mg/l) and R is percentage rate (%).

The physical and chemical properties of KLM-2 geothermal well are presented in Table 4.16.

KLM-2 well, SK-1, SK-13 and SK-19 well were mixed 10%, 20%, 30%, 40% and 50% in the AquaChem program according to the Eq. (4.1) to determine the mixing mechanism of the research wells and the geothermal system in the study area. The reason for the selection of the SK-1, SK-13 and SK-19 well is that they provide low EC, temperature and Boron values during the wet and dry period. So, SK-1, SK-13 and SK-19 well were not affected by the geothermal fluid in the area. The results of the obtained geothermal mixture ratio are presented in Figure 4.32.

According to the results, the Boron values of the SK-6 well affected by the geothermal fluid in the study area are overlapped in the Boron graphs for mixture ratios. These wells are thought to be affected by the geothermal system. Because, high boron values were obtained in the wet and dry periods in these wells. When mixing ratios were calculated, the water chemistry of the SK-1 and SK-6, SK-13 and SK-19 wells during the wet period was considered. The reason for this is that there is a lot of water circulation in this period.

According to Figure 4.32, a mixture was found as 17% depending on the Boron in the SK-6 well.

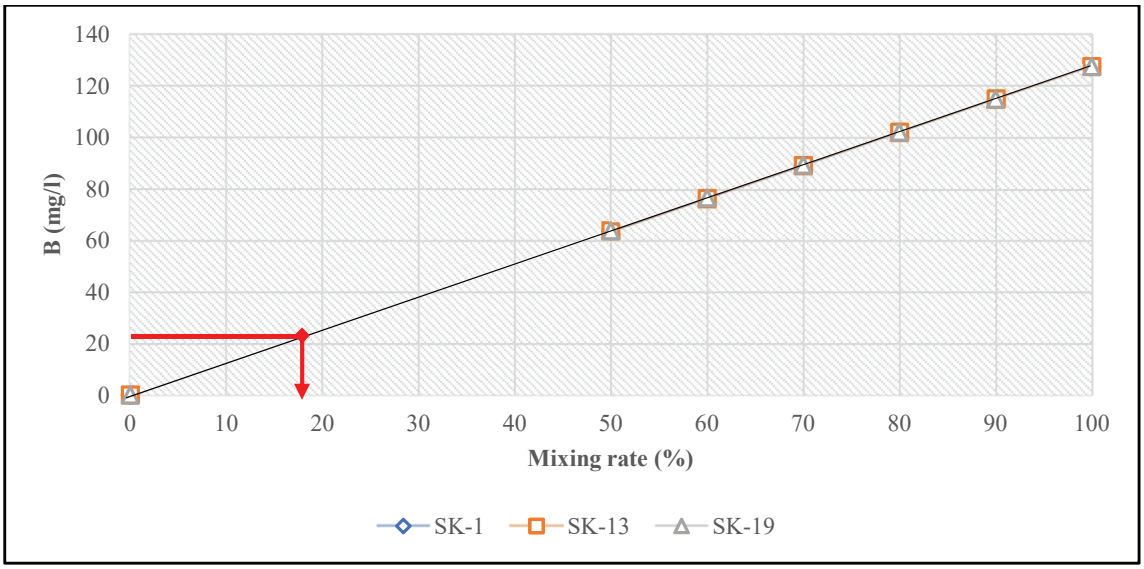

Figure 4.32. Geothermal well mix ratio due to Boron in SK-6 well

CHAPTER 5

CONCLUSION

The consumable water resources are decreasing from day to day in parallel with the decrease of surface and groundwater level as well as with the increase in population both in the world and in Turkey. Turkey is located on a zone where the global climate change effect and the precipitation decrease and the temperature increases. In recent years, the effects of climate change have reached considerable levels. The most important effects of climate change can be explained by the fact that today, due to the effect of high evaporation, there is a continuous decline in surface water resources, lakes, dams and rivers (Aküzüm et al., 2010).

Being an agriculture and industry region, the agriculture and animal husbandry is the subsistence of the population in Alaşehir sub-basin. The recent reduction in precipitation and high evaporation rates in the region has increased the groundwater requisition for agricultural irrigation.

Within the context of this study the groundwater recharge has been carried out for the sustainability of alluvium aquifer in the Alaşehir sub-basin. Numerical and chemical methods were used to determine the groundwater recharge. In addition, since the study area is located in a region where the geothermal system is concentrated, the mixing mechanism of the groundwater and the geothermal system was revealed.

HYDRUS-1D numerical model was used to determine the annual recharge value for 2017 in the Alaşehir sub-basin. According to the HYDRUS-1D numerical model results the recharge value of annual rainfall which was applied to 19 research wells that opened to the alluvium aquifer in the area is between 21.78 mm and 68.52 mm and the recharge value from the average rainfall is 43.09 mm. The amount of recharge obtained from direct rainfall corresponds to 10% of the amount of rainfall. This value also represents the recharge coefficient for the study area.

In the Chloride Mass Balance Method in which the recharge value is determined by chemical methods, the recharge value for 2017 was figured. According to this calculation, the mean recharge value was 74.85 mm/year. Thanks to these results, it was understood that the amount of the recharge from the surface was 16.38%.

Comparing the recharge results obtained from the numerical model and the chemical method, a higher recharge value was obtained for the alluvium aquifer in the chemical method. The reason of this difference is that the recharge values calculated in the HYDRUS-1D model express the recharge value only vertically infiltered from the surface. The HYDRUS-1D model assumes no lateral recharge. The recharge value calculated in the chemical method is higher due to the vertical and lateral recharge in the basin. The west part of the alluvium aquifer is under the influence of lateral recharge.

The Chloride Mass Balance Method emerges as a suitable method for alluvium and karstic aquifers in Turkey. Because the alluvium and karstic aquifers are unconfined aquifers that react quickly to precipitation.

In addition, the mixing ratio of the groundwater and geothermal system in the SK-6 well is 17%. It is suggested that in the Chloride Mass Balance Method, the alluvium aquifer is recharged entirely from rainwater and used in areas where there is no pollutant effect in the system. According to this, in consideration of two different methods for the Alaşehir sub-basin, it is seen that the HYDRUS-1D model in which the amount of 10% recharge value obtained, provides a more accurate approach.

The HYDRUS-1D model has some disadvantages when used for recharge basins. Long-term groundwater monitoring and meteorological monitoring methods using in the HYDRUS-1D model and drilling the research wells for the characterization of the aquifer are the time-consuming and cost-increasing factors. However, in the Chloride Mass Balance Method, recharge value can be estimated more quickly and economically based only on the amount of precipitation and chloride concentrations between groundwater and rainwater.

According to the recharge values obtained from both methods, high evaporation values and excessive water withdrawal in the Alaşehir basin will continue to threaten groundwater resources today and in the future.

APPENDIX A

LABORATORY SOIL EXPERIMENT RESULTS

Table A.1. SK-1 well laboratory soil experiment results

SK-1					
Depth (m)	Water Content (%)	Natural Mass (g/cm^3)	Specific Gravity	Porosity	Soil Class
1.5-3	27.62	1.91	2.72	0.45	SC
3-4.5	15.93	2.18			CL
4.5-6	6.24				GM
6.8-7.5	25.84	2.09			GC
7.5-8.5	12.92				GC
8.5-9	9.25	2.15			GP-GC
9.7-10.5	22.08	2.07	2.71	0.37	GC
11.0-12.0	16.53				GC
12.5-13.5	7.06				GP-GC
13.5-15	17.43	2.05	2.69	0.32	SC
16.5-18	18.78	2.13	2.73	0.34	SC
22-22.5	32.22	1.96			SC
22.5-24.0	25.11	1.97	2.68	0.41	SC
26.4-27	26.21	2.01			
29.5-30	21.86	2.08	2.70	0.37	SC

Table A.2. SK-2 well laboratory soil experiment results

SK-2					
Depth (m)	Water Content (%)	Natural Mass (g/cm^3)	Specific Gravity	Porosity	Soil Class
0-1.5	33.07	1.88	2.62	0.46	SC
1.5-3	33.59	1.72			SC
3-4.5	26.00	1.75	2.72	0.49	SC
4.5-6	28.63				SC
6-7.5	28.34	2.09			SC
7.5-9	19.76				SC
9-10.5	41.54	1.80	2.68	0.53	SC
10.5-12	28.65	1.99	2.71	0.43	SC
12-13.5	22.45				SW-SM

(cont. on next page)

Table A.2. (cont.)

13.5-15	23.87				SM
15-16.5	19.26				
16.5-18	10.42				GW-GM
19.5-21	15.71				GC
21-22.5	18.02				SC
25.5-27	23.78	2.08	2.68	0.37	
27-28.5	25.96	2.01	2.68	0.41	SC
28.5-30	24.59	2.02			

Table A.3. SK-3 well laboratory soil experiment results

SK-3					
Depth (m)	Water Content (%)	Natural Mass (g/cm^3)	Specific Gravity	Porosity	Soil Class
1.3-1.5	9.64				SM
1.7-3	29.67	1.88	2.70	0.42	
3.5-4.5	19.92	2.05			SC
4.8-6	18.27	2.04	2.69	0.34	CL
6.9-7.5	14.70				
8.4-9	14.97	2.07			SC
9.9-10.5	13.15	2.13			SC
10.7-12	16.83	1.97	2.75	0.42	CL
12.5-13.3	22.54	2.06	2.68	0.39	ML
14-15	27.32	1.94	2.70	0.43	CL
15.5-16.5	30.79	1.95	2.72	0.44	
16.5-17.0	28.43	1.96			MH
17-18	29.32				CL
18.5-19.5	20.39	2.14			
20.0-21.0	24.62	2.11	2.72	0.39	CL
21.5-22.5	21.35	2.00	2.61	0.37	
23-24	28.12	1.88			CL
24.5-25.5	26.63	2.21			CL
26.4-27	14.06				GC
28-28.5	12.53				GC
29.2-30	21.46	2.20			SC
30.5-31.4	27.22	1.88			
32-33	30.69	1.93			
33.7-34.5	23.63	2.07	2.72	0.38	CL
34.9-36	25.66	2.11			CH

(cont. on next page)

Table A.3. (cont.)

36-37.5	19.66				
37.8-39	19.40	2.07	2.64	0.34	ML
39.5-40	18.22	2.15	2.72	0.33	SM

Table A.4. SK-4 well laboratory soil experiment results

SK-4					
Depth (m)	Water Content (%)	Natural Mass (g/cm^3)	Specific Gravity	Porosity	Soil Class
1-1.5	24.57	1.99	2.57	0.38	CH
1.5-3	26.94				CL
3-4.5	27.09	2.10			
4.5-6	23.50	1.97			CH
6.5-7.5	32.05	1.90	2.84	0.47	CL
8.0-9.0	25.93	2.00			CH
10-10.5	24.24	1.49	2.72	0.58	
11.5-12	30.39	1.90	2.67	0.46	ML
14.2-15	32.83	1.96			ML
15.7-16.5	26.75	1.93	2.69	0.44	ML
17.2-18	27.62	2.14			ML
19-19.5	25.96	2.04			
20.4-21	31.02	1.92			CL
22-22.5	16.67				CL
23.5-24	32.32	2.03	2.73	0.45	CL
25-25.5	34.66				SC
26.2-27	28.28	1.91			
27.5-28.5	28.73		2.64		
29-30	27.65	1.99	2.73	0.43	CL
30.6-31.5	26.51	2.03	2.71	0.38	SC
32.1-33	20.57	2.17	2.76	0.31	
33.5-34.5	13.49	2.15			
35.1-36	21.41	2.12			CL
36.3-37.5	27.52	2.10			CL
37.5-39	23.11	2.16			
39-40.5	26.29	2.03			
42.5-43.5	22.43	2.12			
46.6-48	21.19	2.17			
48.5-49.5	20.80	2.05			
50-51	20.44	2.06	2.68	0.36	SM

Table A.5. SK-5 well laboratory soil experiment results

SK-5					
Depth (m)	Water Content (%)	Natural Mass (g/cm^3)	Specific Gravity	Porosity	Soil Class
0.9-1.5	28.98		2.72		
2.0-3.0	33.85	1.84	2.63	0.48	
5.0-6.0	22.12				SP-SM
6.5-7.5	42.10	1.98	2.64	0.48	CL
7.9-9	45.74	1.90	2.48	0.47	
9.7-10.5	27.67	1.75	2.66	0.49	CL
11.2-12	19.60	2.22	2.72	0.32	
12.9-13.5	29.92	1.99	2.65	0.42	SM
14.2-15	27.17	2.06			CL
16-16.5	25.00	2.01	2.73	0.41	CL
17.4-18	15.31				GP-GM
18-20					GP
20-20.5	16.55				GM
20.5-21	14.63	2.24	2.74	0.29	GM
22-22.5	3.25				GP-GM
23.4-24	5.66				GM
24.0-25.0	26.20	1.99	2.71	0.42	CL

Table A.6. SK-6 well laboratory soil experiment results

SK-6					
Depth (m)	Water Content (%)	Natural Mass (g/cm^3)	Specific Gravity	Porosity	Soil Class
2.0-3.0	6.72		2.70		SC
4.0-4.5	3.74				GC
7.0-7.5	4.52				GP
10.0-10.5	38.43				GP-GC
11.2-12.0	43.02				GC
14.2-15	3.62				GP
16-16.5	2.53				GP-GC
17.2-18	6.60				GC
19-19.5	14.89				SC
20.3-21	3.61				
23.0-24.0	10.44		2.69		SM
27.5-28.5	10.10		2.74		CL

(cont. on next page)

Table A.6. (cont.)

29-30	9.13				ML
30.5-31.5	10.44				ML
32.3-33	10.69				
34.2-34.5	9.72				GC
34-36	10.29				CL

Table A.7. SK-7 well laboratory soil experiment results

SK-7					
Depth (m)	Water Content (%)	Natural Mass (g/cm^3)	Specific Gravity	Porosity	Soil Class
1.0-1.5	13.37				SC
2.5-3.0	9.04				GC
4-4.5	15.48				SC
5.0-6.0	17.02				CL
6.7-7.5	23.13	2.03			CL
8.2-9.0	13.28	2.03	2.72	0.34	
10.0-10.5	13.12	2.02	2.79	0.36	
11.5-12.0	15.00				
13.1-13.5	7.14				GC
14.5-15	2.26				GP-GC
15-16.5					GP
20.7-21	7.21				GC
24-25.5					
27-28.5	18.27				GC
28.5-44					GP
44.0-45.0	19.59	2.12			GC

Table A.8. SK-8 well laboratory soil experiment results

SK-8					
Depth (m)	Water Content (%)	Natural Mass (g/cm^3)	Specific Gravity	Porosity	Soil Class
2.0-3.0	17.53				GC
4.0-4.5	10.54				GC
5.5-6.0	9.31				GC
7.1-7.5	16.27				SC
8.4-9	21.28				SC

(cont. on next page)

Table A.8. (cont.)

10.2-10.5	24.84				CL
11.6-12	11.00				CL
13-13.5	4.55		2.65		GC

Table A.9. SK-9 well laboratory soil experiment results

SK-9					
Depth (m)	Water Content (%)	Natural Mass (g/cm^3)	Specific Gravity	Porosity	Soil Class
0-1.5	5.24				SP
1.5-3	4.49				GP
3-4.5	0.78				GP
4.5-31.5					GP
31.5-32	12.90				GC
34-34.5	15.78				GC
34.5-45					GP

Table A.10. SK-10 well laboratory soil experiment results

SK-10					
Depth (m)	Water Content (%)	Natural Mass (g/cm^3)	Specific Gravity	Porosity	Soil Class
0-13.5					GP
13.5-15	14.18				SC
15-16.5	11.78				SC
16.95-18	22.39	2.08	2.7	0.37	SC
18.5-19.5	20.52				SC
19.5-24.5					GP
24.5-25.5	24.78	1.95	2.64	0.41	SC
25.5-28.5	16.46	2.12	2.65	0.31	SC
28.5-50					GP

Table A.11. SK-11 well laboratory soil experiment results

SK-11					
Depth (m)	Water Content (%)	Natural Mass (g/cm^3)	Specific Gravity	Porosity	Soil Class
1.0-1.5	29.17	1.76			

(cont. on next page)

Table A.11. (cont.)

2.3-3.0	28.51	1.94	2.78	0.46	ML
3.7-4.5	37.09	1.75			
5.4-6.0	37.23	1.86	2.72	0.50	ML
6.9-7.5	36.87	1.85	2.70	0.50	GC
9-13.5					GP
14.4-15.0	28.13				
16.1-16.5	27.99	1.94			
17.5-18.0	32.92	1.93	2.71	0.46	CL
20.6-21.4	31.01	1.87			SC
22.2-22.5	31.73	2.03			SC
22.5-25.5					GP
26.4-27.0	30.44	1.88			CL
28.0-28.5	27.69	1.91	2.73	0.45	MH
29.3-30.0	19.45	2.12			CL
30.8-31.5	20.26				
32.5-33.0	22.09	2.01			SC
33.9-34.5	27.06				CL
35.5-36.4	22.32	2.02			SC
40.0-40.5	22.21		2.73		GC
41.6-42.0	15.42				
44.6-45.0	19.10				GC
46.0-46.5	14.24				

Table A.12. SK-12 well laboratory soil experiment results

SK-12					
Depth (m)	Water Content (%)	Natural Mass (g/cm^3)	Specific Gravity	Porosity	Soil Class
0.5-1.5	24.07	1.85			CL
2.0-3.0	25.03				GC
3.5-4.5	31.31	1.75			MH
5.5-6.0	19.78	1.97			ML
7.0-7.5	23.68				ML
8.5-9.0	26.42				CL
10-10.5	34.97				CL
11.3-12.0	34.75				
12.5-13.5	27.97	1.98			
14.0-15.0	24.36	2.09	2.78	0.39	CL

(cont. on next page)

Table A.12. (cont.)

17.4-18.0	23.32				CL
24-24.5	27.28				CL
26.0-27.0	24.62				
29.5-30	22.75				CL
32.3-33.0	32.17	1.89	2.71	0.47	CL
33.6-34.5	21.52	2.10	2.68	0.36	SC
35.5-36.5	22.04				
37.0-37.5	18.48				GC
38.5-39.5	26.27				
41.5-42.0	28.86				CL
43.0-43.5	20.67	1.94			CL
44.5-45.0	23.27	1.83			CL
46.1-46.4	22.27	1.91			
47.0-48.0	18.20				SC

Table A.13. SK-13 well laboratory soil experiment results

SK-13					
Depth (m)	Water Content (%)	Natural Mass (g/cm^3)	Specific Gravity	Porosity	Soil Class
1.0-1.5	19.76	1.94	2.73	0.41	CL
2.2-3.0	16.91				CL
3.8-4.5	14.76				CL
4.5-6	10.59				GP
6-7.5	19.88				GP
7.5-10.5	15.75				SC
11.4-12.0	15.67				GC
13-13.5	20.56				CH
13.5-15					GP
15-16.5	6.94				GC
16.5-22					GP
23.5-24	17.80	2.01	2.77	0.39	SC
25.1-25.5	8.82				GC
29-30	17.97				SC
32.4-33	20.36	2.09	2.72	0.36	GC
35.6-36.0	31.04	1.89			
38-39	6.91				GC
41-45	16.95				
47-48	25.63	2.05	2.78	0.41	CL

Table A.14. SK-14 well laboratory soil experiment results

SK-14					
Depth (m)	Water Content (%)	Natural Mass (g/cm^3)	Specific Gravity	Porosity	Soil Class
1-1.5	31.23		2.65		CL
2.0-3.0	31.50		2.72		CL
4.0-4.5	33.21	1.84	2.73	0.49	CL
5.4-6	37.62	1.71	2.83	0.56	CL
7.1-7.5	37.55	1.81	2.71	0.51	CL
8.2-9.0	34.92	1.96			CL
10-10.5	39.60		2.90		CL
11.0-12.0	42.98	1.80			CL
14.0-15.0	33.07	1.74	2.67	0.51	SC
17.0-18.0	22.26		2.70		SC
20.1-21	41.17				SC
23.0-24.0	44.63				SC
26.0-27.0	28.94				CL
29.5-30	28.49	1.86	2.61	0.45	CL
32-33	22.10		2.89		GC
41.0-42.0	17.81				GC
42.5-43.5	35.27	1.91	2.72	0.48	CL
44.0-45.0	23.12	2.10	2.65	0.36	SC
45.5-46.5	20.23	2.05	2.67	0.36	SC
48.5-50	19.78	1.74	2.67	0.46	

Table A.15. SK-15 well laboratory soil experiment results

SK-15					
Depth (m)	Water Content (%)	Natural Mass (g/cm^3)	Specific Gravity	Porosity	Soil Class
0-8.2					GP
8.2-9	21.52	1.83			CH
9.5-10.5	28.08	1.80	2.78		CL
11.0-12.0	25.28				CH
13-13.5	29.52	1.98			CL
16-16.5	26.58				
16.5-21					GP
21-22.5	25.78				SC
23.2-24	26.31	1.93			SC

(cont. on next page)

Table A.15. (cont.)

24.5-25.5	24.20	1.78	2.72		GC
27-28	3.57				GP

Table A.16. SK-16 well laboratory soil experiment results

SK-16					
Depth (m)	Water Content (%)	Natural Mass (g/cm^3)	Specific Gravity	Porosity	Soil Class
2.0-3.0	20.27		2.76		SC
5.0-6	24.62		2.68		SC
8-9.0	26.41	1.91274	2.66		CH
11.0-12.0	34.19				CL
14.0-15.0	30.32				

Table A.17. SK-17 well laboratory soil experiment results

SK-17					
Depth (m)	Water Content (%)	Natural Mass (g/cm^3)	Specific Gravity	Porosity	Soil Class
2.0-3.0	19.18				SC
5.0-6	16.52		2.67		SC
8-9.0	10.96				SC
11.0-12.0	31.28				
14.0-15.0	32.02	1.90	2.68	0.46	SC
20.0-21.0	25.25				
23.5-24.5	31.97				CL
26.0-27.0	28.15	1.93	2.65	0.43	
29.4-30.0	31.00	1.85			
32.0-33.0	34.27	1.96			CL
35.0-36.0	28.15	1.89	2.83	0.48	SC
38.2-39.0	22.28	2.04	2.68	0.38	SC
41.0-42.0	20.52				SC
44.0-45.0	25.77	2.10	2.78	0.39	
47.0-48.0	20.80	2.04	2.65	0.36	SC

Table A.18. SK-18 well laboratory soil experiment results

SK-18					
Depth (m)	Water Content (%)	Natural Mass (g/cm^3)	Specific Gravity	Porosity	Soil Class
2.0-3.0	21.67	1.99	2.64	0.38	SC
5.0-6	11.57				GC
6.0-50.0					GP

Table A.19. SK-19 well laboratory soil experiment results

SK-19					
Depth (m)	Water Content (%)	Natural Mass (g/cm^3)	Specific Gravity	Porosity	Soil Class
0-3					GP
6.0-11.0					GP
11.0-12.0	54.27	1.81			
14.0-15.0	51.06	1.99	2.71		SC
17.0-18.0	32.27	1.85	2.73	0.49	CL
20.0-21.0	42.29	1.98			CL
23.2-24.0	31.52	1.99	2.75	0.45	CL
26.5-27.0	28.98	1.88			
29.6-30.0	37.21	1.72			
30-39					GP
41.0-42.0	27.27	1.94	2.65	0.42	SC
44.0-45.0	36.94	1.81			
48.0-49.0	34.70	1.84	2.67	0.49	CL

Table A.20. SK-20 well laboratory soil experiment results

SK-20					
Depth (m)	Water Content (%)	Natural Mass (g/cm^3)	Specific Gravity	Porosity	Soil Class
11.0-12.0	31.28	1.90	2.78	0.48	SC
14.2-15.0	26.75	1.82			
17.6-18.0	39.64	1.86	2.72	0.47	SC
20.0-21.0	31.55	1.87	2.75	0.48	CL
23.5-24.5	31.97				
29.1-30.0	19.54	2.01			
23.1-24	22.23	2.06	2.70	0.38	SC

(cont. on next page)

Table A.20. (cont.)

26.0-27.0	30.49	1.91			SC
32.0-33.0	23.10	2.39			
35.2-36.0	23.27	2.41			
38.0-39.0	21.08	2.38			
41.0-42.0	23.57	1.93			SC
44.0-45.0	20.44	2.11	2.72	0.36	SC
47.0-48.0	22.01	1.95			SC

Table A.21. SK-21 well laboratory soil experiment results

SK-21					
Depth (m)	Water Content (%)	Natural Mass (g/cm^3)	Specific Gravity	Porosity	Soil Class
2.0-3.0	40.37		2.74		
5.0-6	39.08	1.88			ML
8-9.0	41.27	1.92	2.83	0.52	GC
11-12.0	38.16	1.89			
14.0-15.0	29.87	1.86	2.76	0.48	
17-18.0	30.48				
23-24	32.03	1.97	2.50	0.40	
26-27	25.30	2.13			SC
29-30	20.19	2.02	2.82	0.40	SC
32.3-33.0	26.34	2.01			
35-36	30.98	2.16			SC
41-42	26.90	1.86			
44-45.0	35.94	1.95	2.63	0.39	SC
49-50	25.84				

Table A.22. SK-22 well laboratory soil experiment results

SK-22					
Depth (m)	Water Content (%)	Natural Mass (g/cm^3)	Specific Gravity	Porosity	Soil Class
0-14					GP
14.0-15.0	13.69				GC
15-18					GP
18-21	12.26				GC
21-29					GP

(cont. on next page)

Table A.22. (cont.)

29.0-30.0	10.77				SC
30-39					GP

Table A.23. SK-23 well laboratory soil experiment results

SK-23					
Depth (m)	Water Content (%)	Natural Mass (g/cm^3)	Specific Gravity	Porosity	Soil Class
0-5					GP
5.0-6	9.02				GC
6.0-14.0					GP
14.0-15.0	26.26				CL
15-16.5					GP
16.5-17	16.17				GC
23.0-24.0	21.44				CL
24-					GP

APPENDIX B

GROUNDWATER LEVEL MONITORING GRAPHS (DIVER DATAS)

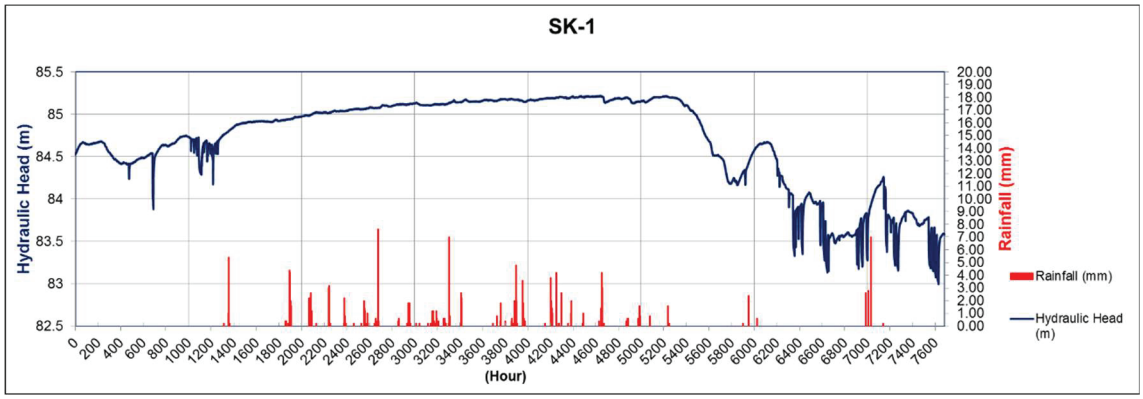

Figure B.1. SK-1 well groundwater level monitoring graphs

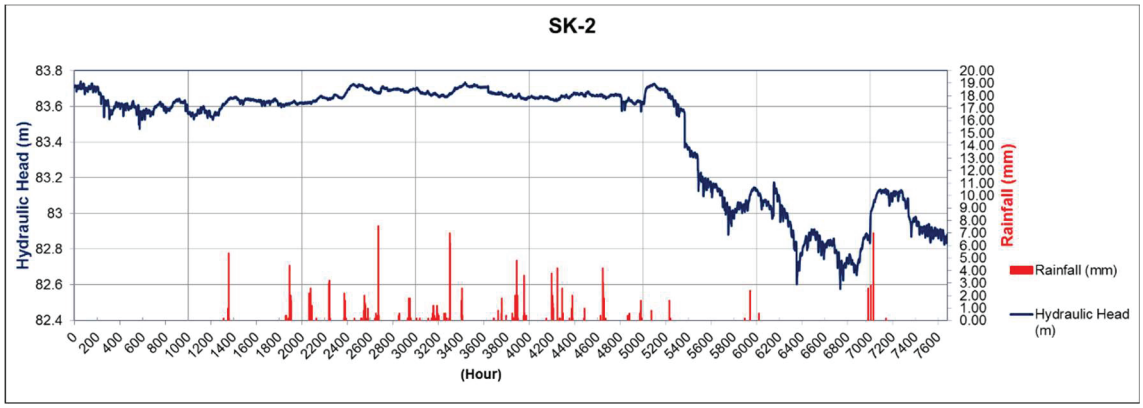

Figure B.2. SK-2 well groundwater level monitoring graphs

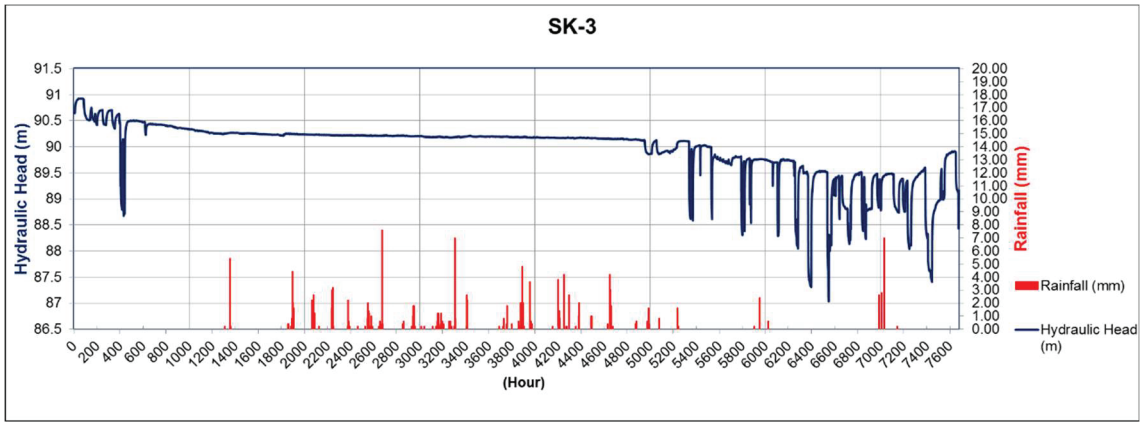

Figure B.3. SK-3 well groundwater level monitoring graphs

Figure B.4. SK-5 well groundwater level monitoring graphs

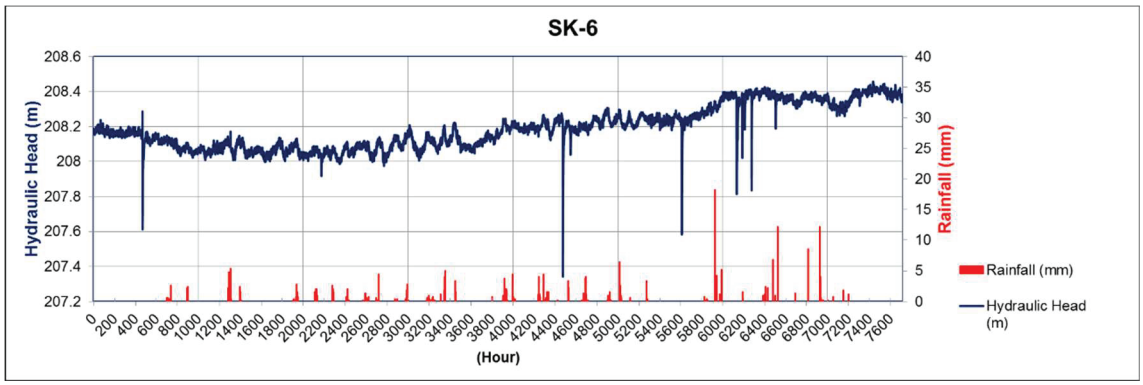

Figure B.5. SK-6 well groundwater level monitoring graphs

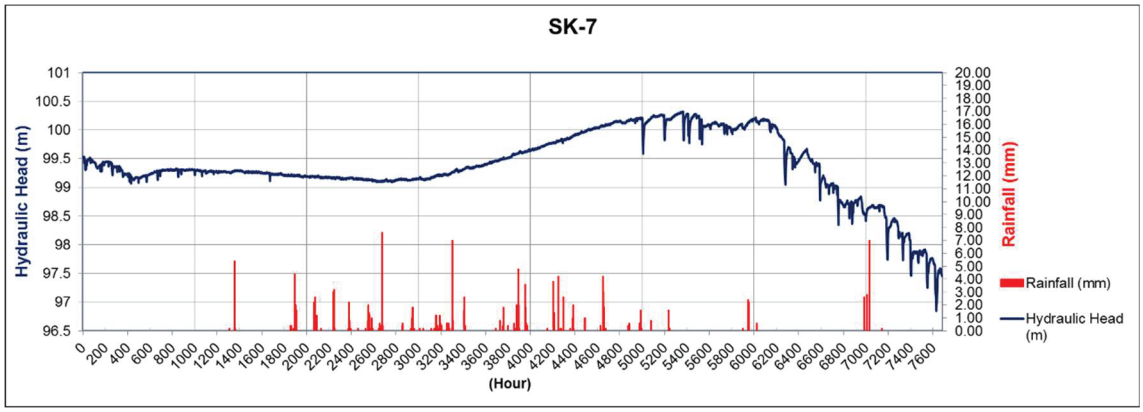

Figure B.6. SK-7 well groundwater level monitoring graphs

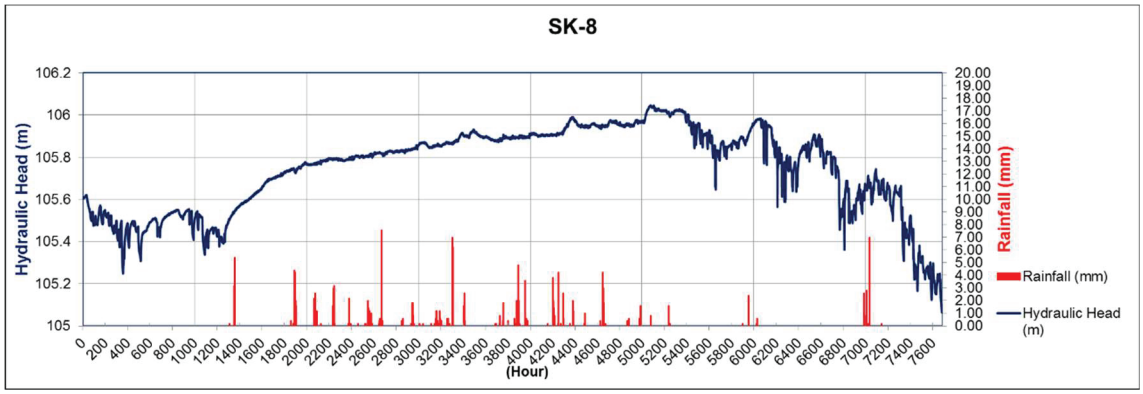

Figure B.7. SK-8 well groundwater level monitoring graphs

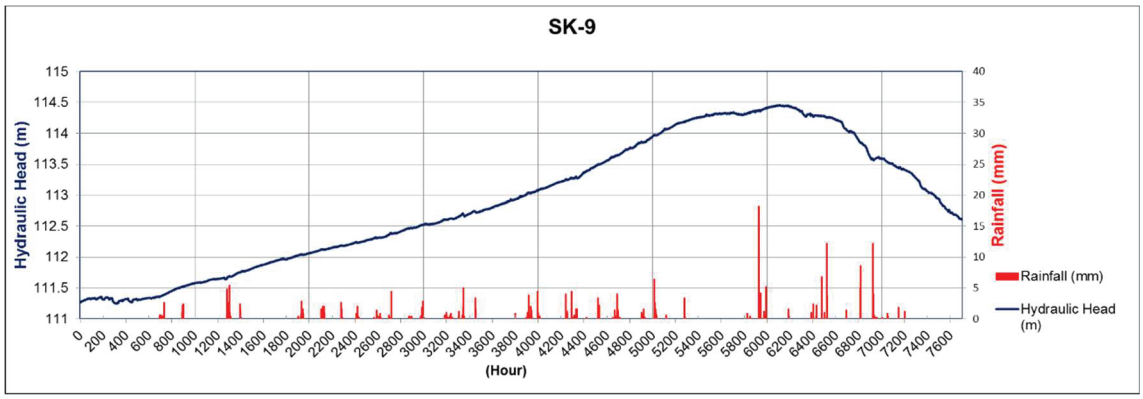

Figure B.8. SK-9 well groundwater level monitoring graphs

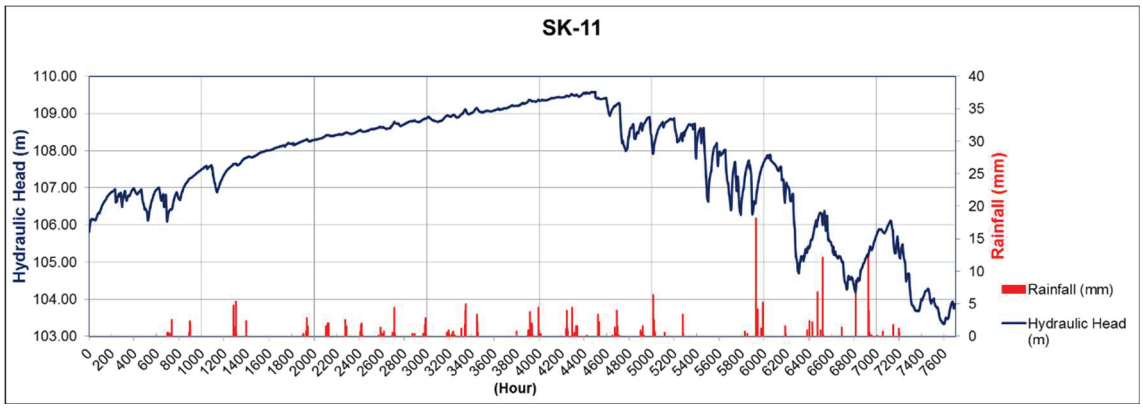

Figure B.9. SK-11 well groundwater level monitoring graphs

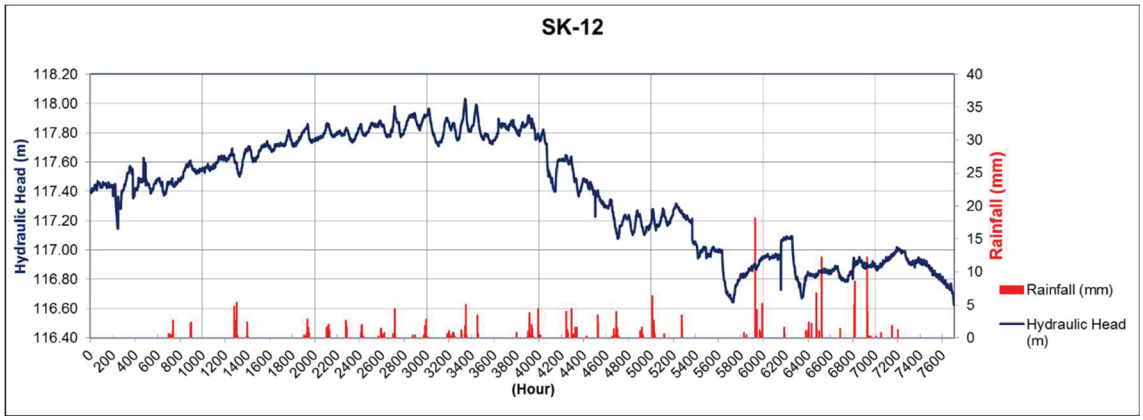

Figure B.10. SK-12 well groundwater level monitoring graphs

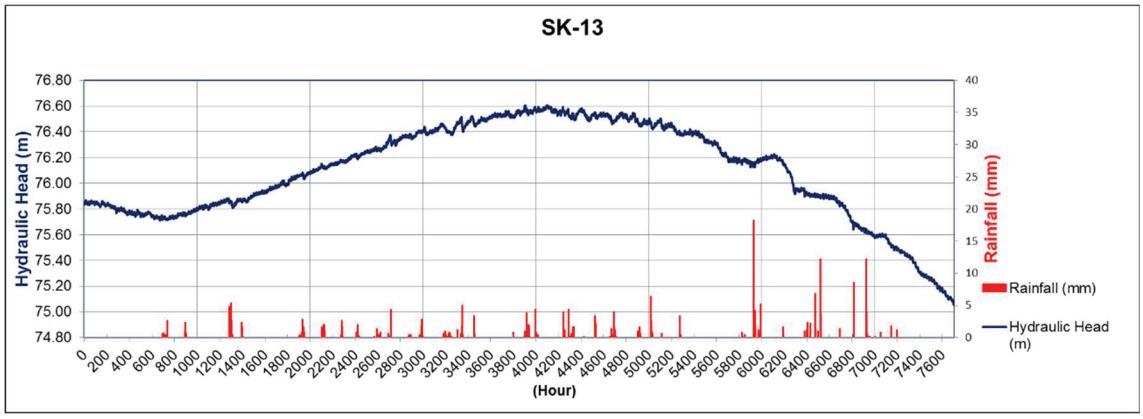

Figure B.11. SK-13 well groundwater level monitoring graphs

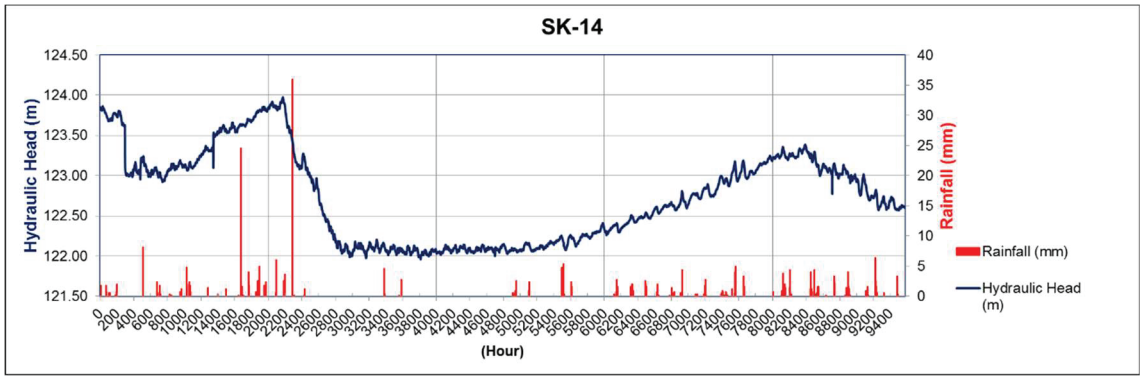

Figure B.12. SK-14 well groundwater level monitoring graphs

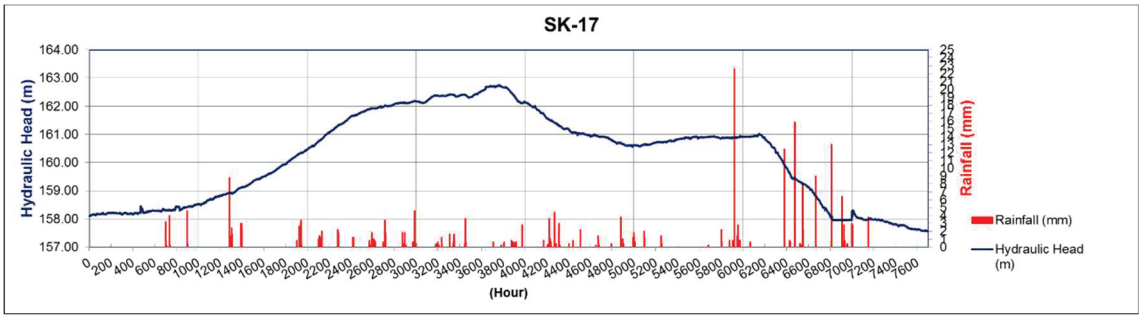

Figure B.13. SK-17 well groundwater level monitoring graphs

APPENDIX C

INFILTRATION GRAPHS OF RESEARCH WELLS

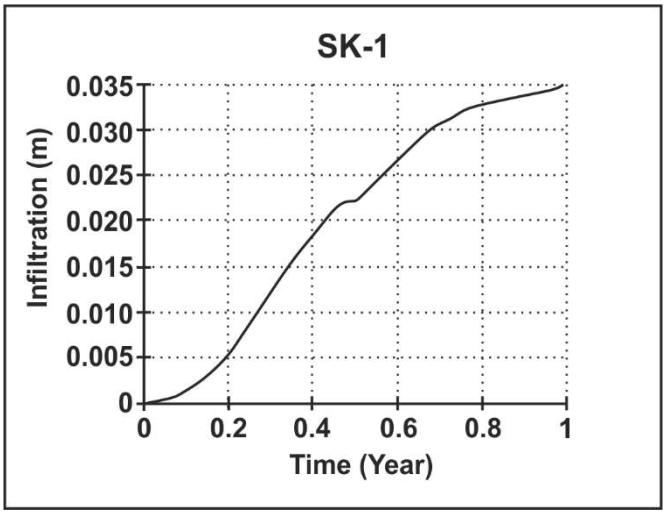

Figure C.1. SK-1 well infiltration graph

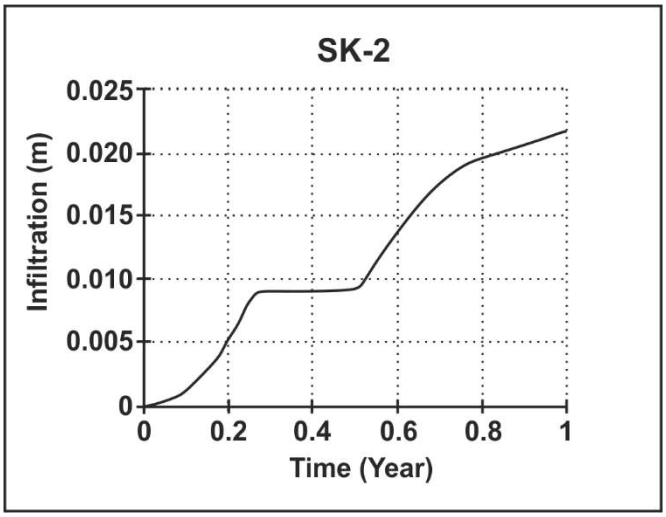

Figure C.2. SK-2 well infiltration graph

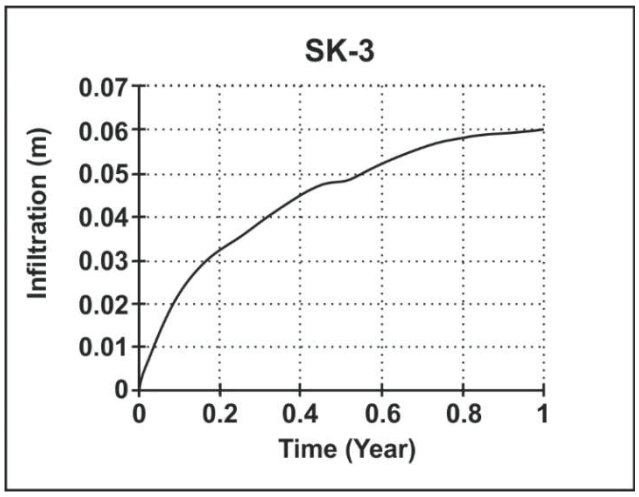

Figure C.3. SK-3 well infiltration graph

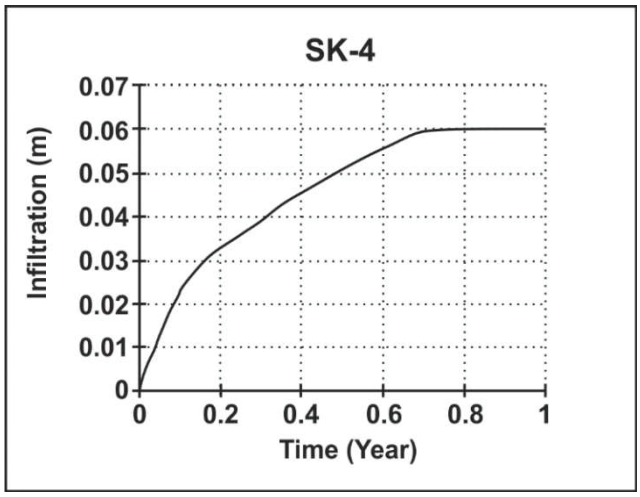

Figure C.4. SK-4 well infiltration graph

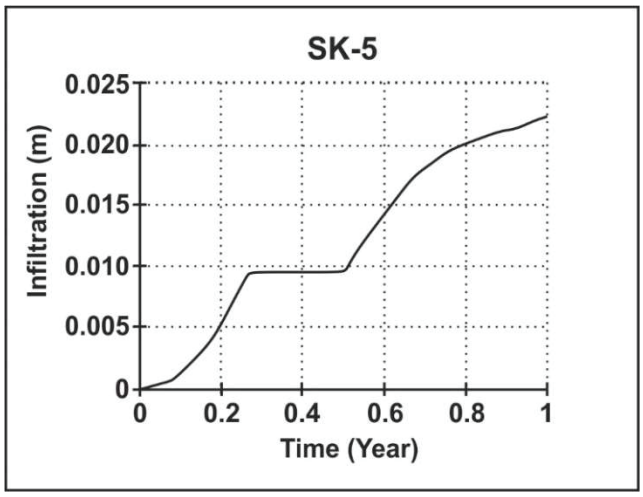

Figure C.5. SK-5 well infiltration graph

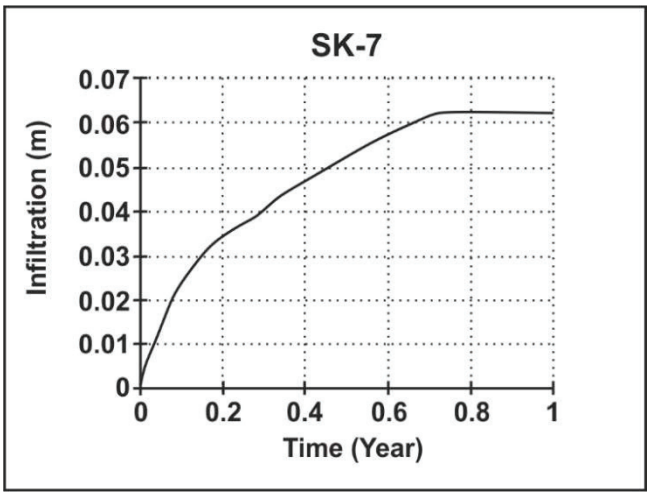

Figure C.6. SK-7 well infiltration graph

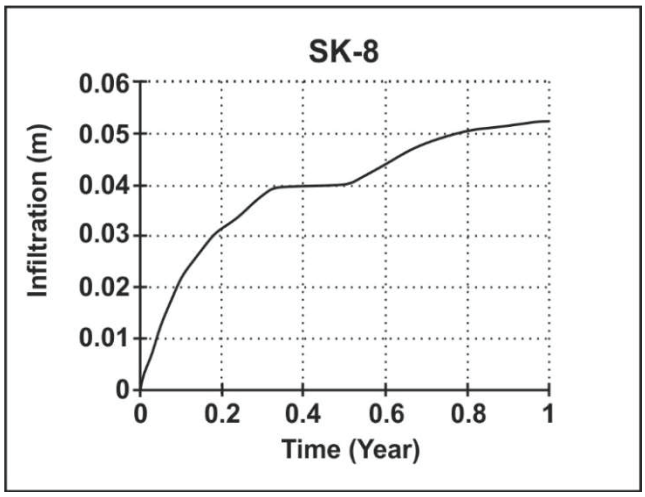

Figure C.7. SK-8 well infiltration graph

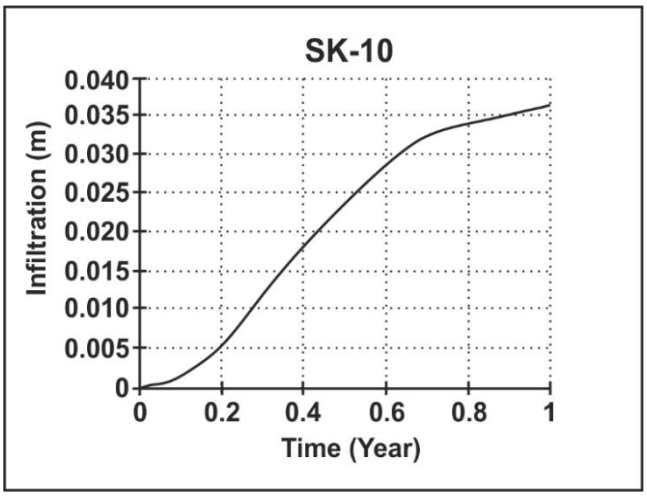

Figure C.8. SK-10 well infiltration graph

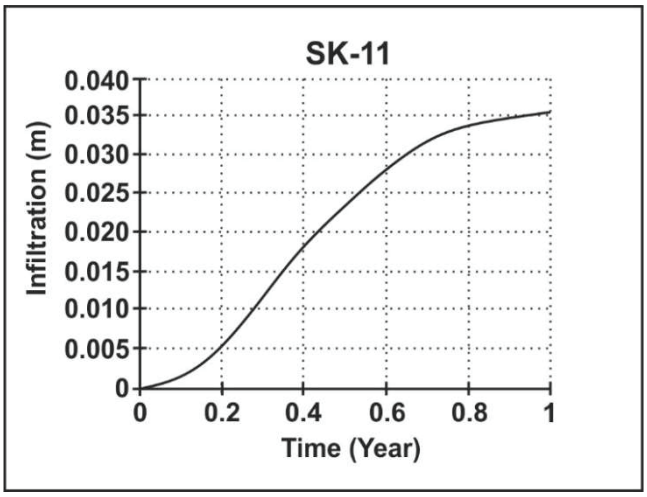

Figure C.9. SK-11 well infiltration graph

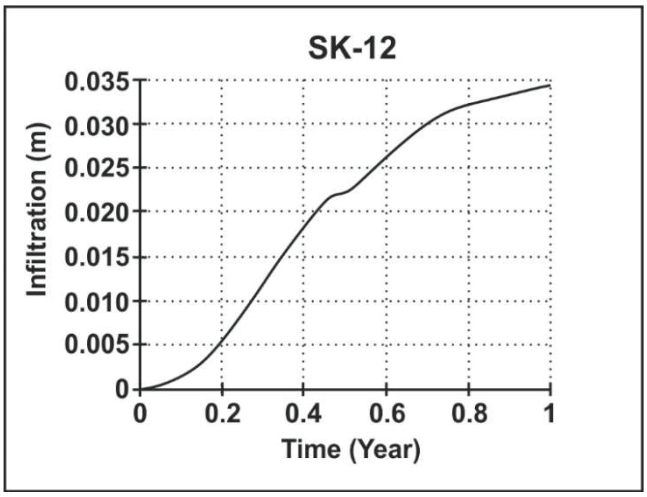

Figure C.10. SK-12 well infiltration graph

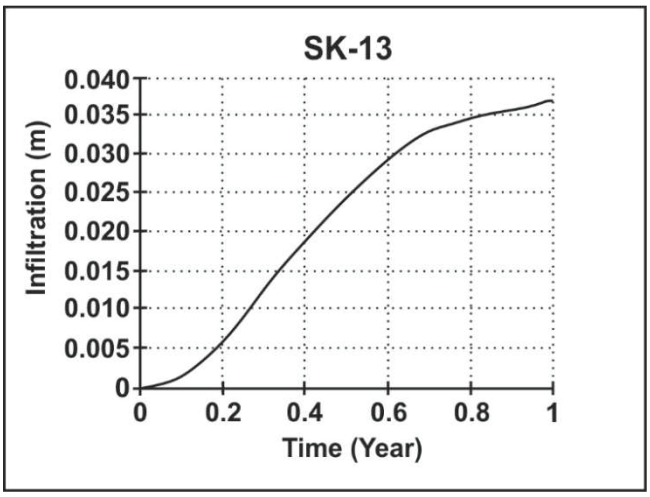

Figure C.11. SK-13 well infiltration graph

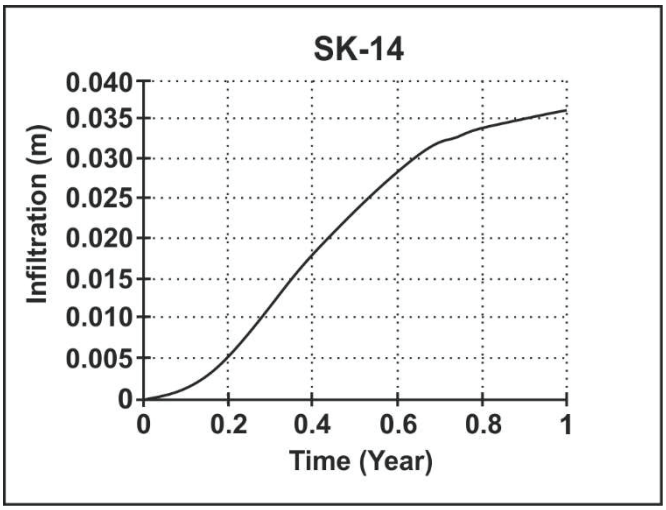

Figure C.12. SK-14 well infiltration graph

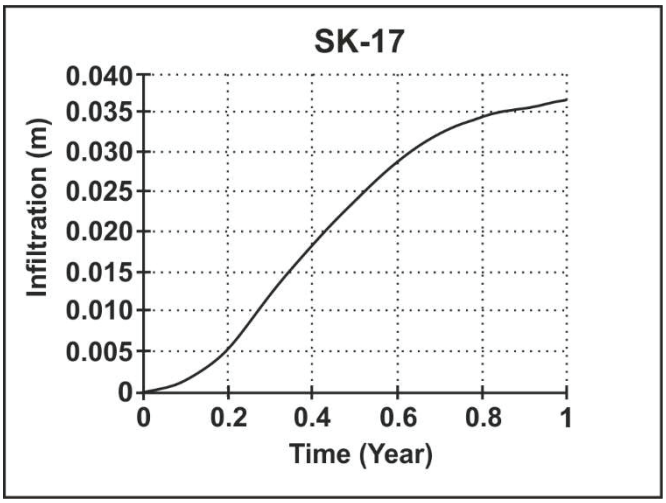

Figure C.13. SK-17 well infiltration graph

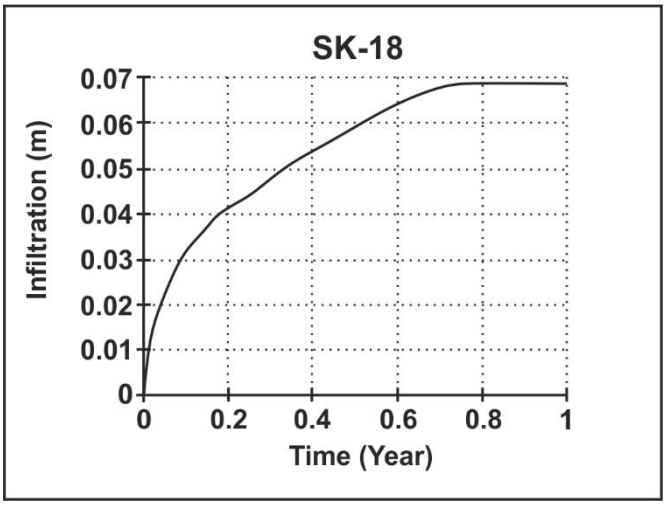

Figure C.14. SK-18 well infiltration graph

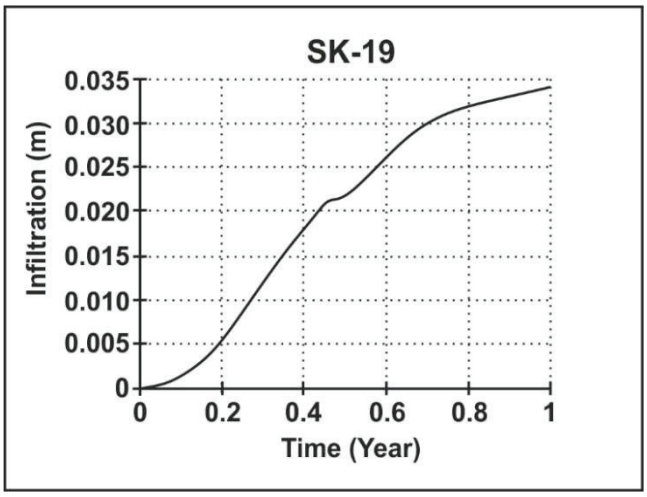

Figure C.15. SK-19 well infiltration graph

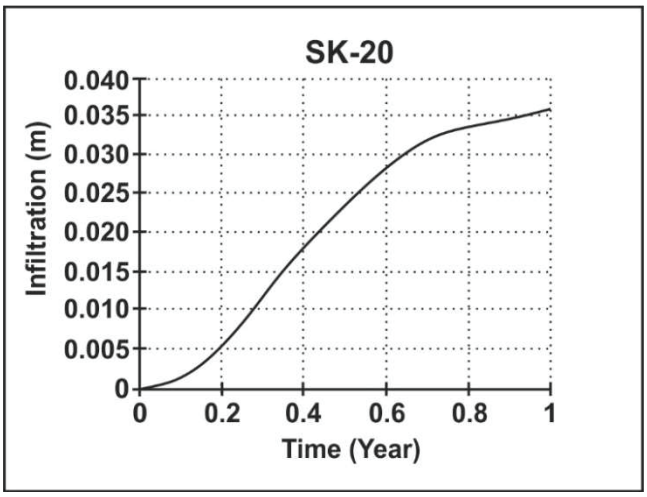

Figure C.16. SK-20 well infiltration graph

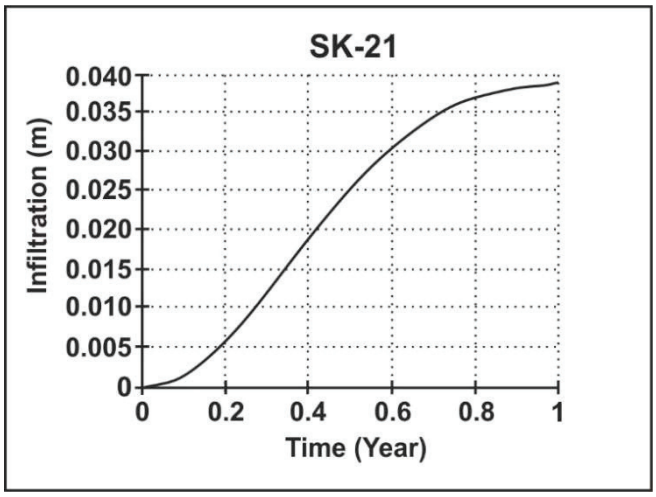

Figure C.17. SK-21 well infiltration graph

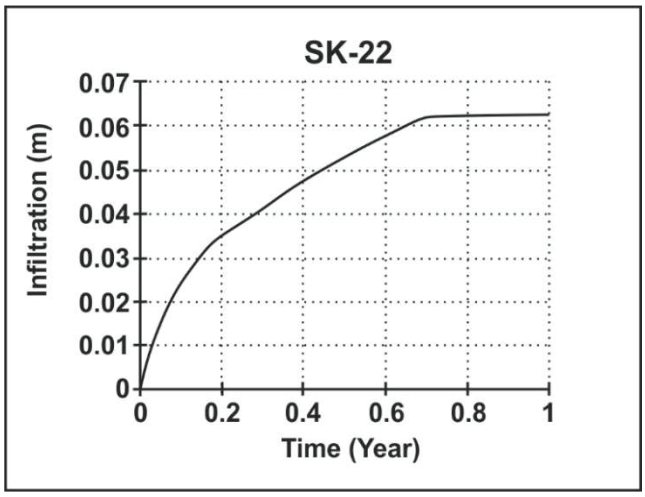

Figure C.18. SK-22 well infiltration graph

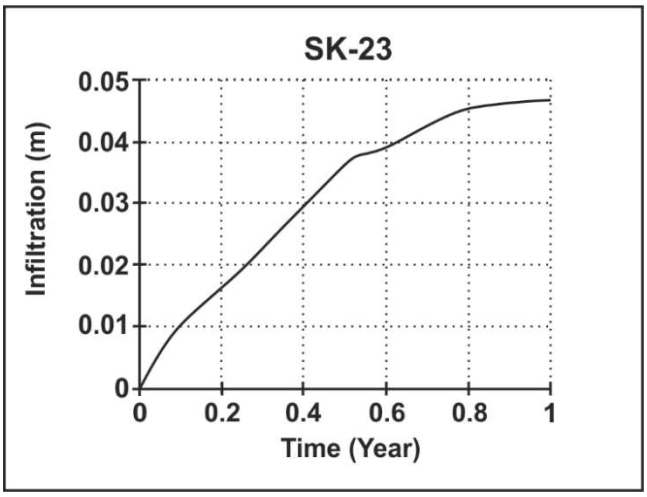

Figure C.19. SK-23 well infiltration graph

APPENDIX D

RESEARCH WELLS HYDRUS-1D MODEL OUTPUTS

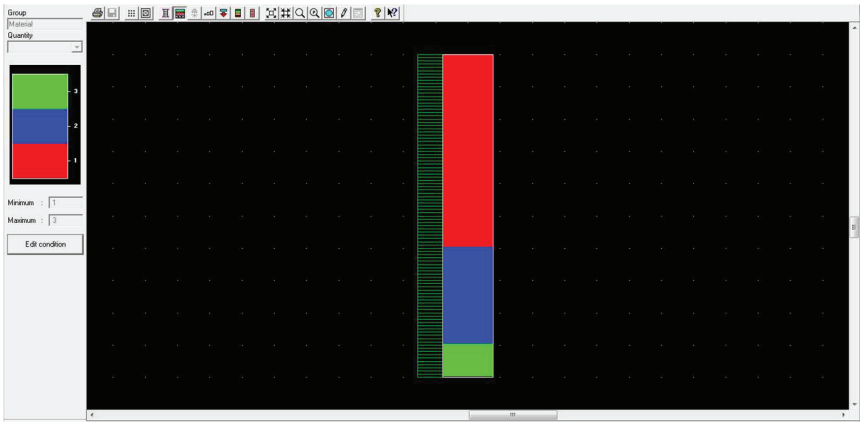

Figure D.1. SK-1 well HYDRUS-1D Model Result

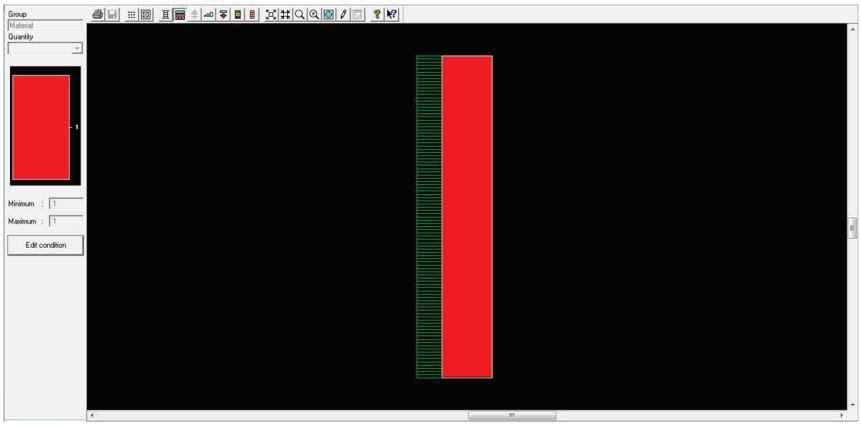

Figure D.2. SK-2 well HYDRUS-1D Model Result

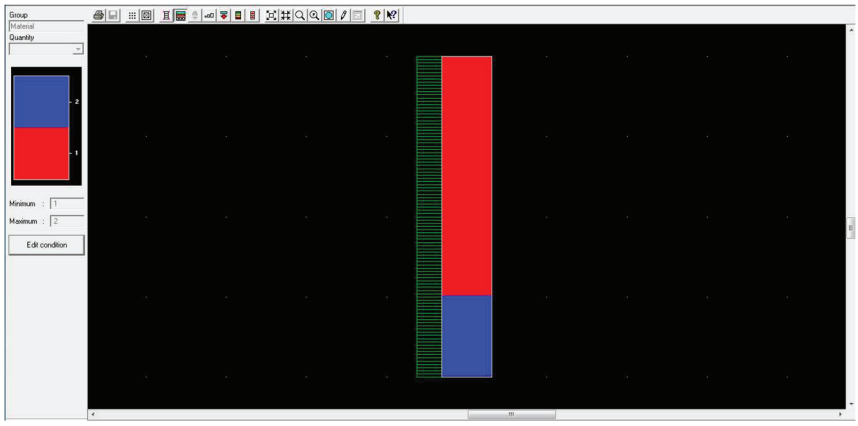

Figure D.3. SK-3 HYDRUS-1D Model Result

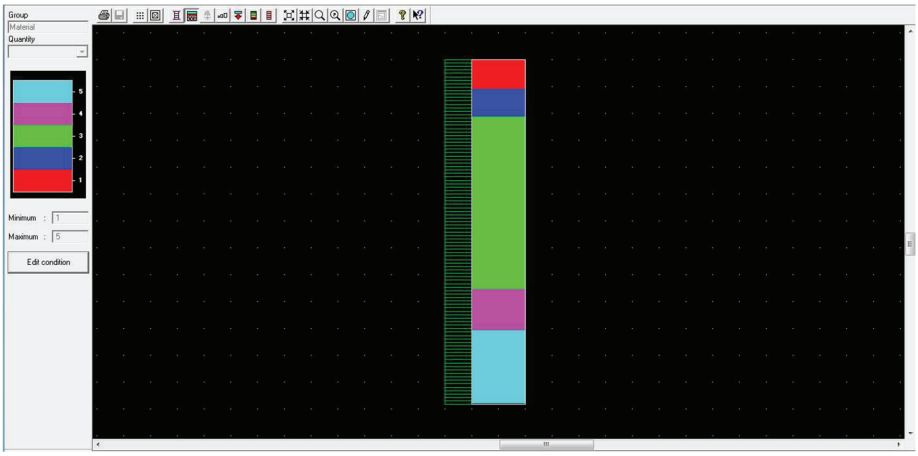

Figure D.4. SK-4 HYDRUS-1D Model Result

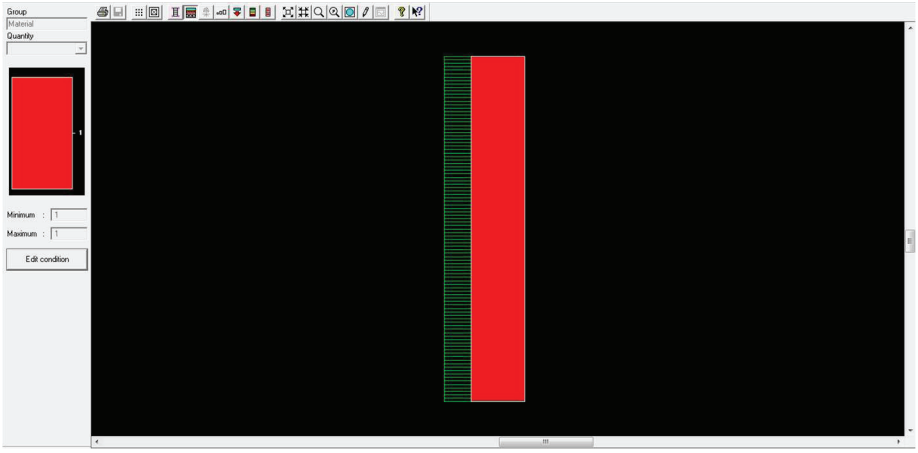

Figure D.5. SK-5 HYDRUS-1D Model Result

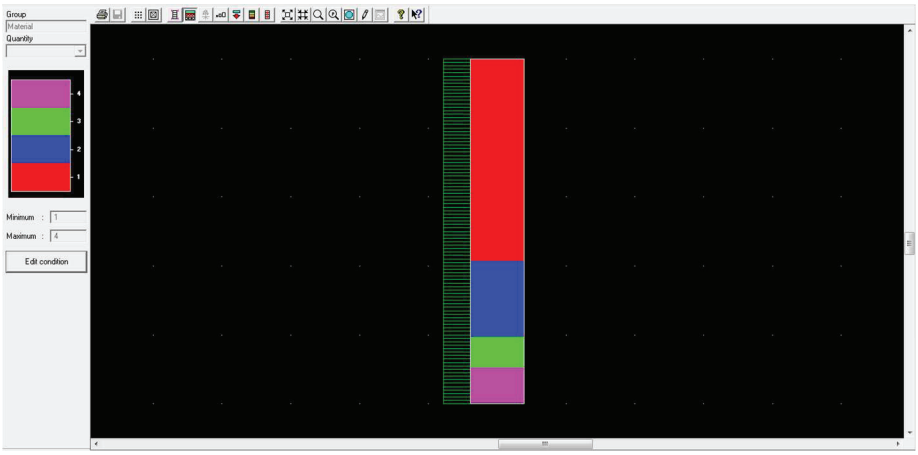

Figure D.6. SK-7 HYDRUS-1D Model Result

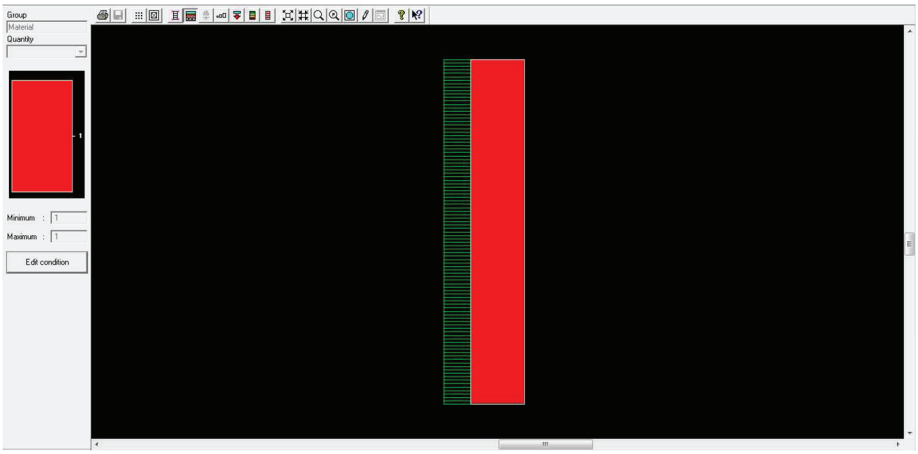

Figure D.7. SK-8 HYDRUS-1D Model Result

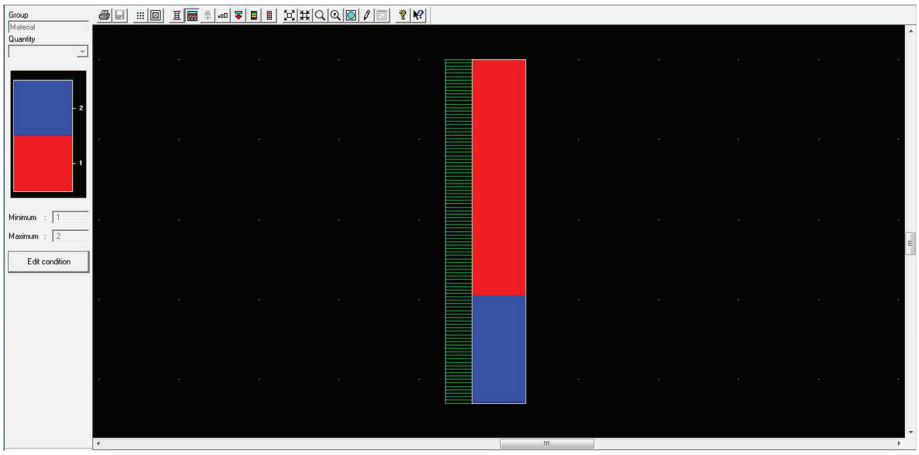

Figure D.8. SK-10 HYDRUS-1D Model Result

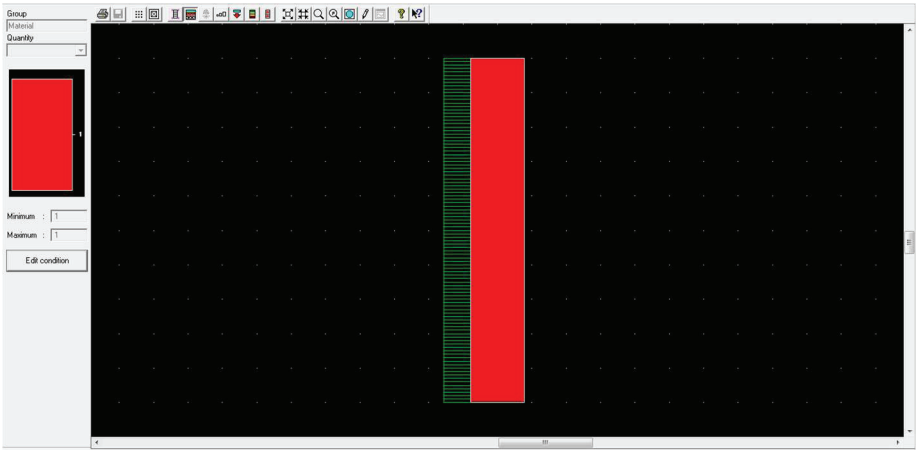

Figure D.9. SK-11 HYDRUS-1D Model Result

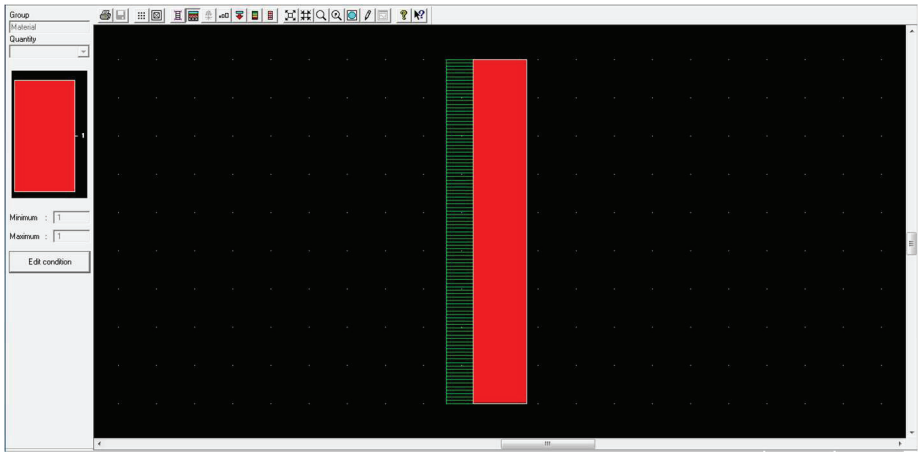

Figure D.10. SK-12 HYDRUS-1D Model Result

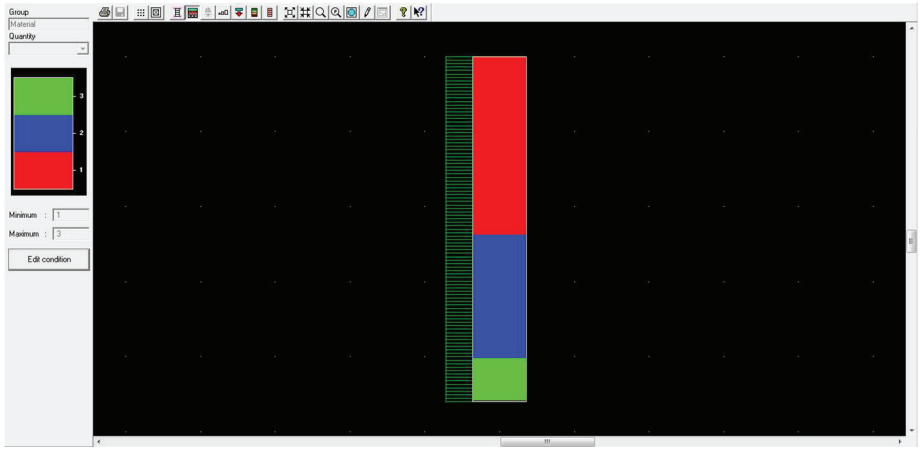

Figure D.11. SK-13 HYDRUS-1D Model Result

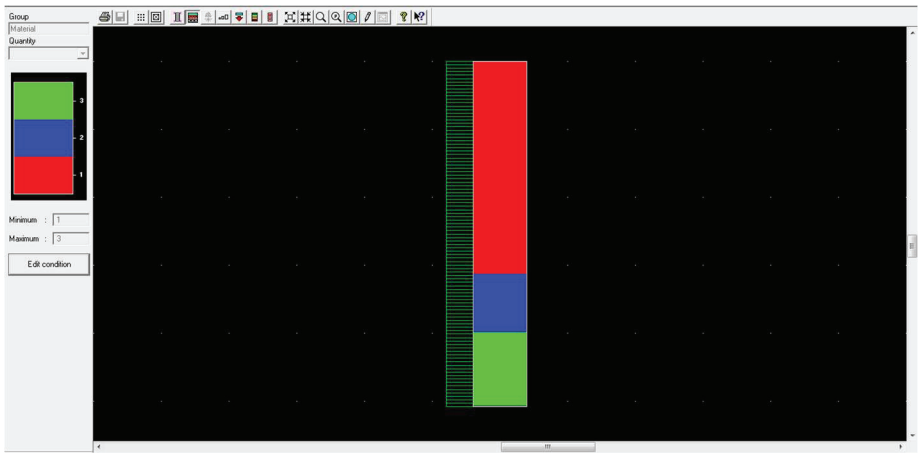

Figure D.12. SK-14 HYDRUS-1D Model Result

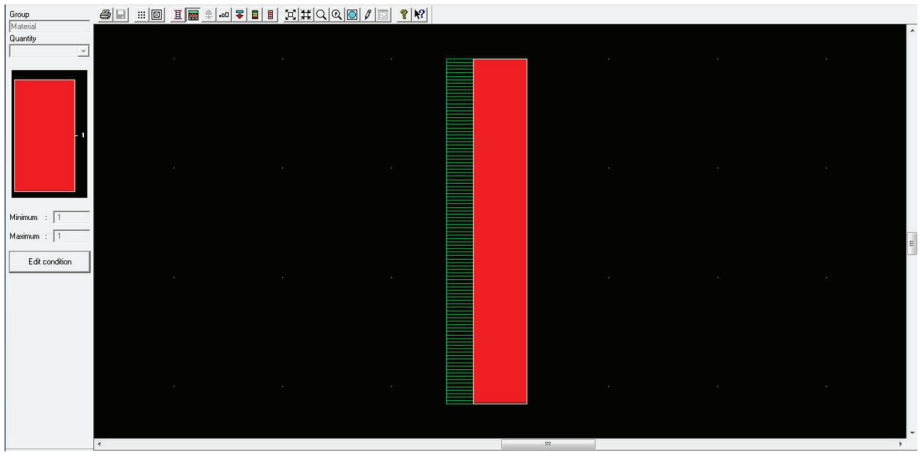

Figure D.13. SK-17 HYDRUS-1D Model Result

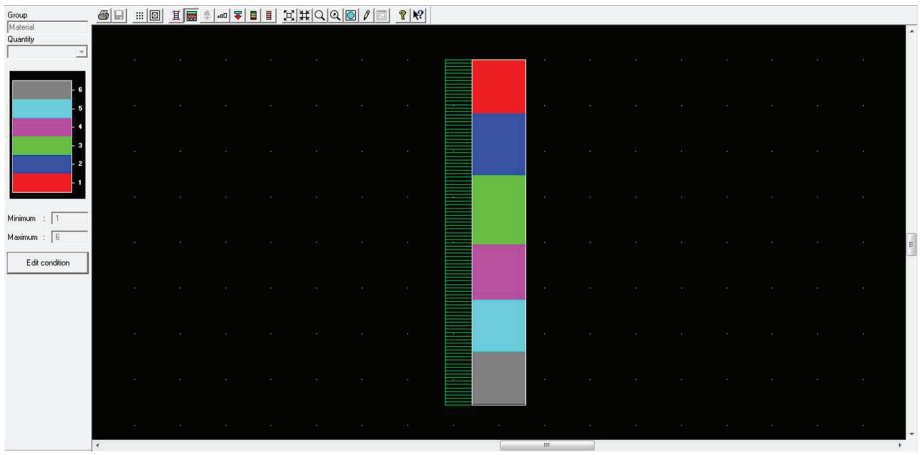

Figure D.14. SK-18 HYDRUS-1D Model Result

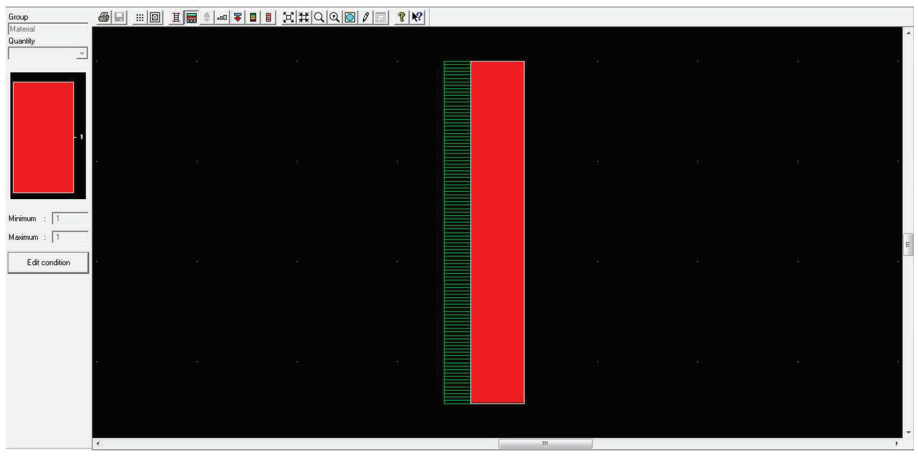

Figure D.15. SK-19 HYDRUS-1D Model Result

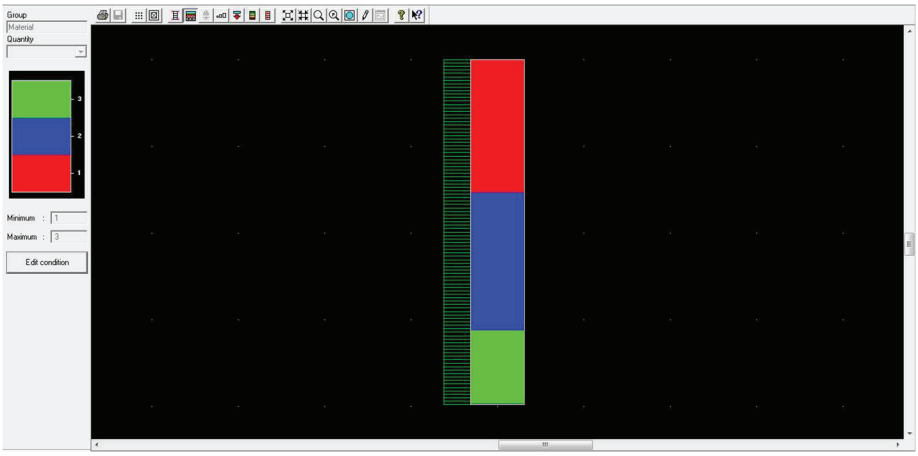

Figure D.16. SK-20 HYDRUS-1D Model Result

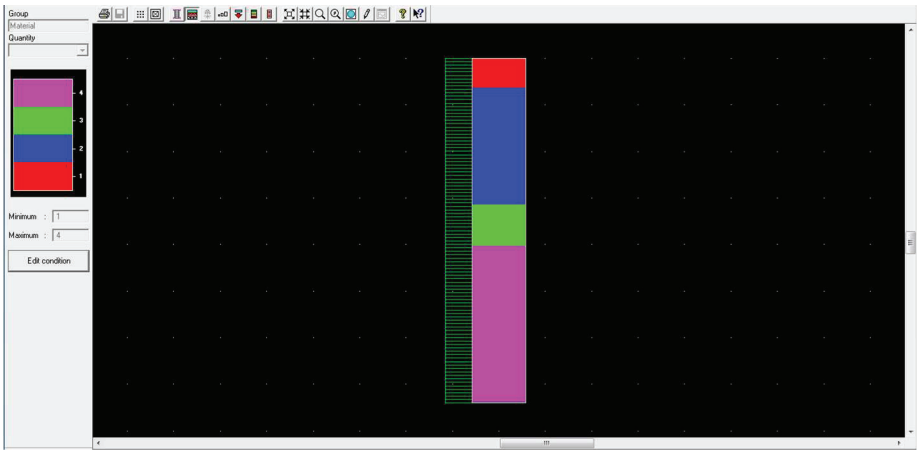

Figure D.17. SK-21 HYDRUS-1D Model Result

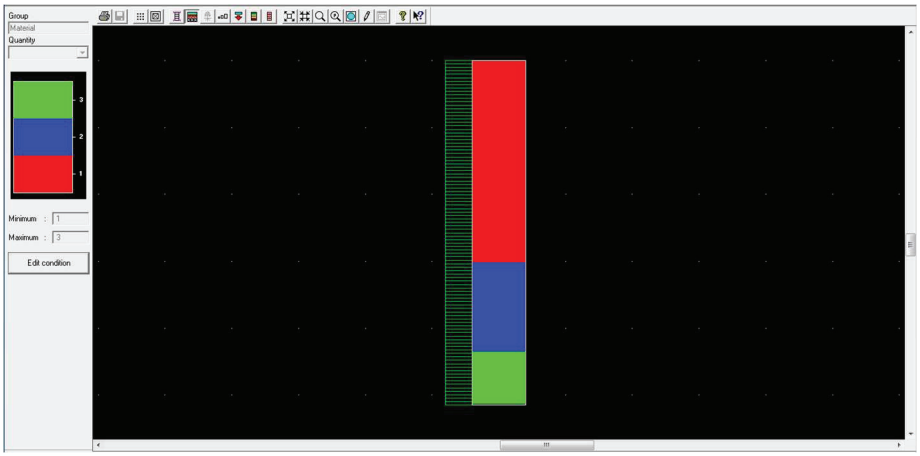

Figure D.18. SK-22 HYDRUS-1D Model Result

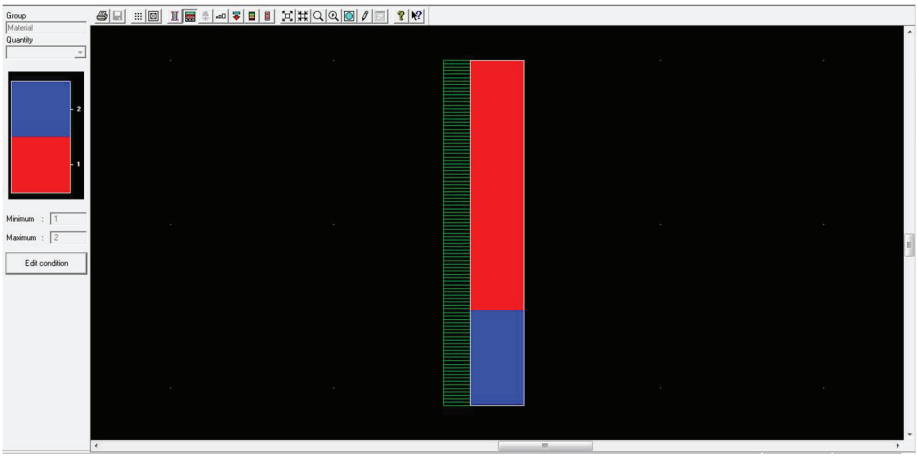

Figure D.19. SK-23 HYDRUS-1D Model Result

REFERENCES

Aküzüm, T., Çakmak, B., & Gökalp, Z. (2010). Türkiye'de su kaynakları yönetiminin değerlendirilmesi. *Tarım Bilimleri Araştırma Dergisi*(1), 67-74.

Alley, W. M., Healy, R. W., LaBaugh, J. W., & Reilly, T. E. (2002). Flow and storage in groundwater systems. *science, 296*(5575), 1985-1990.

Anlauf, R., Rehrmann, P., & Schacht, H. (2012). Simulation of water uptake and redistribution in growing media during ebb-and-flow irrigation. *Journal of Horticulture and Forestry, 4*(1), 8-21.

Anuraga, T., Ruiz, L., Kumar, M. M., Sekhar, M., & Leijnse, A. (2006). Estimating groundwater recharge using land use and soil data: A case study in South India. *Agricultural water management, 84*(1-2), 65-76.

Asano, T. (1985). Artificial recharge of groundwater, section III, Groundwater recharge operations: Butterworth, London.

Back, W., & Hanshaw, B. B. (1965). Chemical geohydrology *Advances in hydroscience* (Vol. 2, pp. 49-109): Elsevier.

Bear, J., & Cheng, A. H.-D. (2010). *Modeling groundwater flow and contaminant transport* (Vol. 23): Springer Science & Business Media.

Blonquist Jr, J., Jones, S. B., & Robinson, D. (2006). Precise irrigation scheduling for turfgrass using a subsurface electromagnetic soil moisture sensor. *Agricultural water management, 84*(1-2), 153-165.

Canik, B. (1998). Hidrojeoloji, yeraltı sularının aranması, işletilmesi, kimyası. *Ankara Üniversitesi Fen Fakültesi*.

Chow, V., Maidment, D., & Mays, L. (1988). Applied hydrology, 572 pp. *Editions McGraw-Hill, New York*.

Chow, V. T. (1964). Handbook of applied hydrology.

Coduto, D. P. (1999). *Geotechnical engineering: principles and practices*.

Cook, P., Edmunds, W., & Gaye, C. (1992). Estimating paleorecharge and paleoclimate from unsaturated zone profiles. *Water Resources Research, 28*(10), 2721-2731.

Darcy, H. (1856). *Les fontaines publiques de la ville de Dijon: exposition et application*: Victor Dalmont.

De Silva, C. (2015). Simulation of Potential Groundwater Recharge from the Jaffna Peninsula of Sri Lanka using HYDRUS-1D Model. *OUSL Journal, 7*.

De Vries, J. J., & Simmers, I. (2002). Groundwater recharge: an overview of processes and challenges. *Hydrogeology Journal, 10*(1), 5-17.

Delin, G. N., Healy, R. W., Lorenz, D. L., & Nimmo, J. R. (2007). Comparison of local- to regional-scale estimates of ground-water recharge in Minnesota, USA. *Journal of Hydrology, 334*(1), 231-249.

Devine, R. S. (1995). The trouble with dams. *Atlantic Monthly, 276*(2), 64-74.

DSİ. (2014). DSİ 02 Bölge Gediz Havzası Yeraltısuyu Planlaması Hidrojeolojik Etüd Raporu, DSİ Ankara.

E.İ.E. (2017). Güneş Enerjisi Potansiyel Atlası (GEPA). Retrieved from Türkiye Cumhuriyeti Enerji ve Tabi Kaynaklar Bakanlığı: http://www.eie.gov.tr/MyCalculator/pages/45.aspx.

Fancher, G. H., & Lewis, J. A. (1933). Flow of simple fluids through porous materials. *Industrial & Engineering Chemistry, 25*(10), 1139-1147.

Grinevskiy, S. O., & Pozdniakov, S. P. (2013). The use of Hydrus-1D for groundwater recharge estimation in boreal environments. *HYDRUS Software Applications to Subsurface Flow and Contaminant Transport Problems, 107*, 1-13.

Gündüz, O., & Şimşek, C. (2011). Influence of climate change on shallow groundwater resources: the link between precipitation and groundwater levels in alluvial systems *Climate Change and its Effects on Water Resources* (pp. 225-233): Springer.

Hartmann, A., Weiler, M., Wagener, T., Lange, J., Kralik, M., Humer, F., . . . Andreo, B. (2013). Process-based karst modelling to relate hydrodynamic and hydrochemical characteristics to system properties. *Hydrology and earth system sciences, 17*(8), 3305-3321.

Healy, R. W. (2010). *Estimating groundwater recharge*: Cambridge University Press.

Hem, J. D. (1970). *Study and interpretation of the chemical characteristics of natural water*: US Government Printing Office.

Herczeg, A., Leaney, F., Stadler, M., Allan, G., & Fifield, L. (1997). Chemical and isotopic indicators of point-source recharge to a karst aquifer, South Australia. *Journal of Hydrology, 192*(1-4), 271-299.

İTASHY. (2013). İnsani Tüketim Amaçlı Sular Hakkında Yönetmelik Hakkında Değişiklik Yapılmasına Dair Yönetmelik. 2858 Nolu Resmi Gazete.

Knoppers, R., & van Hulst, W. (1995). *De keerzijde van de dam*: Novib.

Leaney, F., Crosbie, R., O'Grady, A., Jolly, I., Gow, L., Davies, P., . . . Kilgour, P. (2011). Recharge and discharge estimation in data poor areas: scientific reference guide.

Leaney, F., & Herczeg, A. (1995). Regional recharge to a karst aquifer estimated from chemical and isotopic composition of diffuse and localised recharge, South Australia. *Journal of Hydrology, 164*(1-4), 363-387.

Lu, X., Jin, M., van Genuchten, M. T., & Wang, B. (2011). Groundwater recharge at five representative sites in the Hebei Plain, China. *Groundwater, 49*(2), 286-294.

Luijendijk, E., & Bruggeman, A. (2008). Groundwater resources in the Jabal Al Hass region, northwest Syria: an assessment of past use and future potential. *Hydrogeology Journal, 16*(3), 511-530.

Margat, J., & Van der Gun, J. (2013). *Groundwater around the world: a geographic synopsis*: Crc Press.

Moriasi, D. N., Arnold, J. G., Van Liew, M. W., Bingner, R. L., Harmel, R. D., & Veith, T. L. (2007). Model evaluation guidelines for systematic quantification of accuracy in watershed simulations. *Transactions of the ASABE, 50*(3), 885-900.

Mualem, Y. (1976). A new model for predicting the hydraulic conductivity of unsaturated porous media. *Water Resources Research, 12*(3), 513-522.

Neuman, S. P., Feddes, R. A., & Bresler, E. (1974). Finite element simulation of flow in saturated-unsaturated soils considering water uptake by plants.

Pearce, F. (1992). The dammed: rivers, dams, and the coming world water crisis.

Rabet, R. S. (2014). Alaşehir Ovasında Jeotermal Suların Yeraltı suyuna olan etkileri. Yüksek Lisans Tezi, Dokuz Eylül Üniversitesi, Fen Bilimler Enstitüsü, İzmir.

Rabet, R. S., Simsek, C., Baba, A., & Murathan, A. (2017). Blowout mechanism of Alasehir (Turkey) geothermal field and its effects on groundwater chemistry. *Environmental Earth Sciences, 76*(1), 49.

Richards, L. A. (1931). Capillary conduction of liquids through porous mediums. *physics, 1*(5), 318-333.

Rushton, K., & Ward, C. (1979). The estimation of groundwater recharge. *Journal of Hydrology, 41*(3), 345-361.

Scanlon, B. R., & Cook, P. G. (2002). Theme issue on groundwater recharge. *Hydrogeology Journal, 10*(1), 3-4.

Scanlon, B. R., Healy, R. W., & Cook, P. G. (2002). Choosing appropriate techniques for quantifying groundwater recharge. *Hydrogeology Journal, 10*(1), 18-39.

Simunek, J., van Genuchten, M. T., & Šejna, M. (1999). *The HYDRUS-2D Software Package for Simulating the Two-dimensional Movement of Water, Heat, and Multiple Solutes in Variably-saturated Media: Version 2.0*: Colorado School of Mines.

Simunek, J., Köhne, J. M., Kodešová, R., & Šejna, M. (2008). Simulating non equilibrium movement of water, solutes, and particles using HYDRUS: A review of recent applications. *Soil Water Res, 3*(Special Issue 1), S42-S51.

Simunek, J., Van Genuchten, M. T., & Sejna, M. (2005). The HYDRUS-1D software package for simulating the one-dimensional movement of water, heat, and multiple solutes in variably-saturated media. *University of California-Riverside Research Reports, 3*, 1-240.

Simunek, J., Van Genuchten, M. T., & Šejna, M. (2006). The HYDRUS software package for simulating two-and three-dimensional movement of water, heat, and multiple solutes in variably-saturated media. *Technical manual, version, 1*, 241.

Somaratne, N., Smettem, K., Lawson, J., Nguyen, K., & Frizenschaf, J. (2013). Hydrological functions of sinkholes and characteristics of point recharge in groundwater basins. *Hydrol. Earth Syst. Sci. Discuss, 10*, 11423-11449.

Standard, A. (2011). D2487-11. *Standard Practice for Classification of Soils for Engineering Purposes (Unified Soil Classification System), ASTM International, West Conshohocken, PA*.

Thornthwaite, C. W. (1948). An approach toward a rational classification of climate. *Geographical review, 38*(1), 55-94.

Todd, D. K. (1959). *Ground water hydrology*: John Wiley and Sons, Inc, New York.

Van Genuchten, M. T. (1980). A closed-form equation for predicting the hydraulic conductivity of unsaturated soils 1. *Soil science society of America journal, 44*(5), 892-898.

Walker, G. R., Jolly, I. D., & Cook, P. G. (1991). A new chloride leaching approach to the estimation of diffuse recharge following a change in land use. *Journal of Hydrology, 128*(1-4), 49-67.

Weight, W. D. (2008). *Hydrogeology field manual*: McGraw-Hill.

White, D. E., Hem, J. D., & Waring, G. (1963). *Chemical composition of subsurface waters* (2330-7102).

Wood, W. (2014). Interactive comment on ‘‘Theory of the generalized chloride mass balance method for recharge estimation in groundwater basins characterised by point and diffuse recharge’’by N. Somaratne and KRJ Smettem. *Hydrol Earth Syst Sci Discuss, 11*, C19-C21.

Wood, W. W., & Sanford, W. E. (1995). Chemical and isotopic methods for quantifying ground-water recharge in a regional, semiarid environment. *Groundwater, 33*(3), 458-468.